INFORMATION TO USERS

This manuscript has been reproduced from the microfilm master. UMI films the text directly from the original or copy submitted. Thus, some thesis and dissertation copies are in typewriter face, while others may be from any type of computer printer.

The quality of this reproduction is dependent upon the quality of the copy submitted. Broken or indistinct print, colored or poor quality illustrations and photographs, print bleedthrough, substandard margins, and improper alignment can adversely affect reproduction.

In the unlikely event that the author did not send UMI a complete manuscript and there are missing pages, these will be noted. Also, if unauthorized copyright material had to be removed, a note will indicate the deletion.

Oversize materials (e.g., maps, drawings, charts) are reproduced by sectioning the original, beginning at the upper left-hand corner and continuing from left to right in equal sections with small overlaps. Each original is also photographed in one exposure and is included in reduced form at the back of the book.

Photographs included in the original manuscript have been reproduced xerographically in this copy. Higher quality 6" x 9" black and white photographic prints are available for any photographs or illustrations appearing in this copy for an additional charge. Contact UMI directly to order.

UMI

A Bell & Howell Information Company
300 North Zeeb Road, Ann Arbor MI 48106-1346 USA
313/761-4700 800/521-0600

Université d'Ottawa · University of Ottawa

Assessing the Cause of Irreversible Permeate Flux Decline of Reverse Osmosis Membranes during the Treatment of Wastewater

A thesis submitted to the School of Graduate Studies and Research
in partial fulfillment of the requirements for the degree of

M. A. Sc.

in the

DEPARTMENT OF CHEMICAL ENGINEERING
UNIVERSITY OF OTTAWA

May 1997

Abstract

This study was conducted to determine causes of irreversible permeate flux declines observed during the treatment of waste water. The resistance of reverse osmosis membranes to fouling during the processing of waste water at various crossflow velocities is evaluated. Tests were performed with a three weight percent NaCl solution and with batches of a waste stream that is treated at AECL's Chalk River Laboratories. With the NaCl tests, the mass transfer coefficient of NaCl was determined for crossflows ranging from 30 L/min to 60 L/min. An optimum crossflow of 45 L/min was found. Using the mass transfer coefficients calculated with the NaCl tests, the permeate flux was predicted for the waste stream based strictly on osmotic pressure considerations. With the waste stream, an improved membrane performance was not observed at any of the crossflows tested. At high volumetric recoveries, the observed permeate flux was significantly lower than the predicted permeate flux based on osmotic pressure calculations. The presence of particulates was found to be the primary factor affecting the permeate flux of the waste. This effect was intensified at volumetric recoveries in excess of 55 to 70 percent. It was recommended to remove the source of the particulates by treating the water before it enters the Chalk River Laboratories site. This would prevent severe flux declines and eliminate the need for frequent cleanings and costly membrane replacements.

A three-step cleaning procedure was developed to restore the permeate flux of the fouled reverse osmosis membranes to an acceptable level of 1 L/min. This level is required in order to prevent accumulation with in the process. In the first step, the Triton X-100 detergent solution improved the permeate flux by 73.5 percent for module 1 and by 47.3 percent for module 2. In the second step, a HCl solution at pH 2, caused a 14 percent improvement in permeate flux for module 1 and no observed improvement for module 2. The final step consisted of a solution of NaOH and ethylenediaminetetraacidic acid at pH 12 for module 1 and a solution of NaOH and nitrilotriacetic acid at pH 12 for module 2. An improvement in permeate flux by 20 percent was

observed for both modules. The three-step cleaning procedure restored the permeate flux from a value of 0.5 L/min to 1.1 L/min.

Tests were also conducted to determine if the three-step cleaning procedure had degraded the integrity of the membrane. This was achieved by performing rejection efficiency tests with cesium and strontium. Both species were effectively rejected by the membranes so the three-step cleaning had not affected the separation characteristics of the membrane. The decontamination factor of cesium for a new membrane is approximately 100 (99.0 % rejection efficiency) at 2760 kPa. The fouled membranes had a decontamination factor of 50 (98.0 % rejection efficiency) for cesium both before and after cleaning. The decontamination factor of strontium for a new membrane is approximately 1000 (99.9 % rejection efficiency) at 2760 kPa. The fouled membranes had a decontamination factor of at least 4000 (99.98 % rejection efficiency) for strontium both before and after cleaning. The increased rejection of strontium is associated with the exchange of strontium with precipitated calcium on the membrane surface.

Résumé

L'objet de cette étude consiste à déterminer les causes d'une perte irréversible de flux lors du traitement des eaux usées par osmose inverse (OI). L'entartrage des membranes en fonction de la vitesse d'écoulement tangentiel dans un module d'OI est étudié. Plusieurs essais ont été faits avec une solution de trois pour cent en chlorure de sodium et des eaux usées provenant du laboratoire d'Énergie Atomique Canada (Chalk River, Ontario). Les coefficients de transfert de masse obtenus avec les essais utilisant le NaCl indiquent une performance optimale à un écoulement tangentiel de 45 L/min. Pour le traitement des eaux usées, aucune amélioration du débit du permeat est observé en fonction de l'écoulement tangentiel. Une diminution significative du débit de perméat est observée à des taux de récupération élevés. La diminution importante du débit lors du traitement des eaux usées est attribuée à la présence et la formation de particules dans l'alimentation. Cet effet est très intense à des taux de récupération supérieurs à 55 pour cent. On recommande d'enlever une source majeure de particules en traitant l'eau avant son entrée dans les laboratoires d'EACL. Ceci préviendrait les réductions considérables de flux, réduirait les lavages fréquents et les remplacements de membranes coûteux.

Les bénéfices d'un lavage en trois étapes sont évalués. Un débit de 1 L de perméat/min/élément est nécessaire pour prévenir une accumulation dans le système de traitement des eaux usées d'EACL. Deux modules (1 et 2) on fait l'objet de cette étude. Dans une première étape, une solution de détergent (Triton X-100) à améliorer le flux de 73,5 % et 47,3 % pour les modules 1 et 2 respectivement. Lors de la deuxième étape, une solution de HCl (pH 2) augmente le flux de 14 et 0 % respectivement pour les modules 1 et 2. Et lors d'une étape finale le module 1 est traité avec une solution de NaOH et EDTA (pH 12) et le module 2 une solution de NaOH et NTA (pH 12). Une augmentation de 20 % est observée pour les deux

modules. Pour les deux éléments, le lavage en trois étapes augmente le débit de perméat de 0,5 L/min/élément à 1,1 L/min/élément.

Plusieurs tests ont été faits pour déterminer si la procédure de lavage avait endommagé les membranes. Ceci fut déterminé en faisant des tests avec des sels de césium et de strontium. Pour une nouvelle membrane, le facteur de décontamination du césium est environ 100 (99,0 % de rejet) à 2760 kPa. Les membranes usées avaient un facteur de décontamination de 50 (98,0 % de rejet) avant et après le lavage. Le facteur de décontamination du strontium pour une nouvelle membrane est environ 1000 (99,9 % de rejet) à 2760 kPa. Les membranes encrassées avaient un facteur de décontamination de 4000 (99,98 % de rejet) pour le strontium avant et après le lavage. Les deux espèces sont suffisamment bien rejetées par la membrane. L'augmentation du facteur de décontamination du strontium est attribuée à l'échange du strontium pour le calcium présent dans le dépôt d'entartrage à la surface de la membrane.

Acknowledgments

I would like to express my gratitude to Dr. A. Y. Tremblay, Dr. S. K. Sen Gupta, and Mr. L. P. Buckley for their guidance and support. I owe you much.

I would like to gratefully acknowledge the Waste Treatment Centre staff at AECL's Chalk River Laboratories for their assistance throughout the duration of the project: Carson Bramburger, Eileen Burke, Ken Christink, Paul Corriveau, Pat Duff, Paul Faught, Jim Longfield, Sandy McConnachie, Eddie Mielke, Giles Mohns, Larry Neuman, Mike Nixon, Blair Ruhnke, Ralph Sheilds, Joe Slade, Kevin Sullivan, and Bill Tulk. You all helped to make this experience enjoyable. Thank you.

I would like to thank Ron Peori and Steve Wickware. I couldn't ask to work with two better guys.

A thank you also goes out to George Bauernschmitt, Danielle Beaton, Darren Ezerins, Don Gagnon, Henny Hamel, George Hill, Paul Leeson, John "Scotty" MacLean, Helmut Micheal, Gill Patrick, Gary Raddatz, Dave Rose, Ernie Villeneuve and the NRU lab crew.

I could not have made it through these past two years without the support and patience of my family and friends. You know who you are and thank you for putting up with me.

Äiti, thanks for being there. This is for you.

This thesis could not have been made possible without the financial support of the CANDU Owners Group (COG) through Working Party 49.

Nomenclature

A	membrane constant (m/atm/s)
c	molar volume of water (mol/m^3)
C_{Ai}	concentration of solute (mol/m^3 or mol/L)
C_i	concentration of ionic species i (mol/m^3 or mol/L)
D_{ion}	diffusion coefficient of an ion (m^2/s)
D_{NaCl}	diffusion coefficient of an NaCl (m^2/s)
k	mass transfer coefficient (m/s)
k_{ion}	mass transfer coefficient of an ion (m/s)
k_{NaCl}	mass transfer coefficient of NaCl (m/s)
K	equilibrium constant (dimensionless)
K^c	equilibrium constant adjusted for ionic strength effects (dimensionless)
K_{sp}	solubility product (dimensionless)
N_B	solvent flux (mol/m^2/s)
P_g	gauge pressure (atm)
pK	-log K (dimensionless)
pK_{sp}	-log K_{sp} (dimensionless)
PR	product rate of solution (m^3/s)
PWP	pure water permeability (m^3/s)
R	universal gas constant (L·atm/mol/K)
SA	surface area of the membrane (m^2)
T	temperature (K)
T_B	freezing point of water (K)
T_{sol}	freezing point of salt solution (K)
x_{Ai}	mole fraction of solute (dimensionless)
Z_i	charge of species i (dimensionless)
$\Delta\Pi$	osmotic pressure difference between the feed and permeate at the membrane surfaces (atm)
Δp	applied pressure difference between the feed and permeate at the membrane surfaces (atm)
γ_i	activity coefficient (dimensionless)

$\Pi(C_{Ai})$	osmotic pressure of the solute (atm)
μ	ionic strength (dimensionless)
{ }	activity or active concentration (mol/L)
[ ]	molar concentration (mol/L)

subscripts

1	feed
2	boundary layer
3	permeate

units

Bq	SI (metric) unit of radioactivity 1 Bq represents 1 disintegration per second of radioactive isotope

Abbreviations

AD/DC	active drain / decontamination centre
AECL	Atomic Energy of Canada Limited
BCV	bypass control valve
CRL	Chalk River Laboratories
CV	concentrate control valve
DF	decontamination factor
DRL	derived release limit
EDTA	ethylenediaminetetraacidic acid
EDX	energy dispersive X-Ray
FM2	flowmeter
HP	high pressure
IAEA	International Atomic Energy Agency
LP	low pressure
MCCR	Ministry of Consumer and Commercial Relations
MFU	microfiltration unit
PR	product rate
PWP	pure water permeability
NTA	nitrilotriacetic acid
RCV	recirculation control valve
RO	reverse osmosis
SEM	scanning electron microscope
SWRO	spiral-wound reverse osmosis
TFE	thin-film evaporator
TRO	tubular reverse osmosis
VR	volumetric recovery
VRF	volumetric recovery factor
WTC	Waste Treatment Centre
®	registered trademark
™	trademark

TABLE OF CONTENTS

Page

LIST OF TABLES

LIST OF FIGURES

Chapter 1

Introduction

The nuclear industry has been established for over forty years (International Atomic Energy Agency, 1984) and during that time, considerable waste treatment experience has been acquired. This was mainly due to the very strict environmental regulations associated with liquid and solid wastes generated by the nuclear industry. Since radioactive liquid wastes tend to be generated in larger volumes than solid wastes (International Atomic Energy Agency, 1984), the treatment of liquid waste was needed to reduce storage capacity requirements. Thus, more conventional treatment methods were employed in the early developmental stages of nuclear technology. Conventional treatment of radioactive liquid wastes include ion exchange, chemical coagulation and precipitation, and evaporation. Established nuclear facilities all over the world employ one or a combination of these techniques to treat their radioactive liquid wastes. These treatment methods used by various nuclear facilities will be discussed further in Chapter 2.

According to the International Atomic Energy Agency (IAEA), "the basic objective of radioactive liquid waste treatment is to remove radionuclides from the bulk of waste in order to meet the limits for release of radioactivity into the environment and to concentrate the radioactivity into a small volume for subsequent conditioning and disposal" (IAEA, 1994). With increasingly stringent environmental regulations concerning radioactive and non-radioactive release limits, more efficient and cost effective treatment methods are being sought. The

decontamination of waste being the primary concern and decreasing the quantity of waste that must be conditioned before final disposal a close second, membrane technology is coming to the forefront of radioactive liquid waste processing. This is because pressure driven membrane separations tend to be non-selective. Reverse osmosis, ultrafiltration and electrodialysis have emerged as full scale industrial treatment processes (Gutman, 1981). Electrodialysis (an electrically driven membrane separation process) has also been considered as an alternative to conventional treatments.

The Waste Treatment Centre (WTC) at the Chalk River Laboratories (CRL) site utilizes membrane technology and evaporation for the treatment of their low level radioactive liquid wastes. The focus of this thesis is on the spiral wound reverse osmosis (SWRO) system used by the WTC. The SWRO system has been experiencing difficulties with severe declines in permeate flux. The flux decline was attributed to two different causes: concentration polarization and/or surface fouling of the membrane. These causes will be discussed in more detail in Chapter 2.

The concentration of the feed stream poses a risk to the operational lifetime of the membranes because any potential foulants present in the feed stream will be concentrated to high levels. This makes membrane separation different from other more conventional processes. Chemical precipitation methods, ion exchange and evaporation will treat a feed stream of relatively the same chemical composition and concentration. On the other hand, membrane processes operated in batch mode treat a more concentrated and more potentially hazardous feed stream as the run proceeds.

The objectives of this work were the following:

- To determine the optimum crossflow velocity to minimize fouling of the membranes; and
- To develop an effective cleaning procedure to regenerate the fouled reverse osmosis membranes and recover the permeate flux performance.

The first objective was achieved by determining the mass transfer coefficient of the membrane and predicting the boundary layer concentrations caused by concentration polarization. The mass transfer coefficient experiments were conducted with a salt solution of three weight percent using a pilot-scale system. Further experiments were conducted with the pilot-scale system to determine if an optimum crossflow velocity could minimize concentration polarization and fouling during the processing of a typical waste stream treated by the WTC. The second objective was achieved by testing the effectiveness of a three-step cleaning procedure on the fouled reverse osmosis membranes taken from the spiral wound reverse osmosis system in the Waste Treatment Centre at Atomic of Energy of Canada (AECL) Chalk River Laboratories.

Chapter 2

Literature Survey

This chapter summarizes the existing literature that is relevant to processing radioactive liquid wastes by membrane technologies. The characterization of radioactive wastes are described as conventional techniques used in the treatment of radioactive liquid waste water. Three different membrane technologies have been evaluated as possible alternatives to the more conventional techniques. These technologies and actual applications will be discussed. Strategies to prevent permeate flux decline and membrane cleaning methods are discussed in this chapter. The effect of crossflow velocity on the membrane performance is also described. Finally, the past performance of the SWRO membrane system at the WTC is discussed.

2.1 Radioactive Liquid Waste Characterization and Derived Release Limits

Radioactive liquid wastes are produced in all areas of nuclear power operations: ore processing; fuel fabrication; reactor operation; fuel reprocessing; nuclear research; radioisotope production; and radiotherapeutic and diagnostic nuclear medicine techniques used by hospitals (Chauvet and Carley-Macauly, 1981). Characterization of the liquid waste arising from the various nuclear operations is necessary so guidelines can be created for proper handling and treatment. The waste can be classified according to its chemical, physical, radiological and biological properties or even by the half-life of the radionuclides. The IAEA has classified

radioactive liquid wastes according to its specific activity: low level, intermediate level, and high level radioactivity (IAEA, 1984). The liquid waste that will be dealt with in later chapters is classified as low level liquid waste. The specific activities for low level and intermediate level radioactive waste according to the IAEA are listed in table 2.1. These classifications vary from country to country and even within the same country at different nuclear facilities.

Table 2.1: Classification of Liquid Wastes (IAEA, 1984)

Category		Activity (m^{-3}) mixed β/γ -emitters	Comments
	1	< 37 kBq	No treatment required
Low level waste (LLW)	2	37 kBq to 37 MBq	Treatment required; no shielding required
	3	37 MBq to 3.7 GBq	Treatment required; shielding required depending on radionuclide composition
Intermediate level waste (ILW)	4	3.7 GBq to 370 TBq	Treatment and shielding required
High level waste (HLW)	5	>370 TBq	Cooling required before any treatment

There is no international guideline for discharge limits because local environments generally set the maximum permissible release limits. At AECL's Chalk River Laboratories discharge limits are determined internally. The internal administrative controls ensure effluent discharges are well below the derived release limits (Palmer, 1981). According to the report released by AECL and written by Palmer (1981), the derived release limits (DRLs) represent upper limits for routine emissions of radioactivity from CRL to the surrounding environment. Actual releases are much lower than the DRLs and are regulated by administrative levels. The release limits of a few of the radionuclides monitored by CRL are listed in table 2.2.

Table 2.2: Derived Release Limits (DRLs) for Liquid Effluents from CRL (Palmer, 1981).

Radionuclide	DRL	
	GBq/s	Maximum GBq/month
H-3	11.1	2.92×10^{7}
C-14	7.77×10^{-3}	2.04×10^{4}
Co-60	1.66×10^{-2}	4.44×10^{4}
Sr-89	1.517	4.07×10^{6}
Sr-90	5.18×10^{-2}	1.37×10^{5}
Cs-134	2.48×10^{-3}	6.66×10^{3}
Cs-137	3.44×10^{-3}	8.88×10^{3}

These derived release limits were determined by taking various exposure pathways into account and were based on regulatory dose limits for individual tissues and organs set by the International Commission on Radiological Protection. Various exposure pathways (i.e. fish, vegetation, and water ingestion) to workers on site and to the general public were considered.

2.2 Conventional Radioactive Liquid Waste Treatment

The first treatments used to process radioactive liquid wastes consisted of techniques already used to treat normal chemical wastes; including chemical precipitation, ion exchange and in the more difficult cases, evaporation (Simon and Cecille, 1989).

2.2.1 Chemical Precipitation

The basic objective of chemical precipitation is to concentrate the radionuclides into a smaller volume of sludge and reduce the activity of the larger volume of liquid waste so that it meets discharge release limits (IAEA, 1968). Based on the coagulation-flocculation separation

process, this can be achieved by forming precipitates that will entrap radionuclides by co-precipitation or adsorption (IAEA, 1984).

In low level radioactive liquid wastes, radionuclides are usually present in trace amounts; therefore, a carrier is needed. A carrier can be stable isotope of the radionuclide to be removed or of the same chemical family. Barium, calcium or the stable isotope of strontium are carriers of the radioactive isotope ^{90}Sr (Chauvet and Dippel, 1981). The carriers added will be precipitated out with the radionuclide to be extracted from the solution; this is co-precipitation. The addition of an anion or a cation to the waste or a simple pH adjustment will cause a precipitate to form. The anion or cation should be chosen so that a salt with as low a solubility as possible will be formed. The solubility of a compound is affected by the ionic strength of the solution, the concentration of common ions and by the formation of complexes.

The adsorption of radionuclides can occur in two ways; physical adsorption and chemisorption (Laidler and Meiser, 1982). Physical adsorption consists of a layer of ions depositing on a surface and held together by van der Waals forces. Once the surface is completely covered, adsorption stops. With chemisorption, the adsorbed ions are held to the surface by covalent bonds. Once the surface is completely covered, additional adsorption can take place on the new surface creating a crystal which can continue growing.

Chemical coagulation destabilizes the precipitates formed by increasing the rate at which the colloidal particles aggregate (Amirtharaja and O'Melia, 1990). The process of flocculation brings the colloidal particles together to form larger and more easily settleable particles called floc. Thus, two phases that are easily separated are formed; a purified aqueous solution and a wet sludge rich in radionuclides.

The major advantage of chemical precipitation is the low cost associated with the process. Chemical precipitation is suitable for treatment of large volumes of low level liquid wastes that would not be cost effective to treat by evaporation. Chemical precipitation can also treat liquid wastes containing particulates or high salt concentrations that would cause problems with other treatment methods (IAEA, 1984).

A disadvantage of chemical precipitation is that several radionuclides may be present in the waste stream. Some of the compounds may precipitate at different pH values or may even interfere with precipitation making additional treatment steps necessary. Also in the presence of organics, detergents, complexing agents, oils and greases, decontamination factors are low and very inconsistent (IAEA, 1968). Thus, in order for chemical precipitation to be an effective treatment method for radioactive liquid waste, the chemical and radiochemical properties of the waste treated should be relatively constant (Chauvet and Dippel, 1981).

2.2.2 Ion Exchange

By the time ion exchange was first used for processing radioactive liquid waste, ion exchange procedures in water and wastewater treatment were well known (IAEA, 1984). Ion exchange consists of an insoluble resin that has a functional group that can be exchanged with another ion of the same charge in the solution (Gauchon et al., 1981).

Ion exchangers can be divided into two categories; inorganic exchangers and organic exchangers. Each of these groups have their own disadvantages and advantages. The inorganic exchangers can be either natural or synthetic. The limitations of natural inorganic exchangers (i.e. clay minerals or naturally occurring zeolites) are their relatively low exchange capacities and low abrasion resistance. They also partially decompose in the presence of acids and alkalies (Gauchon et al., 1981). Synthetic inorganic exchange resins have been developed with improved stability and higher exchange capacities (IAEA, 1984) but the lower cost of the natural occurring inorganic resins make them attractive from an economic viewpoint.

Organic exchangers are available as synthetic resins. They have been well developed and a wide variety of cation and anion exchangers are available. Thermal and chemical degradation of the organic exchange resins can take place. Radiation can also cause degradation of the resins as well. Another cause for concern is that during the immobilization of spent organic resin, organic ligands could enhance the mobility of the radionuclides, affecting the safety of long term disposal (IAEA, 1994).

In general, ion exchange has certain limitations for the treatment of radioactive liquid wastewater. Monovalent ions, such as cesium, or ions of low atomic number are difficult to remove. This can be overcome by using resins that are specific to the ion (Gauchon et al., 1981). Thus, many different types of resins would be required to remove the large variety of radionuclides present in the liquid waste stream. Many ion exchange columns or beds would be required increasing the cost of the process substantially. Ion exchange cannot effectively treat wastes with activity associated with colloids or non-ionic species (Gauchon et al., 1981). Also, if the resins cannot be regenerated, the spent resin itself becomes radioactive waste (IAEA, 1984).

2.2.3 Evaporation

Evaporation has been proven to have good decontamination and concentration factors in the treatment of liquid radioactive wastes. When high decontamination factors (>1000) are demanded or when discharge release limits are very low, evaporation will most likely be the conventional treatment of choice despite its high energy costs (IAEA, 1994). The only improvements that can be made to evaporation is lower energy costs and improved scaling and corrosion inhibition.

There are some limitations to thermal evaporation. Some liquid wastes cannot be effectively treated by evaporation. The overall decontamination factor of liquid wastes containing volatile radionuclides like tritium is quite low (IAEA, 1994). Wastes containing detergents, surfactants, or high salt concentrations affect decontamination factors as well (Chauvet and Dippel, 1981). Foaming results from the detergent and surfactants and low decontamination factors result from high salt contents. Highly corrosive liquids should also be avoided since the corrosive tendencies of liquid wastes are enhanced by the elevated temperatures employed by evaporators (IAEA, 1994). The formation of precipitates causes scaling which reduces the efficiency of the evaporator making it even more expensive to operate (IAEA, 1994).

2.3 Membrane Technologies for Radioactive Liquid Waste Treatment

With more stringent environmental regulations concerning discharge release limits and disposal costs rising, alternatives to the more conventional methods of treating radioactive liquid waste are being sought. Membrane technology has been shown to have considerable potential to improve the conventional treatments or to replace them completely (Simon and Cecille, 1989). Membrane processes work at ambient temperature, consume less energy and are simple to operate compared to conventional waste treatment technologies (Panicker et al., 1990). Three membrane technologies in particular have shown great promise in the treatment of radioactive liquid wastes. These are electrodialysis, ultrafiltration, and reverse osmosis (Polyakov et al., 1990).

2.3.1 Electrodialysis

Electrodialysis is a membrane process that utilizes ion permeable membranes and an applied electric potential to separate ionic species from an aqueous solution and non-electrolytes.

Electrodialysis has some advantages for the treatment of radioactive liquid wastewaters. The lifetime of electrodialysis membranes is estimated to be nearly seven years, which is twice the operational lifetime of reverse osmosis membranes (Gutman, 1981). It is also claimed that fouling can be kept completely under control. The fouled ion exchange membranes can be fully regenerated to their original state by a high concentration acid or alkali cleaning (Gutman, 1981). Another means of controlling fouling is accomplished by polarity reversal. The reversal ejects any deposits that may have formed on the membranes during operation (IAEA, 1994). Lower operating pressures are associated with electrodialysis resulting in less pump maintenance and costs (Gutman, 1981).

The limitations of electrodialysis are with respect to the characteristics of the feed. Electrodialysis is limited by the conductivity of the diluate and 10 ppm of salt is assumed the limit of that diluted stream (IAEA, 1994). Compared to reverse osmosis processes,

electrodialysis is less economically attractive for both high conductivity and low conductivity feed streams. The energy consumption of electrodialysis is directly proportional to the amount of salt removed; therefore, electrodialysis is economically unfavourable for feed streams with a salt content above 5000 ppm (Gutman and Knibbs, 1989). As the salt concentration decreases in the diluted stream, the electrical resistance of the membrane increases, increasing the energy consumption of the process. Thus, feed streams with salt concentrations of less than 200 ppm are economically unfeasible when compared to reverse osmosis (Gutman, 1981).

Electrodialysis cannot remove any non-electrolytes; therefore, bacteria, viruses, organics, colloids and silica remain in the diluate (Gutman, 1981). Also, the electrodialysis cell stacks are more complicated than reverse osmosis systems and would require more man hours for maintenance and membrane replacement (Gutman, 1981). This would be extremely unfavourable in radioactive surroundings.

2.3.2 Ultrafiltration

Ultrafiltration membranes reject large molecules; generally organic and fine colloidal suspensions but it does not reject ionic or undisassociated compounds with a molecular weight below 300 daltons (Kulkarni et al, 1992). Ultrafiltration is pressure driven and its separation mechanism is based on the size and shape of the solute in relation to the pores of the membrane. As in reverse osmosis, two streams are produced in ultrafiltration: a concentrate (or retentate stream) and a permeate stream.

The advantages of ultrafiltration are that it is selective in its separation; it operates at lower pressures and higher permeate fluxes than reverse osmosis (Panicker et al., 1990). The advantage of its selectivity is that it is less prone to fouling than reverse osmosis. A consequence of the selectivity is that ultrafiltration membranes cannot be used to treat radioactive liquid wastes on their own. It is more suited for treating radioactive effluents when combined with other processes. A combined treatment of chemical precipitation and ultrafiltration (called seed ultrafiltration) would allow removal of a wider range of radionuclides. Cesium could be

removed with nickel ferrocyanide; strontium with barium sulfate; and alpha emitters with iron hydroxide (Gutman, 1981 and IAEA, 1994). This combined process would create larger molecules that can be more easily separated by ultrafiltration and would require less additives than required by chemical precipitation alone.

Although, ultrafiltration is operated at less severe conditions than reverse osmosis, concentration polarization and fouling can take place. Concentration polarization is the build up of rejected species at the membrane surface. The diffusion coefficient of a molecule determines the rate at which it will move away from the surface of the membrane. Since the diffusion coefficients of the molecules rejected by an ultrafiltration membrane are very small due to their large size, the concentration at the membrane surface may be sufficient enough to create a gel layer (Gutman, 1981). This gel layer sets limits at which the ultrafiltration process can be operated (i.e. volumetric recovery, feed concentration and crossflow velocities).

2.3.3 Reverse Osmosis

Reverse osmosis is a process that reverses the natural phenomenon of osmosis by applying a pressure to a concentrated solution in contact with a semipermeable membrane. Reverse osmosis can only take place if the pressure applied is greater than the osmotic pressure of the solution. Pure solvent will then pass through the membrane forming a dilute solution called permeate and leaving on the feed side of the membrane a more concentrated solution called the concentrate or retentate (Weber, 1972).

The major advantage of reverse osmosis is that it is essentially a non-selective process. It rejects ionic solutes and larger macromolecules. The decontamination factor of each specie depends on the size and charge of the ions as well as the composition of the solution (Gutman, 1981). The rejection of monovalent ions is poor when compared to multivalent ions. The rejection efficiency obtained for cesium, a monovalent ion, is expected to be approximately 90 percent and for multivalent ions it is expected to be 95 percent. Reverse osmosis membranes will also reject larger molecules like organics and fine colloidal suspensions. Membrane transport

phenomena is relatively well known and can be found in Mulder (1991), Ho and Sirkar (1992) and Nobel and Stern (1995).

Radioactive liquid wastes originating from decontamination solutions, floor drainage and laundry wastes contain a wide variety of radioactive contaminants and are well suited for non-specific separation processes like reverse osmosis (Gutman, 1981). There appears to be little published about the irradiation of reverse osmosis membranes, although Gutman (1981) did state that solutions containing 10 TBq/m^3 could be safely treated. However, there is some danger of the radioactivity depositing on the membrane. The close proximity of the irradiating species to the membrane would considerably increase the dosage received.

A disadvantage of reverse osmosis is that pretreatments are required to reduce the amount of suspended solids, organics, iron, microbes, and potential scaling compounds in the feed stream if not to eliminate them completely (Lueck, 1995). The pretreatments required can be complex: coagulation and sedimentation, filtration, and dosing with acids and anti-scaling agents (Gutman, 1981). These pretreatment processes can create more waste streams. Without such pretreatments, severe permeate flux declines can occur.

2.4 Case Studies of Low-Level Radioactive Liquid Waste Treatment

In this section, case studies of the various low-level radioactive liquid waste treatment methods described in sections 2.2 and 2.3 will be presented.

Sebesta et al. (1993) studied the possibility of treating low/intermediate level radioactive liquid wastes with various types of composite ion exchangers. The removal of radiocesium, radiocobalt, and radiomanganese were tested with NiFC-PAN, NaTiO-PAN, MnO-PAN, M315-PAN and Na-4-PAN composite exchangers. The suffix refers to a new preparation method for the composite ion exchangers by using a modified polyacrylonitrile (PAN) as a binding polymer. Radiocesium was removed the most effectively by the NiFC-PAN ion exchanger giving

decontamination factors of 1000. Radiocobalt removal was more complicated. The decontamination factor was strongly influenced by pH and by the addition of carriers.

Berry et al. (1988) proposed improvements to the treatment of slightly active liquid effluent by using precipitation and ion exchange processes. The typical waste concentrations of ^{90}Sr varies between 500 kBq/m^3 and 8 MBq/m^3 and the concentration of ^{137}Cs varies between 200 kBq/m^3 and 1 MBq/m^3. The major chemical species present are calcium, magnesium, and sodium bicarbonate. The original process consisted of a strong-acid cation exchange process with regeneration of the spent resin. The treatment process was improved by the addition of a clarifier/precipitator and chabazite ion exchange columns. The new process flowsheet consisted of chabazite zeolites for the removal of ^{137}Cs, clarification/precipitation of calcium and magnesium (a portion of the ^{90}Sr precipitates as well), filtration, and finally strong-acid cation exchange resin for the removal the remaining ^{90}Sr. Additional studies have gone into evaluating the optimum precipitation process and into alternative flowsheets. Two precipitation processes were tested and their effluent composition and sludge characteristics were evaluated. These include caustic/soda ash precipitation and a scavenging precipitation method conducted with caustic and ferrous sulfate. The caustic/soda ash process performed best when the non-radioactive concentration of cations was minimized. The scavenging precipitation process could adjust to fluctuations in the feed composition. Iron was found to enhance the precipitation of calcium and magnesium when contaminants (i.e. detergent) are found in the feed stream. The ferrous sulfate produced a fluffy, high volume sludge that was difficult to dewater. Three additional flowsheets were considered and looked at eliminating the need for an evaporator.

The treatment of radioactive liquid waste effluents by continuous ion exchange was studied by Ryabchikov et al. (1975). The KU-2-8 cation exchange resin is continuously moved through the washing, regeneration and rinse stages by pulsation flow. Residual activity was found in the treated solution. Radionuclides present in the solution as anions, complexes or as

compounds could not be removed; however, further treatment by an anion exchange unit further purified the solution to an acceptable level. Regeneration of the resin using a 4-5 mol/L HNO_3 solution produced an increase in concentration (by a factor of 2.5) and a reduction in the volume (by a factor of 1.5) of the waste.

Ryabchikov et al. (1983) improved upon their earlier work discussed above with the continuous cation exchange unit by proposing a continuous mixed ion exchange bed to replace individual anion and cation exchange columns. With the volume ratio of the anion (AV-17-8) to cation (KU-2-8) exchange resin at 1:1, regeneration of the cation exchanger by HNO_3 in excess of 200 percent and the regeneration of the anion exchanger by NaOH in excess of 50 percent, complete extraction of the cationic species present in the solution was achieved. However, the removal of some radionuclides in anionic or complex form was not complete. Increasing the excess regenerate of the anion exchange resin to 180 percent and increasing the ratio of anion to cation to 2:1 led to better extraction of the anionic constituents in the solution.

A proposed facility for the treatment of low and intermediate level wastes arising from a nuclear power plant in Russia is described by Kutscher et al. (1993). The concentration of the liquid wastes consists of preheating the waste and pH adjustment before treatment by thermal evaporation. A final addition of chemicals to further increase the concentrate. The solids arising from the evaporator are immobilized by cementation. Unfortunately, no details of the process are included.

A preliminary plan for the treatment of aqueous mixed low-level radioactive wastes at the Argonne National Laboratory was proposed by Vandegrift et al. (1993). The wastes also contain hazardous metals and tend to be highly acidic or basic making the waste corrosive. The objective of the treatment was to convert the mixed aqueous waste to a low level waste and concentrate the hazardous metals to a solid. In general, the waste will be neutralized and the toxic metals will be

precipitated and filtered. The filtrate will be sent to an existing evaporator. The sludge will be disposed after being mixed with sorbents. The precipitation method was chosen because of its simplicity and its inexpensiveness. Wastes that could not be treated by the precipitation method were wastes containing ethylenediaminetetraacidic acid (EDTA), citric acid or organic complexing agents. It was concluded that the most effective chemical treatment for the removal of toxic metals is by sodium sulfide and calcium hydroxide. This treatment precipitates all the hazardous metals found in the waste except barium, arsenic and hexavalent chromium.

Results of a pilot-plant electrodialysis system for the treatment of acidic mixed radioactive liquid wastes were presented by Del Debbio et al. (1986). Prior treatment by ion exchange proved unfeasible for nitric acid concentrations greater than 0.01 N due to the need for frequent regeneration. It was found that greater than 90 percent of both ^{90}Sr and ^{137}Cs were removed. If higher removal efficiencies are required, it would be possible to treat the diluate further by ion exchange since most of the nitrate and acid had been removed by the electrodialysis system. Low removal efficiencies of mercury was found because it was suspected that it was present in the complexed form of mercuric chloride. Fouling of the membranes was observed during experimentation but the operational lifetime is still estimated to be three years.

Chmielewski and Harasimowicz (1995) studied seeded ultrafiltration for the treatment of low level radioactive effluents. In addition to containing radionuclides, the waste contained solid particles, emulsions, and detergents. For this method to be effective, the proper ligand must be chosen for complexation to take place. It was found that a ligand concentration to ion concentration of 5 to 20 times higher was required. Mixing for four hours and allowing the mixture to stand for 16 hours was necessary for sufficient complexation to take place. For seeded ultrafiltration to be an effective treatment, all of the radionuclides must have a high affinity for the ligands and the pH, temperature and concentration of alkaline metal salts must affect the complexes in a similar fashion.

Koenst and Roberts (1978) had evaluated the treatment of low level radioactive liquid wastes by ultrafiltration. It was determined that the retention of the membranes is a function of the contaminants themselves; whether they are ionic, polymeric, colloidal or adsorbed onto suspended solids. It was found that ionic species were not as readily retained.

Freer et al. (1996) conducted membrane pilot-plant studies to replace clarifloculation and filtration as the primary treatment of radioactive liquid wastes. Centrifugal, hollow fiber, and tubular ultrafiltration was well as reverse osmosis membrane technologies were evaluated. The final process flowsheet consisted of tubular ultrafiltration as a pretreatment to reverse osmosis. The tubular ultrafiltration system was chosen over the hollow fiber ultrafiltration unit as a pretreatment step because the tubular system was less prone to fouling, could handle variations in the feed quality, and its simple operation. The centrifugal ultrafiltration system was used to further concentrate the reject stream from the tubular ultrafiltration system. This treatment process demonstrated the ability to meet current and projected discharge limits while reducing waste and chemical dose requirements.

2.5 Membrane Fouling

Several causes of fouling or irreversible permeate flux decline are given by Barger and Carnahan (1991): colloidal particulates depositing onto the membrane surface; slightly soluble organic or inorganic compounds precipitating onto the surface of the membrane; biological growth accumulating within the process and onto the membrane; the membrane surface undergoing a physical or chemical reaction with a feed water constituent; and organic or inorganic compounds flocculating to form large, insoluble polymers that deposit onto the membrane surface. Models to assess the effects of deposition of foulants and concentration polarization have been proposed. New research into the post-treatment of membranes by various

solvents and their effects on permeate flux and rejection efficiency will be discussed. Other methods of minimizing the effects of concentration polarization will also be presented.

Sethi and Wiesner (1995) modeled the performance and cost of crossflow ultrafiltration as a function of particle size distribution. Their work included Brownian diffusion, shear-induced diffusion and bulk convection mechanisms to predict the thickness of the fouling layer on the membrane and its permeate flux. The particle sizes studied ranged from 0.001 μm to 10 μm. A maximum thickness in the fouling layer and a minimum permeate flux was found in the 10^{-1} μm size range. Below the 10^{-1} μm range, the Brownian diffusion increases which results in a decrease in the fouling layer thickness and an increase in permeate flux. Above the 10^{-1} μm range, shear effects become significant which decreases the fouling layer thickness and increases the permeate flux.

Wijmans et al. (1985) showed that the permeate flux of a solution is lower than that of the pure solvent due to the effects of concentration polarization. Theoretically and experimentally the concentration polarization effects could be described equally well by the osmotic pressure model and the boundary layer resistance model.

Bader and Veenstra (1996) tested various concentration polarization models including the Sherwood correlation model, the original film theory model, and the modified film theory model for an ultrafiltration process. The objective of this work is to improve concentration polarization models so that process design and operation parameters can be optimized, thereby, minimizing the effects of concentration polarization (i.e. permeate flux decline). The major limitation of the Sherwood correlation model is that it is difficult to select the appropriate correlation for the constants used in the model for a specific membrane system. In addition to this, the correlations are derived from heat transfer and extended to mass transfer applications. A questionable

assumption of the original film model is the actual rejection efficiency is constant and independent of solute concentration at the membrane surface. The modified film theory model accounts for the change in rejection efficiency with solute concentration at the membrane surface and it combines the effect of diffusion and convective mechanisms in terms of the mass transfer coefficients. The experimental data best fit the modified film theory model especially under turbulent conditions.

Field and Aimar (1993) proposed a model that included both the effects of osmotic pressure and variations in viscosity caused by concentration polarization during ultrafiltration. The model presents an ideal flux as the permeate flux that would occur in the absence of fouling. From this work, it was concluded that the viscosity change in the boundary layer has more importance than the changes in diffusivity in the boundary layer.

Cohen and Probstein (1986) modeled colloidal fouling of reverse osmosis membranes by ferric hydroxide in laminar flow and compared it with their experimental results. The initial fouling occurs quickly by means of a first-order reaction within the boundary layer and is followed by fouling that grows much slower and linearly with time. If the colloidal ferric hydroxide is destabilized by an increase in pH, the fouling rate was not found to increase linearly with concentration. The rate of fouling for destabilized colloids was found to be an unsteady phenomenon dependent on feed foulant concentration, residence time, and degree of flocculation of the colloids upon deposition. Fouling was found to be preventable if the system was operated at a pH that induced a stable colloid and if the system was operated below a threshold permeation velocity determined empirically.

Amjad (1988) and Smith and Huilin (1992) discussed the effectiveness of a number of different commercial anti-scalants in the inhibition of mineral scale formation. Amjad (1988) related his work to reverse osmosis processes. The effectiveness was judged according to the

length of the induction period before crystallization occurs and the rate of crystallization once it has begun. The presence of anti-scalants increased the induction period but did not have any affect on the rate of crystallization. The various parameters studied were the anti-scalant concentration, anti-scalant molecular weight, temperature, pH, and the presence of ferric and zinc ions.

Luu (1994) tested various commercial anti-scalants for inhibiting the formation of $CaCO_3$ and $CaSO_4$ scale. Unfortunately, the fouling test solutions resulted in the formation of various scales regardless of which anti-scalant was used giving inconclusive results. This was attributed to the multi-component test solution forming unpredictable precipitates.

Zeiher (1996) compared commercial and developmental products that are said to control scale and deposition of corrosion products on thin-film reverse osmosis membranes. Common approaches to scale control involve pH adjustments. Sulfuric acid is generally preferred because of its low cost but this is not recommended as iron impurities are often present and may cause fouling. Eleven different products were tested for their ability to control scale and iron oxide deposits. A field test was also conducted on a site with membranes traditionally prone to iron oxide fouling. Two products were singled out for their superior performance in controlling an iron/sulfate scale and a carbonate scale.

Kronmiller (1993) suggested that foulants are formed in layers whether they are inorganic or organic and an understanding of how they form is fundamental in developing pretreatment and cleaning methods. The contact angle of organic acids, oils and tars on the membrane surface effects the adhesion of the foulants to the surface. Kronmiller developed a product that claims to modify the hydrophilicity of the membrane surface so that water is absorbed onto the membrane surface facilitating the transport of water through the membrane.

Reitz (1989) described a computer program developed to evaluate the water chemistry and scale prevention of reverse osmosis desalination systems. The program calculates optimum volumetric recovery rates at which the precipitation of salts will be minimized. The precipitation of salts is kept under control at high volumetric recoveries by the addition of an appropriate amount of a commercial anti-scalant, FLOCON 100. The calculations required to determine the proper anti-scalant dosage are calculated by the computer with respect to the initial analysis of the feed water and the desired volumetric recovery.

Comstock and Durham (1993) developed an apparatus for determining the optimum concentration of a colloidal anti-foulant required and a proper cleaning schedule for a reverse osmosis liquid purification system. A number of different anti-fouling agents can be evaluated for the same feed stream as well as optimum dosage requirements by zeta potential measurements. The cleaning frequency can be predicted with a test cell consisting of a cleaning frequency membrane having a high permeation. The change in the rate of permeate flow of the solution to be processed gives an indication of the operational time permitted between cleanings.

Mukherjee et al. (1994) proposed a method of modifying the surface characteristics of FILMTEC® thin-film composite SW30HR reverse osmosis membranes to prevent fouling by exposing the membranes to various concentrations of hydrofluoric and fluosilicic acid for various time periods. Tests performed with a 0.5 wt% salt solution showed improved permeate flux without any affect on the rejection efficiency for the membranes soaked in either acid bath; and in some cases, an improved rejection efficiency was observed as well. It was determined that the partial fluorination of the membrane surface which increases its hydrophilicity is the cause of the increased permeate flux. The acid baths were found not to affect the membrane lifetime.

Mukherjee et al. (1996) continued to study the improved performance of chemically treated membranes. Two commercially available aromatic polyamide membranes were again the focus

of their work; one being a low pressure membrane and the other a high pressure membrane. Both types of membranes were soaked in solutions of hydrofluoric acid, fluosilicic acid and isopropyl alcohol in water. Again, significant increases in the permeate flux was observed without any decrease in rejection efficiency and in most cases the rejection efficiency increased as well. In the case of the hydrofluoric and fluosilicic acids, the increase in rejection efficiency results from the formation of carboxylic and amidic groups on the membrane surface. This increases the permeate flux by increasing the hydrophilicity of the membrane as well. The increased permeate flux and rejection efficiency of the membranes soaked in isopropyl alcohol results from the limited solvency power of the alcohol. The limited dissolution of the membrane should cause an increase in permeate flux but decrease the rejection efficiency. The more dense high pressure membrane tended to give better permeate flux improvement than the lower pressure membranes.

The chemical treatment of reverse osmosis membranes for enhanced performance was continued by Kulkarni et al. (1996). Two aromatic polyamide based membranes were soaked in hydrofluoric acid solutions. One type (TFCL-LP from UOP Fluid Systems) was manufactured by a process patented by Cadotte (Kulkarni et al., 1996). The composition of the other membrane, DESAL3 from Desalination Systems, has not been made public. The permeate flux and rejection efficiency showed good improvements for the TFCL-LP membrane but no improvement was observed for the DESAL3 membrane. Scanning electron microscope analyses of the membranes revealed that the TFCL-LP surface has a ridge and valley structure where the DESAL3 surface is packed with spherulites. The ridge and valley structure is more susceptible to attack by the hydrofluoric acid causing thinning of the polymeric network. The number of pores are increased without increasing the size of the pores; thus, the permeate flux and rejection efficiency increase.

Modifying the surface of the membrane by chemical treatment can minimize the adsorption of foulants onto the membrane surface; but once a foulant layer is formed, this modified surface

is covered and rendered useless. Kennedy et al. (1974) had done some preliminary work on pulsed feed flow to improve the permeate flux by reverse osmosis. Winzeler and Belfort (1993) went into greater detail and studied the effect of unsteady flows on the depolarization and defouling of ultrafiltration membranes. Various methods of creating unsteady flow were tested; including, flow over rough surfaces, pulsation flow, and flow under conditions which promote instabilities or vortices. The latter appeared to be the most effective in depolarizing solute accumulation near the membrane surface. Unfortunately, pulsation flow and flows that create a large pressure drop are not feasible for reverse osmosis systems since the pumping energy requirements would be extremely high.

Levy and Earle (1994) tested the performance of open channel membrane configurations and membranes with channels formed by spacers for flux and energy requirements. The membranes with the mesh spacer performed better demonstrating higher flux and lower pumping costs. The open channel configurations require more pumping energy to maintain turbulent flow. The channel spacers helps minimize concentration polarization by inducing turbulent flow but there is concern when suspended solids are present in the feed stream. Suspended solids increase the resistance to flow resulting in higher pumping costs. The test solutions consisted of sucrose in deionized water at various viscosities.

Jonsson and Tragardh (1990) reviewed the influences of various factors that cause fouling of ultrafiltration membranes. These factors included the membrane material, pore size, presence of surfactants, pH and ionic strength of the solution. Membranes made of hydrophobic material tend to foul more easily than membranes made of hydrophilic material. At high pH, it was found that membranes made of the same material with varying pore sizes had similar permeate fluxes but as the pH decreased to pH values below the isoelectric pH of the solution, the permeate flux decreased. The membrane with the smallest pore size had the greatest flux decline. The membrane with the largest pore size had relatively no change in permeate flux with the decrease

in pH. It had been found that hydrophobic solutes are adsorbed onto the membrane more easily than hydrophilic solutes. A combination of surfactants and cationic polymers have also been known to irreversibly foul negatively charged membranes. The pH affects the solute-membrane and solute-solute interactions which may lead to more fouling and more densely packed foulant layers. As the ionic strength of the solution increases, less molecules may be retained by the membrane.

Barger and Carnahan (1991) attempted to predict the fouling rate of a polyurea thin-film composite membrane by calcium sulfate. Their method of predicting membrane fouling incorporates the resistance model and their experimental results obtained from concentration polarization tests conducted with sodium chloride. The permeate flux resistance term is the sum of all of the known and unknown individual resistances. One of these resistances include the resistance due to a deposition layer.

Buckley et al. (1987) discussed specific case studies on the causes of reverse osmosis fouling. When a pilot-scale study to test textile waste streams by reverse osmosis was conducted, it was discovered that the rapid fouling of the membranes was caused by the corrosion of 304 grade stainless steel parts. Iron, chrome and nickel had fouled the membrane. Replacement of the offending parts by upgraded steel alleviated the problem. In another case, a calcium hydroxide flocculation and crossflow microfiltration pretreatment resulted in the fouling of the reverse osmosis unit downstream. Oxalic acid was precipitating out as calcium oxalate. The pretreatment was improved by removing oxalic acid, operating at pH values below the ionization of oxalic acid, and removing the excess calcium with soda lime. In general, complete analysis of the feed stream is required with particular attention being paid to the species low in concentration as these species are frequently responsible for the fouling of the membranes. Chemical speciation programs become useful in obtaining a better characterization of the

solution at different pH operating values and operating volumetric recoveries. With this information, effective pretreatment strategies can be implemented.

Colloidal fouling of reverse osmosis membranes was studied by Elimelech and Zhu (1994). The tests concluded that pore blockage of the membranes was not the primary fouling mechanism since the colloidal fouling could be reversed by chemical cleanings. The fouling was observed under high, moderate, and low ionic strength conditions and the charge of the membrane and of the solute were taken into consideration. Under high to moderate ionic strength whether the membrane and solute are oppositely or similarly charged, the deposition of the solute onto the membrane is favoured. A thick fouling layer is expected to form resulting in a decrease in permeate flux and rejection efficiency.

Amjad et al. (1991) reviewed the various causes of permeate flux decline and presented cases and prevention techniques for each. The various causes discussed include the following: scaling by sparingly soluble salts; iron, aluminum, and manganese oxide/hydroxide fouling; biological fouling; and fouling by suspended solids and colloids. When permeate flux decline is observed, it is best to conduct a complete examination of the deposits on the membrane surface to determine the appropriate pre-treatment required.

Pervov (1991) reported on work done to test the efficiency of methods for inhibition of calcium sulfate and calcium carbonate scale on spiral wound cellulose acetate membranes. Pervov claims that spacer present in the spiral wound membranes allow fouling to take place since the contact sites between the spacer and the membrane provide local resistance to flow. This lowers the flow rate and increases the concentration polarization in those areas. It was found that both compounds precipitate out of solution during reverse osmosis despite that the solubility limit of each compound had not been exceeded. The inhibitors tested did not eliminate fouling but did delay the crystallization rate, even though precipitation still occurred below the

solubility limit of calcium sulfate and calcium carbonate. It was also found that an increase in the salinity of the solution decreased the fouling rate.

2.6 Membrane Cleaning Techniques

Membrane fouling is the major limitation of membrane processes causing permanent flux decline, rejection efficiency losses, high pressure drops and excessive operating costs due to the cost of chemical cleaning solutions and membrane replacement. Despite effective pretreatments, fouling of membrane modules will occur at some point in time and to some extent. Ever since membranes have been used on an industrial scale, research has gone into identifying the foulants and removing them from the membrane surface with hopes of eliminating the problem of fouling completely.

Warren and Comstock (1995) suggested various cleaning procedures for different types of foulants. Inorganic scalants, biological foulants, organics, colloids, metal hydroxides, and chemical precipitates are typical reverse osmosis membrane foulants. Sequential cleanings of different solutions are recommended because reverse osmosis membranes are rarely fouled by one foulant alone. Tips on how to identify the probable type of foulant are given and a cleaning recipe is given for each type of foulant. Cleaning operations, conditions, and equipment for optimum results are suggested as well.

Leger and Hawker (1987) investigated the elemental composition, mineral composition, and physical structure of the foulants formed from treating surface water as a potable water supply. Membranes from eight different water treatment plants were studied. Membrane autopsies were performed to help identify the foulants and two different types of fouling were observed. One foulant type was a deposit that was easily removed by wiping with a rubber squeegee and the other type was thickly encrusted on the membrane and could not be easily removed. X-ray fluorescence and diffraction, infrared spectroscopy, total elemental and selective

dissolution analyses identified the easily removable foulant as organic material, colloidal aluminum layer silicate clay minerals, quartz, iron, and zinc compounds. The thickly encrusted foulant was identified as a calcium carbonate scale. Recommendations for further research into preventing fouling and removing the foulants were given.

Sayed Razavi et al. (1996) recovered the permeate flux of fouled negatively charged polysulfone ultrafiltration membranes by a four-stage cleaning procedure consisting of a wash with sodium hydroxide, protease detergent, and sodium hypochlorite followed by flushing with water. A hydrochloric acid wash was tested but found to be ineffective. The foulant layer consisted of lipids and a protein-polysaccharide matrix resistant to surface shear stresses. The cleaning with the protease detergent gave the highest increase in permeate flux. The combined treatment of the caustic solution and detergent removed a significant amount of the foulant. The caustic solution is suspected to weaken the ionic bonds of the foulant deposit and making the foulant layer more porous. This allowed the detergent to be more effective. The sodium hypochlorite acted as a swelling agent allowing the foulants within the membrane pores to become dislodged and flushed out.

Amjad (1989) reviewed the most common types of membrane fouling and the various possible techniques to identify the foulants. The importance of understanding the morphology of the foulants is fundamental in selecting the proper cleaning solution. The various factors that must be taken into consideration are discussed as well as the foulant removal mechanism of the various cleaning solutions.

Hickman (1991) reviewed various foulants and their effects on membrane performance. He also recommended cleaning techniques for membranes fouled by one type of foulant and for membranes fouled by a multi-component system. The types of foulants discussed include colloidal, organic, and biological fouling, as well as, scaling and precipitation on the membranes.

In most cases, the best cleaning technique consists of a two step cleaning method of a low pH cleaner to dissolve iron and other metal oxide and carbonate scales followed by a high pH cleaner to remove organic and colloidal fouling.

Siler (1992) compared low pressure and high pressure reverse osmosis treatment methods with NaOH and FILMTEC Alkaline Cleaner. The membrane was fouled purposely with a solution containing salt, sparingly soluble metals, and bacteria. Cleaning by neither NaOH nor the FILMTEC cleaner alone achieved a complete restoration in permeate flux or rejection efficiency. The best regeneration was achieved by NaOH followed by the FILMTEC cleaner resulting in permeate fluxes equivalent to the permeate fluxes observed before fouling of the membranes took place. The decontamination factor was also improved with this cleaning sequence. It is suggested that the NaOH was able to breakdown the bonds between the colloidal inorganic hydroxides and the biological foulants on the membrane surface allowing the FILMTEC cleaner to assault the biological foulants. Cleaning in the reverse order renders the FILMTEC cleaner redundant since the NaOH is required to first break up the inorganic constituents.

Ebrahim and El-Dessouky (1994) evaluated the effectiveness of the manufacturer's recommended cleaning solution against the effectiveness of commercial membrane cleaning agents for reverse osmosis membranes fouled during the treatment of seawater. One of the membranes tested was a spiral-wound FILMTEC SW30HR membrane module. The manufacturer's recommended cleaning solution of EDTA and NaOH resulted in a decreased permeate flux and a decreased salt rejection efficiency. The commercial cleaning agent, Floclean AES 510, resulted in a slight improvement in permeate flux and an increase in salt rejection efficiency. These results are considered preliminary but the authors believe that the commercial agent, Floclean AES 510, was generally more effective than the cleaning solution recommended by the manufacturer.

Ebrahim (1994) presented a review of physical, chemical, and physio-chemical cleaning techniques of reverse osmosis membranes. The physical cleaning methods discussed include forward flushing, back flushing, permeate back pressure, vibration, air drain and water refill, air sparge, CO_2 back permeation, and sponge ball cleaning. The physio-chemical cleaning methods involve physical cleaning methods as well as chemical cleaning agents for increased effectiveness. The chemical cleaning methods discussed include manufacturer's recommendations as well as commercial cleaning products. Regeneration methods of reverse osmosis membranes and alternative methods of identifying membrane foulants without the need for a destructive autopsy are outlined as well.

Nilsson and Hallstrom (1991) attempted to identify whether the fouling mechanism of protein on an ultrafiltration membrane was caused by pore blockage or by cake formation. This was done by plotting the total fouling resistance versus the resistance of the pore blockage. The y-intercept (when the pore blockage resistance is equal to zero) should give the cake layer resistance if the cake layer formation occurred first. It was found that the principal cause of the flux reduction was due to pore blockage. An attempt to pretreat the membrane with ethanol was made resulting in slower permeate flux declines but behaved similarly to an untreated membrane after the pretreated membrane fouled.

Lindau and Jonsson (1994) tested five different cleaning agents on ultrafiltration membranes that had been fouled by oily wastewater. The membranes treated wastewater containing 150 mg/L of oil and were cleaned with a variety of acidic and alkaline cleaning agents. The acidic cleaning agents resulted in a much higher pure water permeate flux which declined quickly with respect to time. The alkaline cleaning agents increased the pure water flux but not to the same extent that the acidic cleaning did. Although, the permeate flux increase observed after cleaning with the alkaline solution remained constant over time. The acidic

cleaning agents may have dissolved some inorganic compounds embedded in the organic foulant layer creating a more porous foulant layer. This would give the high temporary pure water flux increase. As the pressure was applied during the pure water permeability tests, this porous foulant layer would become compacted resulting in a decline in permeate flux.

In addition to the work Pervov (1991) conducted with scale inhibition discussed in section 2.5, he also developed a method to determine the optimum cleaning solution and schedule for calcium sulfate and calcium carbonate scale on cellulose acetate membranes. The cause of the scaling and the ability of the cleaning agent to dissolve the scale must be determined. A solution of citric acid and ammonia was circulated through the fouled membranes until the calcium concentration in the cleaning solution reached a constant value. This was repeated with a fresh cleaning solution until the calcium concentration in the cleaning solution did not increase further. This was repeated until no significant amount of calcium was removed from the membrane surface. Each cleaning cycle removed less and less of the scalant which suggests that various layers of scalant are present on the membrane surface with different structures, densities, and affinity for the cleaning solution. A plot of the cleaning solution consumption and the time interval between cleanings gives the minimum cleaning solution required.

2.7 EDTA versus NTA

Traditionally, EDTA had been used as a chelating agent in membrane cleaning methods and had even been incorporated into commercial membrane cleaning product formulas. Unfortunately, chelating agents such as EDTA solubilize heavy metals and radionuclides; thereby, remobilizing the complex during disposal. This may allow the substance to leach out of the disposed solid waste form into the environment. EDTA has also been found in relatively high concentrations in 15 year old radioactive waste demonstrating its persistence in the environment (Means et al., 1978). Due to this concern about the possible environmental implications of EDTA, more environmentally sound alternative chelating and complexing agents

are being sought for use in membrane cleaning solutions. Nitrilotriacetic acid (NTA) is one of those chelating agents. A comparison of the complexing power and degradation rates of EDTA and NTA, as well as their remobilizing abilities of heavy metals and radionuclides is discussed.

Means et al. (1980) studied the relative degradations of three chelating agents, including EDTA and NTA, under several conditions to determine if any of the chelates degraded to a more significant extent than the others. This would help determine if any of the chelates are superior from an environmental view point. The experimental set up allowed the researchers to determine the biodegradation rates and non-biodegradation rates (including photodegradation, chemical degradation and sorption) under various conditions. It was found that for all of the chelates studied, the presence of nutrients and oxygen accelerates degradation. Degradation caused by photolysis was insignificant for both EDTA and NTA. The short-term overall degradation of EDTA exceeded that of NTA but NTA degraded to a higher degree than EDTA over the long term. In the long term (12 to 15 years), 99.5 to 99.85 percent of the NTA had degraded compared to 92.0 to 99.0 percent of EDTA. The total chemical degradation and adsorption of NTA was slightly higher than EDTA. Means et al. came to the conclusion that EDTA degrades at a slower rate than NTA under most circumstances.

Bolton et al. (1993) studied the biodegradation of several chelating agents, including EDTA and NTA, in surface soil and various types of subsurface sediments. NTA was found to be the most biodegradable where EDTA was found to be the most persistent of the chelating agents studied. It was also found that the heavy metal forms of the chelates, such as Cd-NTA or Ni-EDTA, had a much slower degradation rate than the Ca, Fe, or H form of the chelates.

Egli (1992) reviewed the biodegradation of EDTA and NTA in laboratory and natural environments. The different strains of aerobic bacteria that can biodegrade each chelating agent were identified as well as their biochemistry of degradation. In the laboratory, EDTA was quite

easily degraded but in sewage treatment plants and in the natural environment, EDTA tends to be quite persistent. Studies in Switzerland indicate that EDTA does not degrade as quickly as NTA in natural environments (Egli, 1992). In 1992, higher concentrations of EDTA have been found in Swiss rivers than NTA, despite the fact that EDTA has been largely replaced by NTA in laundry detergents since 1986. Egli also states that the heavy metal ion complexing power of EDTA being a few orders of magnitude higher than that of NTA, results in a higher possibility of remobilization of the heavy metals into the environment.

Tunay and Kabdasli (1994) studied the effect of EDTA, NTA, and succinic acid on heavy metal precipitation. EDTA, NTA, and succinic acid were selected for their respective strong, medium, and weak complexing powers. Calcium was used as a binding agent for the ligand to free heavy metals. It was determined that precipitation by high pH can be obtained if sufficient amounts of calcium bind to the ligand freeing the heavy metals. The predictive concentration diagrams involving the heterogeneous equilibria could be used to help determine optimum operating conditions for complexed metal precipitation.

Toste (1992) studied the degradation of complexing and chelating agents by γ-irradiation by ^{60}Co. The degradation of EDTA and NTA were observed at a dose rate of 75 000 R/hr and a temperature of approximately 90°C. EDTA was found to be 77.5 percent degraded and NTA was found to be 66.7 percent degraded after 100 hours of exposure. The degradation rate of EDTA was found to be exponential where the degradation rate of NTA appeared to be linear. The susceptibility of a chelating agent to degradation is affected by their structural and chemical properties which can be altered by the presence of cations. Cations bind differently to different chelating agents; therefore, NTA may be protected to some degree by the cations present in solution. Degradation was found to be affected by pH, metal ion concentration, temperature and radiation dosage.

Means et al. (1978) discovered that EDTA was responsible for the migration of ^{60}Co from intermediate-level liquid disposal pits at Oak Ridge National Laboratory. The distribution coefficient of cobalt in the shale decreases by several orders of magnitude in the presence of EDTA, reducing the adsorption capacity of the shale. No other chelating agents were detected. Although, if NTA had been present in the waste originally, it was not expected to be found because of its high biodegradability. The use of EDTA in decontamination operations is questioned as its powerful complexing power contributes to the mobilization of radionuclides. NTA was named as a suitable substitute for EDTA because of its high biodegradability and relatively strong complexing power (Means et al., 1978).

2.8 Effect of Crossflow Velocity on Membrane Performance

The crossflow velocity is known to influence various parameters that affect the performance of membranes. It can affect the concentration polarization layer which in turn affects the mass transfer coefficient, permeate flux and rejection efficiency.

Knibbs (1984) and Ramamurthy et al. (1993) investigated the effect of crossflow velocity on the permeate flux. Ramamurthy et al. found that the permeate flux increased with increasing velocity. This was attributed to the higher mass transfer coefficient obtained at the higher crossflow velocities giving a thinner concentration polarization layer. Knibbs did not find any direct correlation between the permeate flux and crossflow velocity but did estimate the fouling layer to decrease with increasing crossflow velocity. Winfield (1986) mentioned that fouling can be minimized by maintaining a satisfactory crossflow velocity.

Bodzek and Konieczny (1994) mathematically modeled the ultrafiltration of latex effluents which helped determine the influence that the crossflow velocity has on the permeate flux rate. It was found that the crossflow velocity notably affects the permeate flux. The permeate flux

increases with an increase in crossflow velocity. There is no apparent effect on the rejection characteristics of the membrane by the crossflow velocity.

Gaddis (1992) studied the effects of crossflow velocity and pressure on ultrafiltration flux. A model is proposed correlating pressure, concentration and surface shear (which is directly related to crossflow velocity) on the permeate flux. The model is only applicable to pre-gel conditions. In laminar flow, the surface shear is said to be directly proportional to the mean velocity across the membrane surface to some exponent. The concentration of the solution will govern the value of the exponent. In turbulent flow, the surface shear is directly proportional to the square of the mean velocity multiplied by a friction factor. Experimental work was found to be in agreement with the model.

2.9 Published Literature on AECL's CRL Waste Treatment Facility

In this section, the published literature on the operation and performance of the WTC at AECL's CRL site will be discussed. Specific attention will be drawn to the spiral-wound reverse osmosis (SWRO) system. The composition of the waste stream processed by the WTC will be described. A general overview of the WTC will be given. The operational difficulties experienced with the SWRO system will be discussed as well as their current SWRO membrane cleaning methods.

2.9.1 Composition of Active Drain/Decontamination Centre Waste

At present, two radioactive liquid waste streams produced at the Chalk River Laboratories site are being processed by the Waste Treatment Centre (Sen Gupta, 1996). One stream is produced by the central Decontamination Centre (DC) where cleaning of reactor components, protective plastic clothing, and respirators takes place. The other, an Active Drain (AD) stream, originates from a large number of research laboratories and radioisotope production facilities.

The composition of each of these streams is shown in table 2.3. From table 2.3, it can be seen that the DC waste tends to contain more total solids and the AD stream tends to contain more radionuclides. These two streams are blended in a ratio of 1:1 and total approximately 2200 m^3 per year. This blended stream is referred to as the Active Drain/Decontamination Centre (AD/DC) waste stream.

Table 2.3: AD/DC Waste Feed Analysis (Sen Gupta et al., 1996)

	DC Waste			AD Waste		
	Min.	Max.	Avg.	Min.	Max.	Avg.
pH	2.3	7.0	3.7	3.1	8.6	6.3
Conductivity (µS/cm)	620	2400	1400	65	940	48
Total Solids (g/L)	0.3	2.3	1.3	0.05	1.5	0.5
Fe^{3+} (mg/L)	1.0	97	13.5	ND[1]	25	3.5
Na^{+} (mg/L)	1.0	320	120	15	340	120
Ca^{2+} (mg/L)	0.3	50	5.2	1.0	80	1.5
Mg^{2+} (mg/L)	0.5	33	4.0	1.0	40	5.9
NO_3^- (mg/L)	3.0	130	19.7	0.6	180	36
Cl^- (mg/)	3.0	280	92	3.7	78	30
SO_4^{2-} (mg/L)	0.5	120	40	0.5	200	46
PO_4^{2-} (mg/L)	70	910	530	ND[1]	180	26
CO_3^{2-} (mg/L)	21	250	85	NA[2]	NA[2]	NA[2]
Turbidity (NTU)	33	240	76	16	56	33
Gross α (Bq/mL)	ND[1]	7.1	1.1	ND[1]	420	77
Gross β/γ (Bq/mL)	1.0	530	160	200	150 000	16 000
Tritium (Bq/mL)	37	7 600	850	37	18 000	8 100

ND[1] - Not Detected; NA[2] - Not Analyzed

2.9.2 Description of the WTC at AECL's CRL

Sen Gupta and Slade (1993) describe the Waste Treatment Centre that manages 2200 m^3 of low-level liquid radioactive liquid wastes annually at the CRL Site of AECL Research.

The AD/DC waste, as described in section 2.9.1, is volumetrically reduced by a combination of crossflow microfiltration, SWRO and tubular reverse osmosis membrane technologies. The reject streams, as well as the backwash from the microfiltration unit and the wastes arising from the chemical cleanings of all the systems are further volume reduced by evaporation. A schematic of the WTC is shown in figure 2.1.

The crossflow microfiltration unit utilizes a nominal filter pore size of 0.2 μm and retains particles, suspended solids, and microorganisms from the feed. The microfiltration system configuration and its operation will not be discussed in detail as the focus of this thesis is on the SWRO system. An important note is that the filtrate production rate is approximately 42 L/min.

The filtrate from the microfiltration unit is sent to the SWRO system for further purification. In the SWRO system, there are nine pressure vessels configured in a three-stage 5:3:1 tapered design. Each vessel can hold one 4 inch (10 cm) diameter by 12 inch (30 cm) long and five 4 inch (10 cm) diameter by 40 inch (100 cm) long membrane modules for a total of 6 modules. The membrane modules are FILMTEC® thin-film composite Seawater High Rejection (SW30HR) modules and will be described in section 4.6. A Goulds 3333 multi-stage centrifugal booster pump feeds the system and operates at an applied pressure of 2760 kPa and a typical crossflow of approximately 40 L/min (Sen Gupta et al., 1996). Operating in feed-and-bleed mode, the system achieves an overall volumetric recovery of around 80 to 85 percent. At this point, the total solids concentration in the reject stream is about 10 g/L. The permeate is sampled and if it meets the internal administrative controls for discharge limits, it is released to the Ottawa River. If the permeate does not meet the internal administrative controls, it is recycled to the SWRO.

The tubular reverse osmosis (TRO) system treats the reject stream from the SWRO system. The permeate from the TRO system is sampled and, if required, it is sent back to the

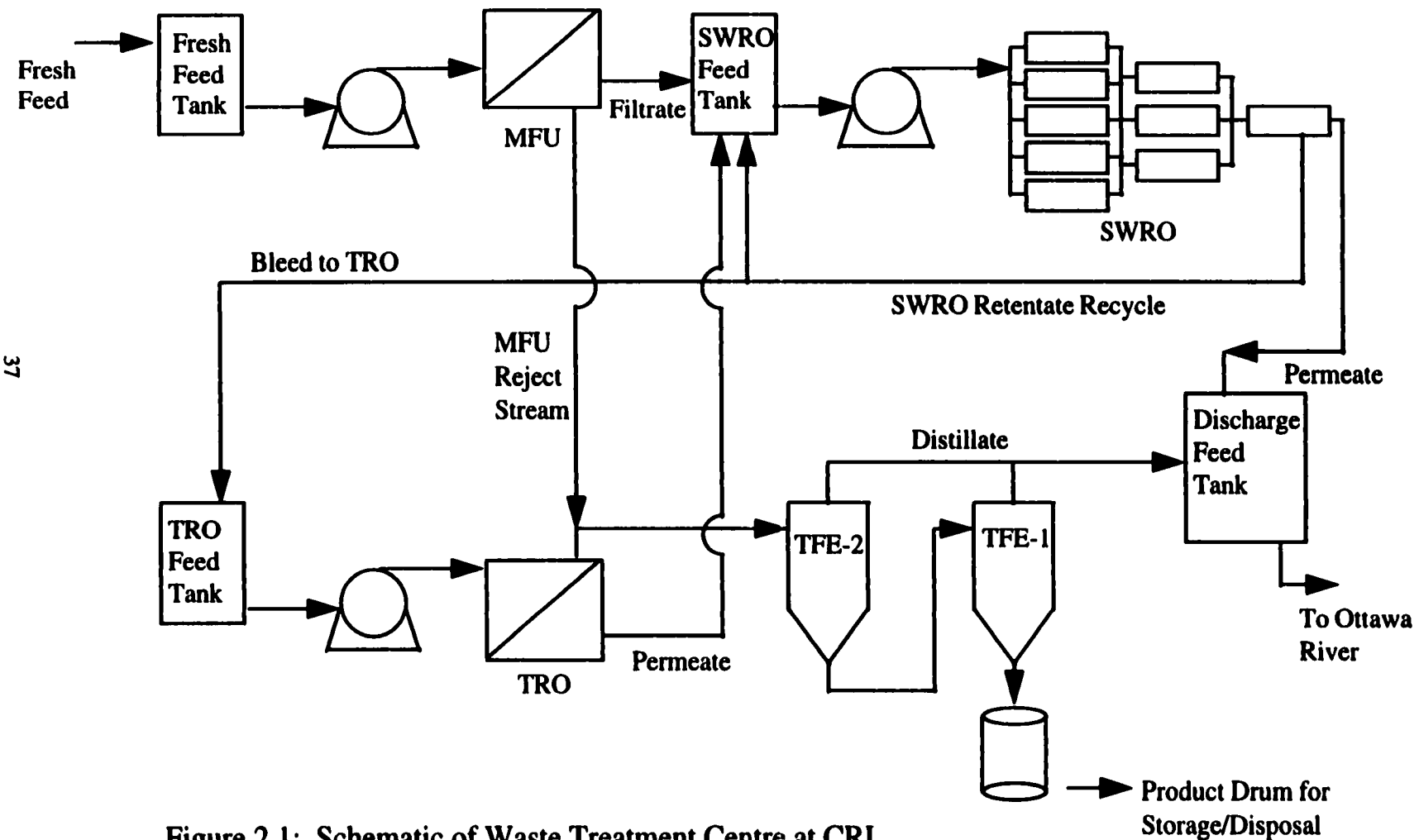

Figure 2.1: Schematic of Waste Treatment Centre at CRL

front end of the SWRO system for further purification. The reject stream, at approximately 80 g/L of total solids, is sent to two thin-film evaporators.

One of the thin-film evaporators (TFE-1) is used to immobilize the liquid waste concentrates with bitumen, and the other thin-film evaporator (TFE-2) is used to volumetrically reduce the microfiltration backwash and tubular reverse osmosis reject stream (Sen Gupta et al., 1994). The bottoms of the TFE-2 are sent to the TFE-1 for immobilization with bitumen. The distillate of both of the evaporators are sampled and, meeting discharge criteria, are released to the Ottawa River.

2.9.3 Permeate Flux Decline Observed with the Plant-Scale SWRO System

The difficulties experienced with the permeate flux decline by the plant-scale SWRO system at Chalk River Laboratories were discussed by Sen Gupta et al. (1996) and Sen Gupta and Rimpelainen (1997). The flux decline for two sets of membranes is shown in figure 2.2. The permeate flux is shown per membrane element (or module). Since one membrane element has an area of 6.28m^2, 1L/min/element is equal to 2.65×10^{-6} $m^3/m^2/s$. The permeate flux was normalized to an applied pressure of 2760 kPa and 25°C by a method proposed by Bukay (1984) as described in Appendix A. The membranes were changed at approximately 3800 hours of operation and again at approximately 7000 hours of operation. The duration of a run is approximately 14 hours when using a new set of membranes. After fouling, the time to process the same volume of waste can increase to as much as 36 hours (Longfield, 1997). Immediately after replacement, the permeate flux is high in both of these cases. The initial drop in the permeate flux is caused by concentration polarization. If the permeate flux decline was attributed solely to concentration polarization, the permeate flux would be expected to bounce back up to the initial permeate flux after a simple flushing of the system with water. From figure 2.2, it is evident that the permeate flux does not rebound back to its initial value and a steady decline in the permeate flux is observed over the course of operations. Even after chemical

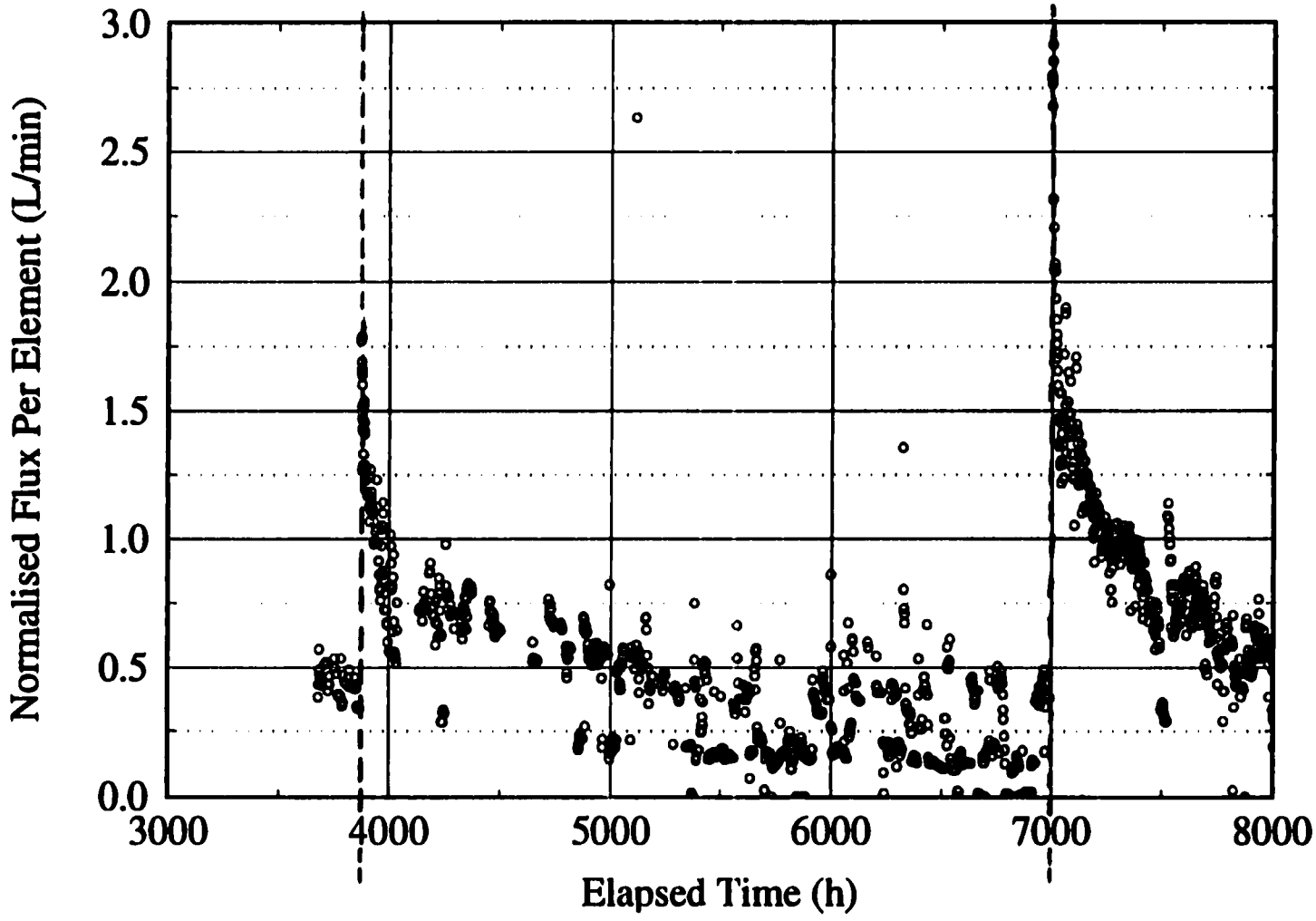

Figure 2.2: Permeate Flux Decline Observed during Processing with Plant-Scale System ----- membrane replacement

cleanings, the permeate flux is not fully regenerated. Although, the chemical cleanings did result in an improvement of 100 percent of permeate flux, this improved performance could not be maintained.

Several precautions were taken after the membrane replacement at 7000 hours of operation in hopes of preventing the severe permeate flux decline observed with the previous set of membranes. The volumetric recovery was set to 80 percent, lowered from 85 percent for the previous set of membranes; anti-scalant chemicals were added to the feed solution; and the chemical cleanings were performed at more regular intervals. As can be seen from the data points after 7000 hours of operation in figure 2.2, these precautions did not have any significant effect on the membrane performance and a steady permeate flux decline was observed for the new set of membranes similar to decline observed for the previous set of membranes. From these observations, it was obvious that irreversible fouling was taking place on the membrane surface.

There was also a decline in the rejection efficiency as well as a decline in the permeate flux. This decline in rejection efficiency is evident in figure 2.3. Figure 2.3 shows the conductivity rejection efficiency versus elapsed operational time. For the first set of membranes, the rejection efficiency was 99 percent until the elapsed operational time reached 6500 hours when it dropped to 95 percent. A rejection efficiency of 95 percent is not sufficient for the daily treatment of the AD/DC wastes and the membranes had to be replaced. A few scattered points showing lower rejection efficiencies (before the drop in rejection efficiency occurred) is attributed to excessive nitrate and sodium ions present in the system after cleanings.

2.9.4 Cleaning Procedures of the Waste Treatment Centre at CRL

Slade (1996) described the cleaning procedure used by the WTC for their SWRO system. Cleaning of the membranes modules in the plant scale system is performed when the permeate flow drops more than 15 percent or if the pressure drop across the membrane pressure vessels

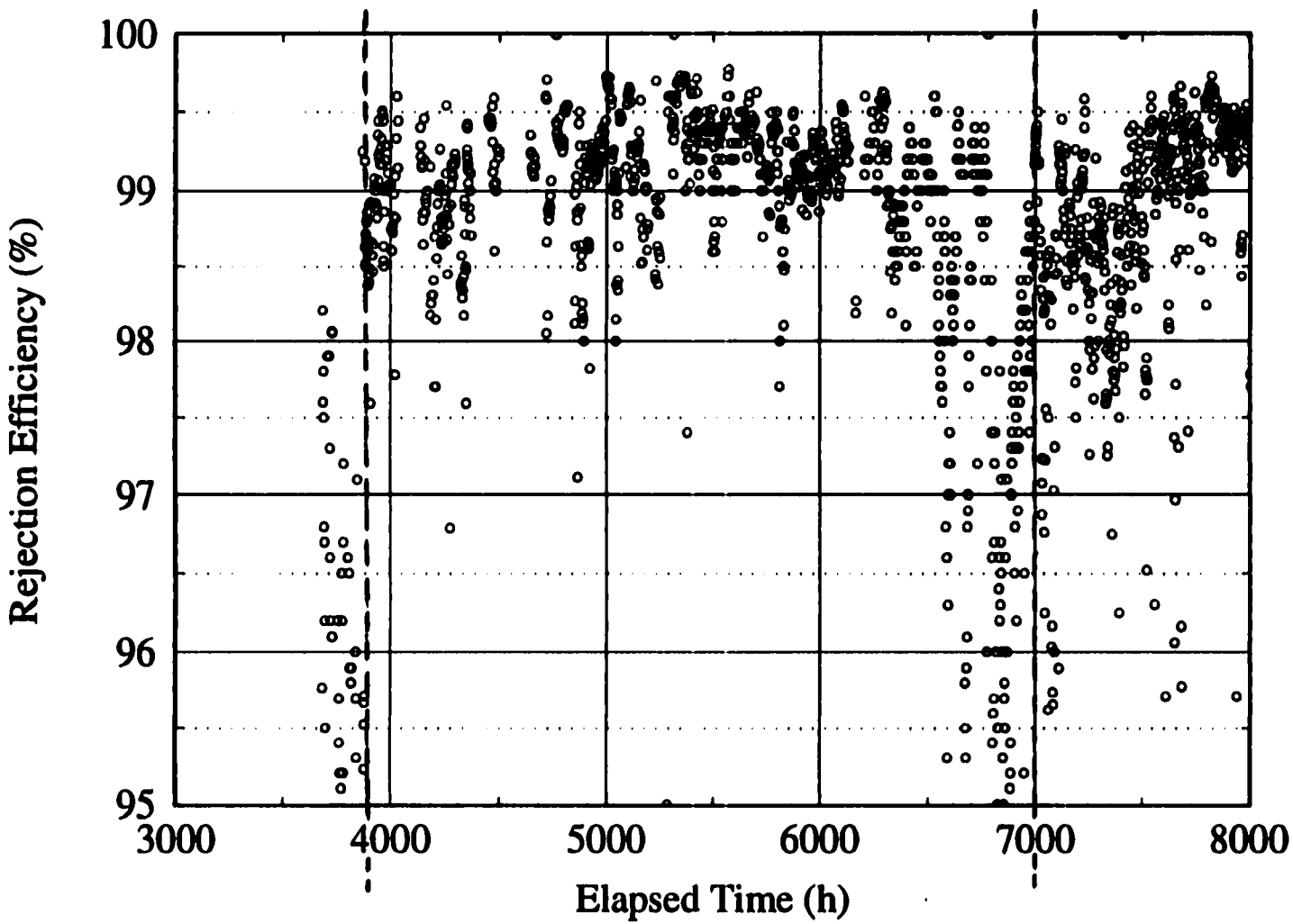

Figure 2.3: Rejection Efficiency of Membranes during Processing with Plant-Scale System ----- membrane replacement

exceeds 15 percent of the normal operating pressure. The average volume of the AD/DC waste processed between cleanings is approximately 100 cubic meters.

The system is first flushed with permeate to rinse the AD/DC waste out of the membrane modules. The cleaning agent, Memclean (KingLee Technologies, San Diego, California), is mixed with reverse osmosis permeate at a 0.2 volume percent concentration resulting in an alkaline cleaning solution with a pH of 12. The cleaning solution is recirculated through the system: at elevated temperatures around 30°C; at a flowrate of approximately 4 to 8 litres per minute; and at pressures below 500 kPa to fully distribute the solution throughout the system. After a few minutes, the recirculation of the cleaning solution is stopped and the membranes are allowed to soak for four to eight hours. Following the soaking, recirculation of each of the three stages recommences separately at high flowrates of approximately 40 litres per minute for a period of 30 to 60 minutes. Finally, the system is rinsed with reverse osmosis permeate to remove the cleaning solution from the membrane modules.

Chapter 3

Theory

3.1 Concentration Polarization

Concentration polarization is the accumulation of rejected solute at the membrane surface creating a solute concentration higher than that of the bulk solution. As the water permeates the membrane, the diffusion of solute away from the membrane surface back to the bulk solution is not as great as the convective flow of solute to the membrane (Bhattacharyya and Williams, 1992). This results in a higher concentration of solute near the membrane surface or boundary layer. Figure 3.1 illustrates the concentration polarization effect.

Concentration polarization is known to affect membrane performance in many ways. This increase in solute concentration near the membrane surface creates a higher osmotic pressure causing the permeate flux through the membrane to decrease. The increased concentration of solute at the boundary layer may exceed the solubility limit of some species causing precipitates to form and promoting fouling of the membrane. Increased solute flux through the membrane leads to decreases in the membrane rejection efficiency. Since increased concentration polarization can cause a decrease in the permeate flux and rejection efficiency, a decrease in the

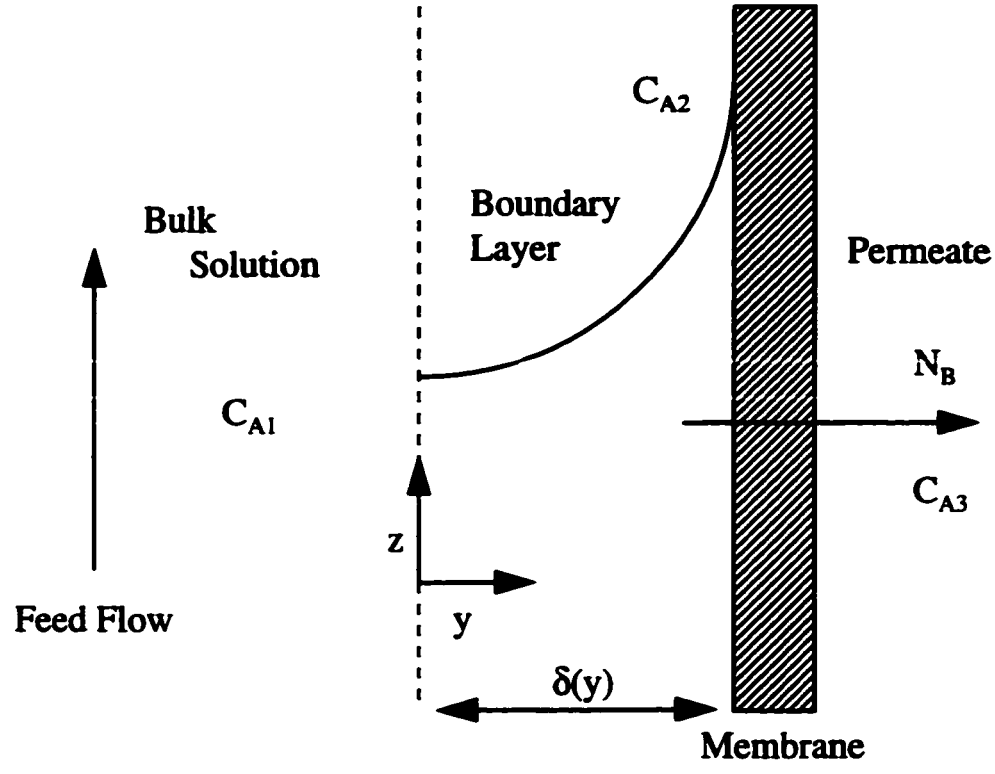

Figure 3.1: Concentration Polarization Effects

mass transfer coefficient is also observed. The next section gives the mathematical relationships found between the mass transfer coefficient, the permeate flux and the rejection efficiency.

3.2 Mass Transfer Coefficient Calculations

According to Treybal (1980), the mass transfer coefficient is the rate at which a component is transferred from one phase to another. In the case of membrane systems, the membrane acts as a semi-permeable barrier between the feed and permeate solutions; thus, the mass transfer coefficient refers to the rate at which a component is transferred through the membrane.

The mass transfer coefficient of salt (k_{NaCl}) was found using the freezing point depression method (Kruss, 1977 and Merten, 1966). The first step was to determine the osmotic pressure of the permeate, $\Pi(C_{A3})$. This is given by the following equation:

$$\Pi(C_{Ai}) = 9.8286 \times 10^5 \left(\frac{1}{T_{sol}} - \frac{1}{T_B} \right). \tag{1}$$

The freezing point depressions for the salt solution at various concentrations was taken from the 66th edition of the CRC Handbook of Chemistry and Physics (Weast, 1985). The osmotic pressure near the membrane surface, $\Pi(C_{A2})$, can then be found (Tremblay, 1989):

$$\Pi(C_{A2}) = \Pi(C_{A3}) + P_g \left(1 - \left[\frac{PR}{PWP} \right] \right). \tag{2}$$

Once $\Pi(C_{A2})$ is known, the concentration near the membrane surface, C_{A2}, can be predicted using the table found in Weast (1985). A computer program found in Appendix B is used to calculate the osmotic pressures of the permeate and the boundary layer concentrations for easy transfer to Lotus 1-2-3 files. The mass transfer coefficient can then be calculated using the equation 3:

$$N_B = ck \ln\left(\frac{x_{A2} - x_{A3}}{x_{A1} - x_{A3}}\right); \tag{3}$$

where,

$$N_B = \frac{PR}{SA} \times c. \tag{4}$$

The mass transfer coefficient of the various fouling species can be calculated by the two-thirds rule (Matsuura et al., 1974),

$$\frac{k_{ion}}{k_{NaCl}} = \left(\frac{D_{ion}}{D_{NaCl}}\right)^{2/3}, \tag{5}$$

where the diffusivities of various ions can be found from the 76th edition of the CRC Handbook of Chemistry and Physics (Lide, 1995).

3.3 Boundary Layer Concentration Calculations

As mentioned previously in section 3.1, concentration polarization creates a higher concentration of solute near the membrane surface. Having found k_{ion} using equation 5, it is possible to calculate the concentration of each of the fouling species near the membrane surface (boundary layer concentrations) using equations 3 and 4. This is relatively straight forward for species that do not form multiprotic acids. The calculations involving the boundary layer concentrations of species that can form a multiprotic acid, such as phosphate, are more involved.

The concentration of trivalent phosphate, PO_4^{3-}, cannot be measured directly. Instead, total analytical phosphate concentrations include the species H_3PO_4, $H_2PO_4^-$, HPO_4^{2-}, and PO_4^{3-}. To determine the concentration of PO_4^{3-}, applicable equilibria equations must be used.

In order to obtain a better estimate of PO_4^{3-} concentration in the AD/DC waste, the solution must be treated as non-ideal. As the concentration of ions in a solution increases, the electrostatic interactions between ions increase and the activity of the ions becomes less than their measured concentration (Snoeyink and Jenkins, 1980).

$$\{i\} = \gamma_i [i] \tag{6}$$

The activity coefficient (γ) of the ions in aqueous solution must be taken into consideration when solving the equilibria equations. To calculate the activity coefficients, the ionic strength of the solution (μ) must first be determined (Snoeyink and Jenkins, 1980):

$$\mu = \tfrac{1}{2}\Sigma\left(C_i Z_i^{\,2}\right); \tag{7}$$

where, C_i = concentration of ionic species, i and

Z_i = charge of the species, i

The activity coefficient can be calculated by the Güntelberg approximation (Snoeyink and Jenkins, 1980):

$$-\log \gamma_{\pm} = \frac{0.5|Z_+ Z_-|\mu^{1/2}}{1+\mu^{1/2}}; \tag{8}$$

where Z_+ = the charge of the positive ion,

Z_- = the charge of the negative ion, and

$\gamma_{\pm}$ = mean of the two activity coefficients.

The applicable equilibria equations for the triprotic acid of phosphate are given below:

$$H_2O \Leftrightarrow H^+ + OH^-; \qquad K_W = 10^{-14} = \{H^+\}\{OH^-\}; \tag{9}$$

$$H_3PO_4 \Leftrightarrow H^+ + H_2PO_4^-; \qquad K_{a.1} = \frac{\{H^+\}\{H_2PO_4^-\}}{\{H_3PO_4\}} = 10^{-2.1}; \tag{10}$$

$$H_2PO_4^- \Leftrightarrow H^+ + HPO_4^{2-}; \qquad K_{a.2} = \frac{\{H^+\}\{HPO_4^{2-}\}}{\{H_2PO_4^-\}} = 10^{-7.2}; \tag{11}$$

$$HPO_4^{2-} \Leftrightarrow H^+ + PO_4^{3-}; \qquad K_{a,3} = \frac{\{H^+\}\{PO_4^{3-}\}}{\{HPO_4^{2-}\}} = 10^{-12.3}. \tag{12}$$

Taking ionic strength effects into account, the equilibrium constants become the following:

$$K_{a,1}{}^c = \frac{K_{a,1}}{\gamma_+\gamma_-} = \frac{[H^+][H_2PO_4^-]}{[H_3PO_4]}; \tag{13}$$

$$K_{a,2}{}^c = \frac{\gamma_-}{\gamma_+\gamma_{2-}} K_{a,2} = \frac{[H^+][HPO_4^{2-}]}{[H_2PO_4^-]}; \text{ and} \tag{14}$$

$$K_{a,3}{}^c = \frac{\gamma_{2-}}{\gamma_+\gamma_{3-}} K_{a,3} = \frac{[H^+][PO_4^{3-}]}{[HPO_4^{2-}]}. \tag{15}$$

The mass balance on the phosphate species is given by the following equation,

$$C_{t,PO_4} = [H_3PO_4] + [H_2PO_4^-] + [HPO_4^{2-}] + [PO_4^{3-}]. \tag{16}$$

The concentration of trivalent phosphate was found by combining the equilibria equations 13, 14, 15 and mass balance equation 16 and solving for $[PO_4^{3-}]$:

$$[PO_4^{3-}] = C_{T,PO_4}\left(1\Big/\frac{[H^+]^3}{K_{a,1}{}^c K_{a,2}{}^c K_{a,3}{}^c} + \frac{[H^+]^2}{K_{a,2}{}^c K_{a,3}{}^c} + \frac{[H^+]}{K_{a,3}{}^c} + 1\right); \tag{17}$$

where C_{T,PO_4} = the total analytical phosphate concentration in moles per litre.

3.4 Calculations of Permeate Flux Predictions Based on Osmotic Pressure and Boundary Layer Concentrations

The permeate flux predictions are based on predicting the boundary layer concentrations of the various species present in solution and calculating the osmotic pressure associated with them.

The permeate flux can also be expressed as (Bhattacharyya and Williams, 1992):

$$N_B = A(\Delta p - \Delta\Pi). \tag{18}$$

In the absence of any solute in the feed stream (i.e. the feed stream consists of pure water), the osmotic pressure value becomes equivalent to zero and the $\Delta\Pi$ term disappears and equation 18 becomes the following:

$$PWP = A \cdot \Delta p \ . \tag{19}$$

If the osmotic pressure of the permeate can be considered negligible, $\Delta\Pi$ can be calculated strictly from the boundary layer concentration (C_{A2}):

$$\Delta\Pi = \Pi(C_{A2}) = C_{A2}RT \ . \tag{20}$$

By using equation 3 (assuming that x_{A3} is negligible as well) and equations 18 and 20, the boundary layer concentration of a specific ion, C_{A2}, and its related osmotic pressure, $\Pi(C_{A2})$, can be calculated simultaneously using equation 21:

$$\ln\left(\frac{C_{A2}}{C_{A1}}\right) - \frac{A}{k}(\Delta p - \Delta\Pi) = 0 \ . \tag{21}$$

The permeate flux can then be predicted based on the total osmotic pressure calculated from boundary layer concentrations using equation 18.

3.5 MINTEQA2, A Metal Speciation Equilibrium Model

MINTEQA2, a metal speciation equilibrium model for surface and ground water (U.S. Environmental Protection Agency, 1991), is capable of solving hundreds of equilibrium equations simultaneously to predict the equilibrium concentrations of different species in solution. It is also capable of predicting the compounds that will exceed saturation and precipitate out of solution. The databases contain information regarding the enthalpies of reaction, the equilibrium constants for aqueous complexes, solubility products for precipitating species, standard potentials for redox reactions, partial pressures for gases, and activity coefficient constants for non-ideal solutions.

Table 3.1 lists a number of possible complexes that may be found in the AD/DC waste and their equilibrium constants (EPA, 1991).

Table 3.1: Possible Aqueous Complexes Present in the AD/DC Waste and their Equilibrium Constants

Complexed Specie	-log K (pK)	Complexed Specie	-log K (pK)
$CaOH^+$	-12.6	$Fe(SO_4)_2^-$	5.4
$CaHCO_3^+$	11.3	$FeCl^{2+}$	1.5
$CaCO_3$ (aq)	3.2	$FeCl_2^+$	2.1
$CaSO_4$ (aq)	2.3	$FeCl_3$ (aq)	1.1
$CaHPO_4$ (aq)	15.1	$MgOH^+$	-11.7
$CaPO_4^-$	6.5	$MgCO_3$ (aq)	3.0
$CaH_2PO_4^-$	21.0	$MgHCO_3^+$	11.4
Ca-Citrate	4.7	$MgSO_4$ (aq)	2.2
Ca-Citrate-H	3.0	$MgPO_4^-$	6.6
Ca-Citrate-H_2	1.3	$MgH_2PO_4^+$	21.1
$FeOH^{2+}$	-2.2	$MgHPO_4$ (aq)	15.2
$FeHPO_4^+$	17.8	Mg-Citrate	3.4
$FeSO_4^+$	3.9	Mg-Citrate-H	8.2
$Fe(OH)_2^+$	-5.7	Mg-Citrate-H_2	11.6
$Fe(OH)_3$ (aq)	-13.6	$NaCO_3^-$	1.3
$FeH_2PO_4^{2+}$	25.0	$NaHCO_3$ (aq)	10.1
Fe-Citrate	12.6	$NaSO_4^-$	0.7
Fe-Citrate-H	19.8	$NaHPO_4^-$	12.6

Table 3.2 lists a few of the potential precipitates.

Table 3.2: Possible Solid Precipitates Formed in the AD/DC Waste and their Solubility Products

Solid Precipitate	-log K_{sp} (pK_{sp})
$CaCO_3$ (s) calcite	8.5
$CaSO_4 \cdot 2H_2O$ (s) gypsum	4.8
$Ca_5(PO_4)_3OH$ (s) hydrapatite/hydroxyapatite	44.2
$FePO_4 \cdot 2H_2O$ (s) strengite	26.4
Fe_2O_3 (s) hematite/ferric oxide	4.0
$FeCO_3$ (s) siderite	10.6
$MgCO_3$ (s) magnesite	8.0

3.6 Volumetric Recovery and Volumetric Recovery Factor

The purpose of the membrane technologies at the WTC is to volumetrically reduce the waste that will be immobilized in bitumen and sent to storage for eventual disposal. The volumetric reduction of waste can be expressed as volumetric recovery (VR):

$$VR = \frac{\text{Permeate Volume}}{\text{Initial Feed Volume}} \times 100\% \quad . \tag{22}$$

The volumetric recovery factor (VRF) can be determined from the VR and expressed as a fraction using equation 23:

$$VRF = \frac{1}{1 - VR} \quad . \tag{23}$$

3.7 Rejection Efficiency and Decontamination Factor

The reverse osmosis membrane selectively allows the passage of solvent while retaining solute. The degree of separation of the solvent from the solute can be expressed as the rejection efficiency. The rejection efficiency can be determined using equation 24:

$$\text{Rejection Efficiency (\%)} = 1 - \frac{\text{Permeate Concentration}}{\text{Feed Concentration}} \times 100\% \tag{24}$$

The decontamination factor (DF) is another way of expressing rejection efficiency:

$$DF = \frac{\text{Feed Concentration}}{\text{Permeate Concentration}} = \frac{100}{100 - \text{Rejection Efficiency}} \tag{25}$$

The DF is more sensitive to changes in rejection efficiency, especially when approaching 100 percent rejection efficiency. For example, a rejection efficiency of 99.98 percent gives a DF of 5000, where a rejection efficiency of 99.99 percent gives a DF of 10 000. However, due to the sensitivity of the DF to changes in the rejection efficiency the error in DF can become quite large at the higher rejection efficiencies. Based on the lower detection limit of the equipment used in the strontium analysis, a rejection efficiency of 99.98 percent for strontium (DF of 5000) can give an error in DF of more than 800.

Chapter 4

Experimental Equipment and Procedure

In this section, the pilot-scale spiral wound reverse osmosis (SWRO) system will be described in detail, as well as modifications made to the system since its installation in the Waste Treatment Centre. The procedure used to determine the mass transfer coefficient of the membrane module in Chapter 5 will be discussed as will be the experiments conducted with the AD/DC waste stream. The procedure used in the attempt to clean the fouled membrane modules in Chapter 6 will also be discussed in this section. The specifications of the membranes used for the experiments described in Chapters 5 and 6 will be given. The equipment used for the wastewater analysis will be described and their detection limits for various species.

4.1 Pilot-Scale Spiral Wound Reverse Osmosis System

A pilot-scale SWRO system purchased from Seprotech Systems Inc. (Ottawa, Ontario, Canada) was employed for all of the experimental work performed. This system was designed specifically to concentrate solutions containing radionuclides. Polypropylene and 316 stainless steel construction was chosen to prevent contamination of the feed, concentrate, and permeate

streams and to minimize contamination of the pilot-scale system itself by absorption of the radioactive species present in the wastewater.

Figure 4.1 shows a simplified schematic of the pilot-scale SWRO system. The system was originally designed to run in batch volumetric reduction mode. Two pressure vessels are available for use: a primary membrane vessel and a polisher membrane vessel. This allows the product water to be further purified (polished). Two thousand litres of AD/DC waste were treated by microfiltration and held in a 2000 litre tank. Four hundred litre batches of this waste was processed at a time from a separate tank. A 100 litre wash tank is available for cleaning solutions or for smaller batch reductions.

The waste from the feed tank is pumped through a 5 μm cartridge pre-filter to the suction side of the high pressure pumps. The feed pump is a Model ICS from Goulds Pumps Inc. (Kitchener, Ontario, Canada). The high pressure pumps are Hydra-Cell Industrial Pumps (Model H25SPSVHHHH) from Wanner Engineering Inc. (Minneapolis, Minnesota, USA). A pressure sensor and switch is located after the pre-filter to assure that a low suction pressure would not cause damage to the high pressure pumps. Both of the pumps have a second pump as a redundancy feature. Any pump can be isolated in case of failure and the second pump, either low or high pressure, can be put into service as backup.

The pressurized feed is sent to either membrane pressure vessel. Each vessel can hold up to two 4 inch (10 cm) diameter and 40 inch (100 cm) long SWRO membrane modules. Between the diaphragm style high pressure pumps and the membrane pressure vessels is a pulsation dampener (Model 60AS-1500S), Young Engineering Manufacturing, Inc. (Arcadia, California, USA). The feed flowrate (before modifications to the system) to the membrane pressure vessels is fixed at approximately 55 L/min to 60 L/min.

The pre-membrane pressure is measured by a pressure sensor located at the pressure vessel inlet. A pressure switch also ensures that the maximum high pressure limit cannot be exceeded. The discharge side of each high pressure pump also has a high pressure relief valve to

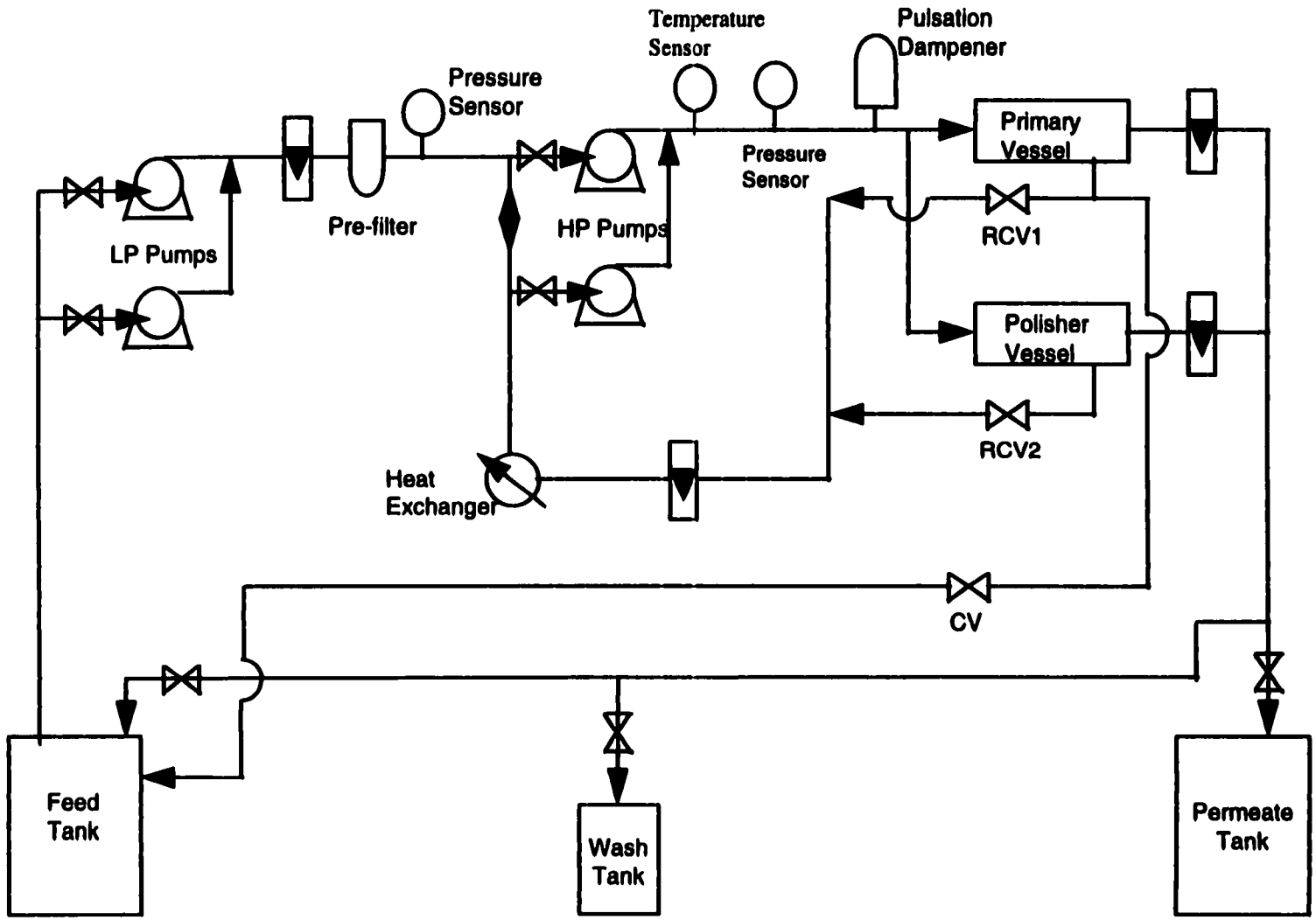

Figure 4.1: Original Pilot-Scale SWRO System
LP - Low Pressure HP - High Pressure

prevent any damage caused by excessively high pressure. The operating pressure is adjusted by the recirculation and concentrate control valves.

The permeate is collected in the permeate tank. The retentate is split into two streams. One stream is sent back to the feed tank and the other is recirculated back to the suction side of the high pressure pump. The recirculation stream passes through a recirculation control valve (RCV1 or RCV2), a flowmeter (FM2), and a plate and frame heat exchanger. A pressure sensor is located on the line leading back to the feed tank to measure the post-membrane pressure. This stream then passes through a concentrate control valve (CV) on the way to the feed tank where it drops to atmospheric pressure.

4.2 Modifications Made to Pilot-Scale SWRO System

Various modifications were made to the pilot-scale SWRO system. A simplified flow schematic of the modified system is shown in figure 4.2. The major modification was to allow for a variable crossflow velocity though the membrane modules. Any modifications to a licensed system, such as the pilot-scale SWRO system, requires approval by the Ministry of Consumer and Commercial Relations (MCCR). According to the Boiler and Pressures Act, any modifications made to existing equipment that processes aqueous solutions containing radionuclides and operating at pressures above 15 psig must be submitted to the MCCR.

A line from the discharge side of the high pressure pump to the tanks bypasses the membrane pressure vessels. A needle valve (BCV) controls the flow through the bypass line; thus, controlling the flow to the pressure vessels. This allows the crossflow velocity to be changed. The crossflow and pre-membrane pressure can be controlled by adjusting RCV1, RCV2, CV, and BCV. A high pressure flowmeter was also installed with two feet of straight piping on either side of the flowmeter. Some existing connections had to be modified to compensate for this increase in height.

Other minor adjustments were made to make the system more versatile. More permeate lines and valves were added so that the permeate could be sent back to any of the three

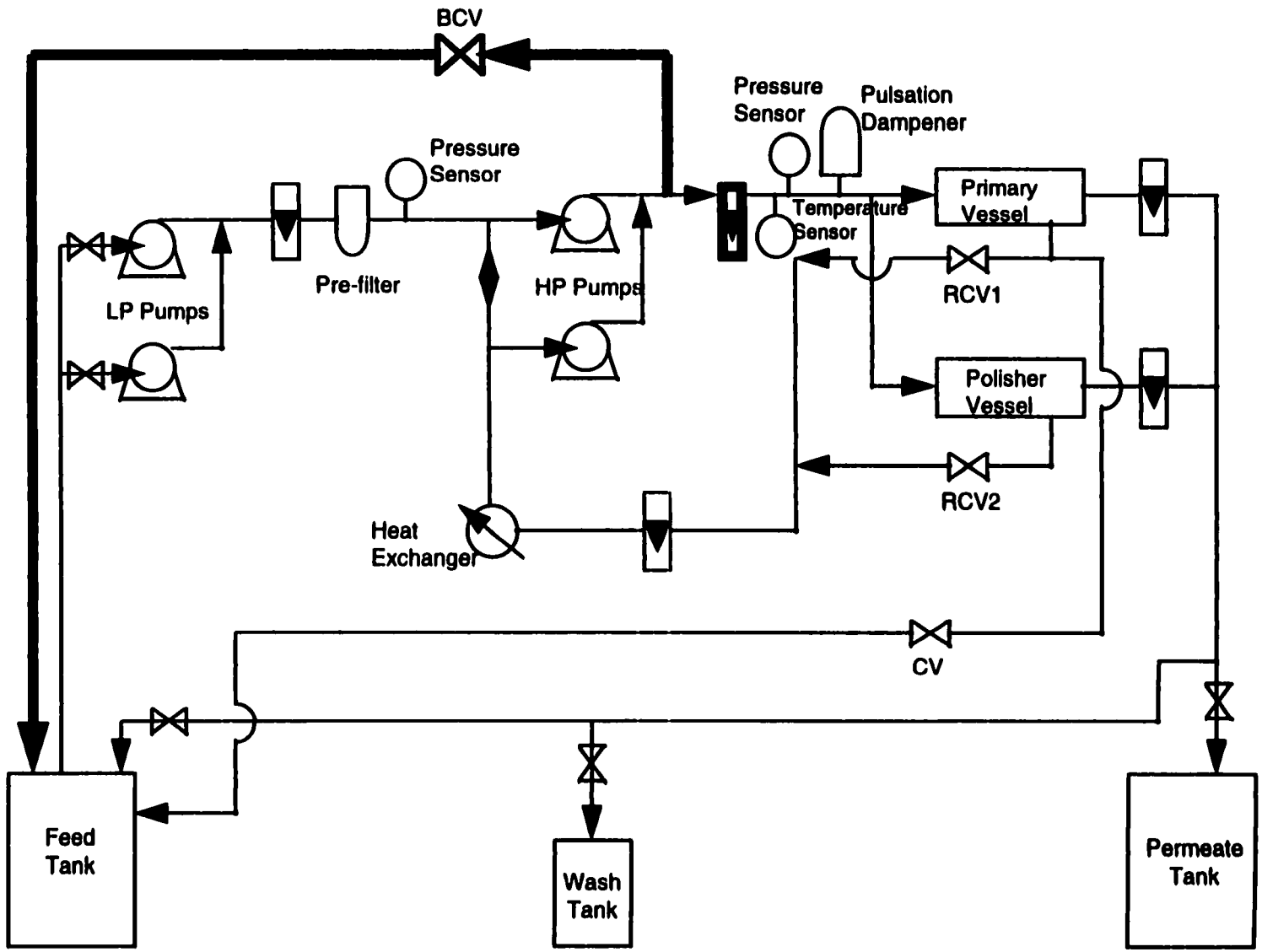

Figure 4.2: Modified Pilot-Scale SWRO System, LP - Low Pressure, HP - High Pressure, ▬ modifications

tanks. This allows the system to be run in full recirculation mode. The feed for the pilot-scale SWRO system is the filtrate from the plant run microfiltration unit. Originally, the filtrate from the microfiltration unit would be collected into drums and then pumped into the appropriate tanks of the pilot-scale SWRO system. Lines were installed from the microfiltration unit to the tanks of the pilot-scale SWRO system so that the tanks could be filled more easily. This modification also allows the combined microfiltration/pilot-scale system to be run in feed-and-bleed mode as well as batch volumetric reduction mode. This is fundamental in duplicating the conditions of the plant-scale system, which is operated in feed-and-bleed mode, with experiments conducted with the pilot-scale system. However, all of the experiments conducted for this work were performed in batch mode.

The two 400 litre tanks were replaced with two 2000 litre tanks. The system can now be run to higher volumetric recoveries in batch mode. With the increased feed tank size, the highest volumetric recovery achievable was increased to 99 percent from 95 percent. The increased tank size required them to be vented to the ventilation system of the building.

4.3 Experimental Procedure for Determining Mass Transfer Coefficients

A series of experiments were performed on a FILMTEC® thin film composite SWRO membrane. Five 400 L batches of AD/DC waste were volumetrically reduced by the pilot-scale SWRO system at crossflows of 30 L/min, 60 L/min, 45 L/min, 52.5 L/min and 37.5 L/min (in that order).

Each 400 litre batch volumetric reduction of AD/DC waste was performed at an average applied pressure of 2760 kPa (400 psi). The pressure was brought up to this value using the concentrate control valves, the recirculation control valve and the bypass valve shown in figure 4.2. The recirculation control valve and the bypass valve must both be adjusted to obtain the desired crossflow velocity and applied pressure. The desired operating temperature was 25°C. The experiments were performed at temperatures ranging from 22°C to 27°C. The permeate flux

measurements were normalized with respect to a temperature of 25°C and a pressure of 2760 kPa using equation A1 in Appendix A. The volumetric recovery targeted for all five batches of AD/DC waste was approximately 85 percent.

Samples were taken at the start of the run at zero percent volumetric recovery and taken periodically during the volumetric reduction of each batch of AD/DC wastes. These samples were analyzed by the laboratories on site for iron, sodium, magnesium, calcium, bicarbonate, and hydroxyl concentrations as well as for turbidity, conductivity and pH. The equipment used in these measurements will be discussed in later sections. Measurements were taken at the same time as the samples.

The permeate flux performance with a three weight percent salt solution and the pure water permeability of the membrane were measured before and after each volumetric reduction of AD/DC wastes. These tests were done to determine if any deterioration of the membrane performance had taken place.

The mass transfer coefficient of salt (k_{NaCl}) was determined once after the AD/DC run at a crossflow velocity of 52.5 L/min and immediately after the last AD/DC run at a crossflow velocity of 37.5 L/min.

The experiments performed with the salt solutions to determine the mass transfer coefficient of salt for the membrane module were run in full recirculation mode to keep the salt concentration constant throughout the duration of the run. Again, the experiments were performed at an applied pressure of 2760 kPa and at a temperature of 25°C. Any variation from these values were taken into account by normalizing the permeate flux by equation A1 in Appendix A. The crossflow velocity was first adjusted to 30 L/min. Measurements and samples were taken after the system was left running at 30 L/min for approximately one hour to completely flush the permeate channel. The system was then adjusted to crossflows of 37.5 L/min, 45 L/min, 52.5 L/min and 60 L/min for approximately 30 minutes (at each crossflow) to ensure that steady state was reached before measurements were taken. Samples and

measurements were taken in triplicate at each crossflow and the samples were analyzed for conductivity.

The pure water permeability tests were conducted in a similar manner to the mass transfer coefficient experiments performed with the salt solutions although samples were not required.

4.4 Fouled Membrane Cleaning Procedure

An attempt to clean two fouled membrane modules taken from the SWRO system in the WTC at CRL was made. These experiments were conducted before the mass transfer coefficient experiments were performed. This is because the experimental cleanings could be performed awaiting MCCR approval for the modifications to the pilot-scale SWRO system. Crossflow velocity was not a parameter that needed to be studied during the cleaning experiments; thus, no crossflow velocity changes were required.

Two fouled membrane modules (module 5-6 and module 3-6) were taken from the head of the first stage of the plant-scale SWRO system. These modules were numbered according to which pressure vessel they were situated (pressure vessel 5 and 3) and the 6 refers to the head of the pressure vessel. For simplicity, module 5-6 will be referred to as module 1 and module 3-6 will be referred to as module 2 in the remainder of this section.

The cleaning was attempted on each module using the pilot-scale SWRO system before any modifications were made. Only one module was tested at a time to test the flux and rejection efficiency of the individual modules after each cleaning step. Each module underwent the same basic cleaning steps except in step 3 EDTA was replaced with NTA when module 2 was tested. The cleaning of the membrane consisted of the steps described in table 4.1:

Table 4.1: Three-Step SWRO Membrane Cleaning Procedure

Step	Cleaning Procedure
1	A solution of approximately 1 vol % Triton X-100 was recirculated for one hour with the low pressure pump.
2	A HCl acid solution at an approximate pH of 2 was recirculated for one hour with the low pressure pump.
3	A solution of NaOH and 2 wt% EDTA (or NTA) at a pH 12 was recirculated with the low pressure pump. EDTA was recirculated through module 1 for approximately two hours and NTA was recirculated through module 2 for approximately one hour.

Pure water permeability tests (PWP) were performed before and after each cleaning step to measure any improvement in the permeate flux. The rejection efficiencies of cesium and strontium were also found before and after each cleaning step. The pure water permeability tests and rejection efficiency tests were performed at the maximum crossflow of the system (between 55 and 60 L/min) and at a temperature of 25°C. The applied pressure was varied from 200 psi (1380 kPa) to 800 psi (5500 kPa) in 100 psi intervals. The system was left at 1380 kPa for approximately 20 minutes to completely flush the permeate channel before any measurements (or samples in the case of the rejection efficiency tests) were taken. The system was run at each applied pressure for approximately 15 minutes. The permeate fluxes were normalized with respect to a temperature of 25°C and pressure of 400 psi (2760 kPa) using equation A1 in Appendix A.

Tests were also conducted with a 1:1 ratio of active drain (AD) and decontamination centre (DC) wastes called the AD/DC wastes. The AD/DC waste recovery runs were performed on both modules after the cleaning attempt with and without the five micron filter installed. Module 2 also underwent an additional AD/DC waste run before any cleaning, pure water permeability or rejection efficiency tests were performed. The AD/DC tests were volumetrically reduced to 85 percent. The tests were performed at 2760 kPa, 25°C and at a

crossflow of approximately 55 to 60 L/min. Again, the permeate fluxes were normalized to 2760 kPa and 25°C.

4.5 Rejection Efficiency Tests Performed with Cesium and Strontium

Tests were conducted with solutions containing very dilute concentrations of cesium and strontium to determine the effect the cleaning procedure had on the integrity of the membrane.

Cesium chloride and strontium nitrate were dissolved in deionized water giving a feed concentration of approximately 50 mg/L of ^{133}Cs and 10 000 mg/L of ^{88}Sr (both non-radioactive) for the first membrane module cleaned. Testing of the permeate stream resulted in concentrations below the detectable limits for both species. Subsequent cesium and strontium rejection efficiency tests conducted with the second membrane module cleaned were performed with a feed stream containing approximately 150 000 mg/L each of cesium and strontium.

The tests performed with cesium and strontium solutions were conducted before any cleaning steps had been undertaken on the membrane and after each cleaning step. Permeate flux measurements and feed and permeate samples were taken at various applied pressures ranging from 200 psi (1360 kPa) and 800 psi (5500 kPa) before and after the entire three-step cleaning procedure had been performed. After cleaning steps 1 and 2, measurements and samples were taken only at 400 psi (2760 kPa).

The concentration of the non-radioactive cesium was determined using a Varian Atomic Absorption 20 GTA 96 Graphite Furnace spectrophotometer . The concentration of non-radioactive strontium was determined using a Tru Logic Systems TL 6000 inductively coupled plasma assembly.

4.6 Description of Membrane Modules

The clean membrane module used in the experiments described in section 4.3 and the fouled modules that underwent the cleaning described in section 4.4 were FILMTEC® thin-film

composite Seawater High Rejection (SW30HR-4040) modules manufactured by Dow Chemical Company (Minneapolis, Minnesota, USA). The membrane composite consists of a polyester support web, a microporous polysulfone interlayer and an ultrathin polyamide membrane on the surface facing the feed stream. The specifications and operating limits of the SW30HR-4040 membrane module are given in table 4.2.

Table 4.2: Specifications and Operating Limits of SW30HR-4040 Membrane Module

Product Water Flow Rate	2.6 L/min
Minimum Salt Rejection Cl^-	99.2 %
Typical Salt Rejection Cl^-	99.4 %
Maximum Operating Pressure	6.9 MPa (1000 psi)
Maximum Operating Temperature	45°C (113°F)
Maximum Feed Turbidity	1 NTU
Free Chlorine Tolerance	<0.1 ppm
pH Range	2-11 (Continuous Operation)
	1-12 (Short-term (30 min.) Cleaning)
Maximum Feed Flow	60 L/min (16 GPM)

4.7 Analysis Equipment

The analysis of the wastewater is done by the NRU Analytical Laboratory on site. The pH is measured by a Pope Model 1500 pH Meter. The conductivity is measured by a Radiometer CDM-83 Conductivity Meter with Dip Cell. The turbidity is measured by a Hach Model 2100A Turbidity Meter. Iron and aluminum concentrations are measured by a Perkin Elmer Model 2380 Atomic Absorption Spectrophotometer. Sodium, magnesium calcium, chloride, nitrate, phosphate and sulfate concentrations are analyzed by a Dionex DX-100 Ion Chromatograph with AS40 Autosampler and A1-450 computer interface and software. The carbonate, bicarbonate and hydroxyl concentrations and the total alkalinity are determined by a two stage titration to pH 8.1 and pH 4.5.

A scanning electron microscope (SEM) along with an energy dispersive X-ray (EDX) was used to help identify possible foulants on the membrane surface. The electron micrographs were produced using a JEOL-840A shielded SEM equipped with a Tracor-Northern EDX spectrometer.

4.8 Detection Limits of All Analyses Used

The lower detection limits of each species using the various analysis techniques are listed in table 4.3. All of the detection limits listed are valid for undiluted samples.

Table 4.3: Lower Detection Limits of Analytical Instruments for Various Species (Atomic Absorption Spectrometer, Ion Liquid Chromatograph and Inductively Coupled Plasma measurements are within 5%, 10% and 2% respectively).

Species	Instrument	Lower Detection Limit
Aluminum	Atomic Absorption Spectrometer	1.1 ppm
Calcium	Ion Liquid Chromatograph	100 ppb
Cesium	Atomic Absorption Spectrometer	1 ppb
Chloride	Ion Liquid Chromatograph	10 ppb (low range)
	Ion Liquid Chromatograph	200 ppb (high range)
Iron	Atomic Absorption Spectrometer	100 ppb
Magnesium	Ion Liquid Chromatograph	100 ppb
Nitrate	Ion Liquid Chromatograph	10 ppb (low range)
	Ion Liquid Chromatograph	600 ppb (high range)
Phosphate	Ion Liquid Chromatograph	30 ppb (low range)
	Ion Liquid Chromatograph	500 ppb (high range)
Sodium	Ion Liquid Chromatograph	100 ppb
Strontium	Inductively Coupled Plasma	5 ppb
Sulfate	Ion Liquid Chromatograph	20 ppb (low range)
	Ion Liquid Chromatograph	400 ppb (high range)
Species with Atomic Weight of Sodium and Above	Energy Dispersive X-Ray	1% of volume analyzed

Chapter 5

Evaluation of Crossflow Velocity on Permeate Flux

As discussed in section 2.9, the plant-scale SWRO system at CRL was experiencing operational difficulties. Frequent membrane replacements were required to maintain reasonable permeate fluxes and permeate quality. During the time period between April 1994 and July 1995, a permeate flow drop from 1.0 L/min to 0.25 L/min was observed after 2500 hours of operation (refer to figure 2.2). Rejection efficiency decreased from 99.5 percent to 95 percent in that same 2500 hours of operation (refer to figure 2.3).

Research was performed with the AD/DC waste stream using the pilot-scale system to determine how the operational life of the membranes used in the plant's SWRO system at CRL could be extended. The pilot-scale SWRO system consistently achieved high permeate fluxes that could be restored after simply flushing the system with pure water. It was thought that the higher crossflow of 55 L/min for the pilot-scale system compared to the 40 L/min crossflow of the plant-scale system was a principal factor in the superior permeate fluxes of the pilot-scale system. Steps were taken to determine what role crossflow velocity was playing in the irreversible fouling of the SWRO membranes in the plant-scale system. In section 5.1, the foulants on the plant-scale SWRO membrane are identified. An unfouled membrane is

characterized in section 5.1 by permeability tests using pure water and rejection efficiency tests using a three weight percent sodium chloride solution. In section 5.2, the mass transfer coefficient of the membrane is determined at five different crossflow velocities from the PWP and salt rejection efficiency tests performed in section 5.1. The boundary layer concentrations of the foulants (identified in section 5.1) are determined in section 5.3 as well. In section 5.4, comparisons are made between a permeate flux predicted from osmotic pressure calculations and the actual flux observed during the volumetric reduction of the AD/DC waste stream at the various crossflows studied. The raw data for the experimental work performed for chapter 5 is shown in Appendix C.

5.1 Identification of Potential Fouling Species

Efforts have been made to determine the major fouling species of the membrane that led to the irreversible fouling discussed in section 2.9.3. A scanning electron microscope along with an energy dispersive X-ray (SEM/EDX) was used on precipitate samples as well as on fouled membranes to determine which elements are precipitating. The EDX examination can only give an elemental analysis of the precipitate and not the actual compounds formed. An equilibrium solution computer program, MINTEQA2 (U.S. Environmental Protection Agency, 1991), predicts which compounds will precipitate out of solution. This program was used to identify suspected precipitate compounds formed.

Several membrane samples were cut from fouled membrane modules and from a clean, unused membrane. The membrane samples were analyzed by SEM/EDX. An SEM of an area of the clean membrane is shown in figure 5.1. Figure 5.2 shows the SEM photograph of a membrane that became fouled after 3200 hours of operation. The SEM photograph of a fouled membrane clearly shows an accumulation of precipitates and deposits on the surface of the membrane. A typical elemental analysis of the fouled membrane by EDX is given in figure 5.3.

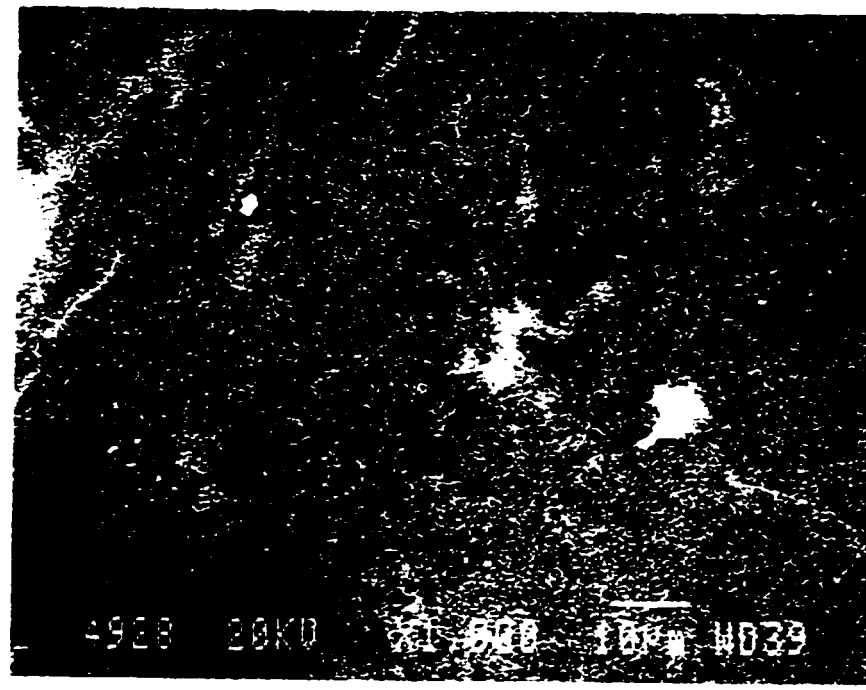

Figure 5.1: SEM Photograph of Clean, Unused Membrane

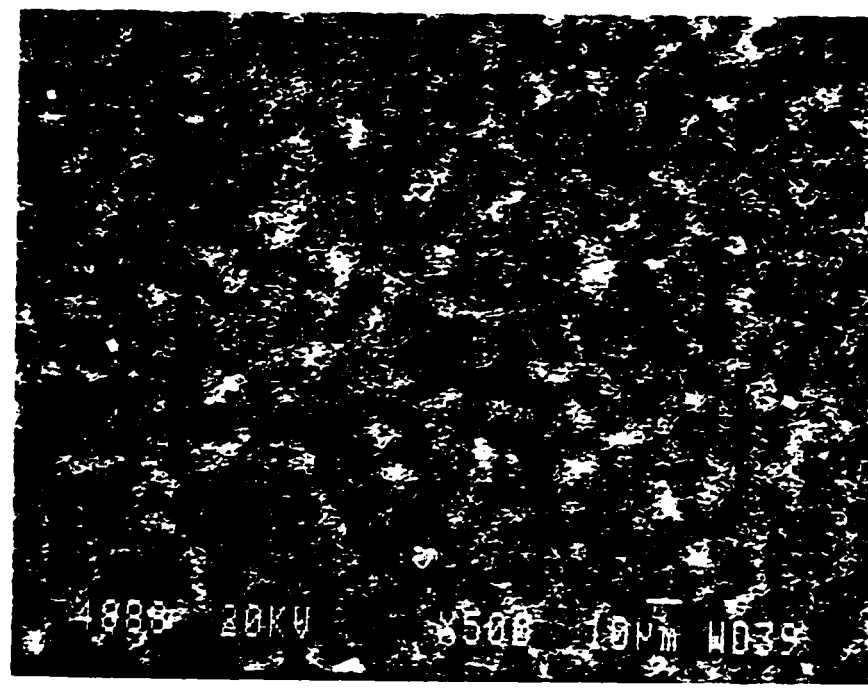

Figure 5.2: SEM Photograph of Fouled Membrane

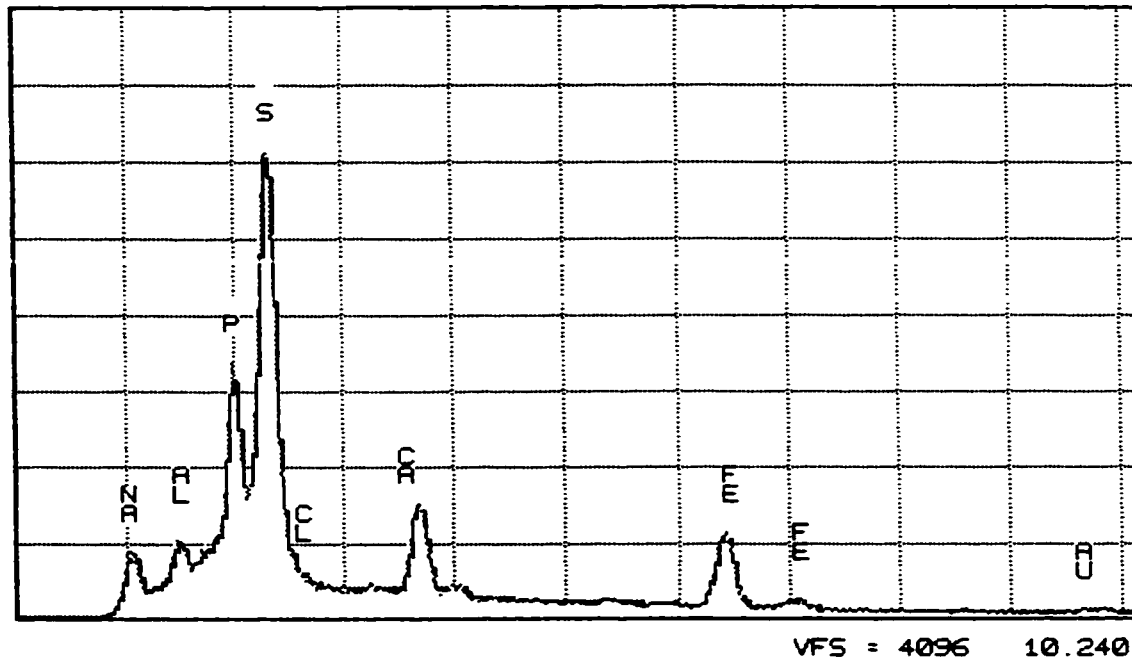

Figure 5.3: EDX Output of Fouled Membrane After 3200 Hours of Operation Treating AD/DC Waste

Peak intensity is proportional to the number of atoms present on the membrane surface.

Two elements identified by EDX can be eliminated from the analysis for various reasons. These elements include gold (Au) and aluminum (Al). Analyses of the AD/DC waste have indicated that neither of these compounds are present in the waste. Gold shows up in the spectrum because the samples analyzed by the SEM are coated in gold to aid in their conductivity. A source of aluminum is the nozzle covering the end of the spectrometer of the EDX. It is suspected that some of the secondary electrons scattering back from the sample are striking the edges of the aluminum nozzle. These secondary electrons release electrons from the aluminum and are identified as aluminum on the EDX elemental analysis. Figure 5.3 identifies sulphur as a major constituent of the elemental analysis of the fouled membrane. In order of decreasing proportions, the other elements present on the membrane surface are sodium, phosphorus, iron and calcium.

Analyses of the AD/DC waste at zero percent volumetric recovery and calculating the concentration of each species at 20, 40, 50, 60, 65, 70, 75, 80 and 85 percent volumetric recoveries provides the input concentrations for the MINTEQA2 computer program. Refer to example A.2 in Appendix A for a sample calculation. Analyses of pH, conductivity, turbidity have been made of the AD/DC waste and atomic absorption and ion liquid chromatography analyses have identified various species present in solution in the AD/DC waste. The concentration of citrate was predicted from the volumes of detergent added by the DC to the DC waste stream. These species and their concentrations are listed in table 5.1.

The concentrations of all of the species present in the AD/DC waste at 85 percent volumetric recovery found in table 5.1 were inputted into the MINTEQA2 program. The program predicted the formation of calcium hydroxyapatite, $Ca_5(PO_4)_3OH$, and an iron oxide, Fe_2O_3. No other compounds were predicted to precipitate. (The results of the MINTEQA2 compilation at 85 percent volumetric recovery of the data in table 5.1 are given in Appendix D). This result did not correspond to the species identified on the fouled membrane by the EDX analysis shown in figure 5.3. No sulfate nor sodium precipitates were predicted by the

Table 5.1: Average Concentrations of Species Present in AD/DC Waste

Analysis		Test #1 at 0% VR March 18/96	Test #2 at 0% VR May 6/96	Test #3 at 0% VR June 13/96	Average of Tests at 0% VR	Average of Tests at 85% VR
pH		6.8	6.2	6.2	6.4	6.4
Conductivity	(uS/cm)	1340	1330	1360	1343	8956
Solids	(g/L)	1.1	0.98	1.6	1.2	8.2
Iron	(mg/L)	4.8	5.4	4.83	5.0	33.4
Sodium	(mg/L)	246	266.3	276	263	1752
Magnesium	(mg/L)	2.8	4.1	3.2	3.4	22.4
Calcium	(mg/L)	13.5	14.2	14.7	14.1	94.2
Aluminum	(mg/L)	NA	<1.1	NA	<1.1	<1.1
Chloride	(mg/L)	119	136.1	135	130	867
Nitrate	(mg/L)	78	67	167	104	693
Phosphate	(mg/L)	455	458.9	528	481	3204
Sulfate	(mg/L)	61	58.6	65	62	410
Bicarbonate	(mg/L)	46	46	58	50	333
Citrate	(mg/L)	NA	NA	NA	87.5	583
Turbidity	(N.T.U)	NA	NA	1	1	7

MINTEQA2 program despite that these two species are identified as major constituents on the fouled membrane.

To determine exactly which elements were precipitating out of solution, samples of the AD/DC waste at approximately 85 percent recovery were taken. Two of these sample waste solutions were vacuum filtered using a 0.1 micron Millipore filter. These filters were then analyzed by SEM/EDX. The SEM photographs are shown in figures 5.4 and 5.5. The EDX results of the photographs shown in figures 5.4 and 5.5 are shown in figures 5.6 and 5.7. Figure 5.6 identifies phosphorus, calcium, iron and some magnesium had precipitated. Figure 5.7 shows a phosphorus, a calcium and a silicon precipitate. In the case of this sample, neither iron nor magnesium was identified by the EDX. It is expected that the precipitates identified on both filter samples would be the same since both samples filtered the same waste water. Most likely, both filters do contain all of the precipitates identified in figures 5.6 and 5.7. Unfortunately, the EDX can only analyze a very small area of the filter; no larger than 12 mm in diameter. In many cases, the area analyzed is only micrometers in diameter. In analyzing this small area, some of the precipitate species can be easily missed since they are not uniformly distributed on the filter. EDX analyses were performed on many different areas of the filter and a combination of the precipitated species were always identified but, neither sulphur nor sodium were ever found on either filter.

The large sulphur peak shown in figure 5.3 does not correspond to the precipitates found on the filters (figures 5.6 and 5.7). Nor does the sulphur correspond to the species predicted to precipitate by the MINTEQA2 program. It was speculated that the source of the sulphur peak may have originated from the membrane itself. The backing of the membrane is made of polysulfone. To determine if this was the case, an EDX examination was performed on a unused clean membrane. Figure 5.8 shows the results of the EDX on the clean membrane. A large sulphur peak is evident and it is most likely that the sulphur identified in figure 5.3 may not be a precipitate but part of the membrane itself.

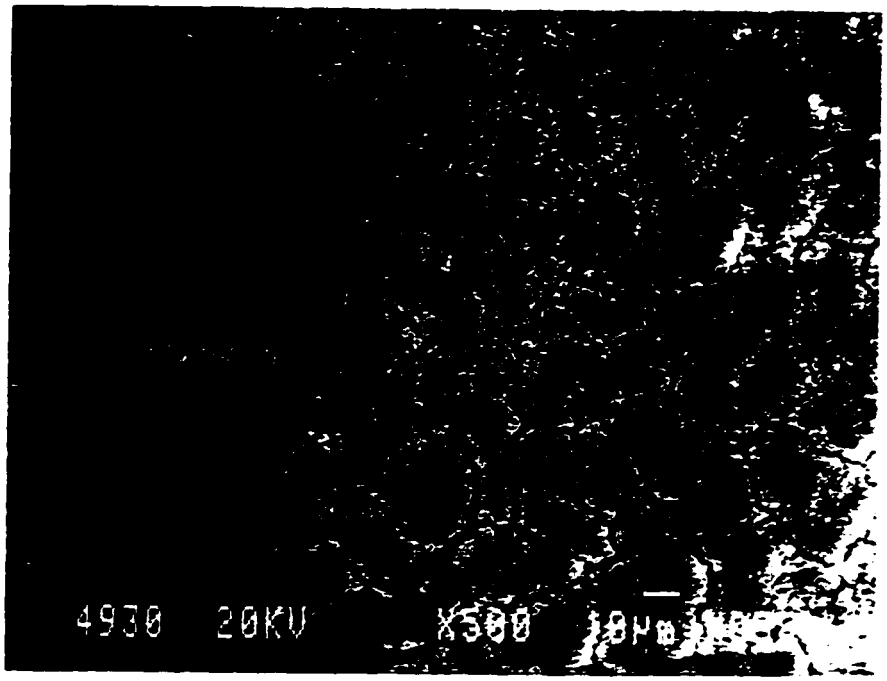

Figure 5.4: SEM Photograph of Vacuum Filtered Sample 1

Figure 5.5: SEM Photograph of Vacuum Filtered Sample 2

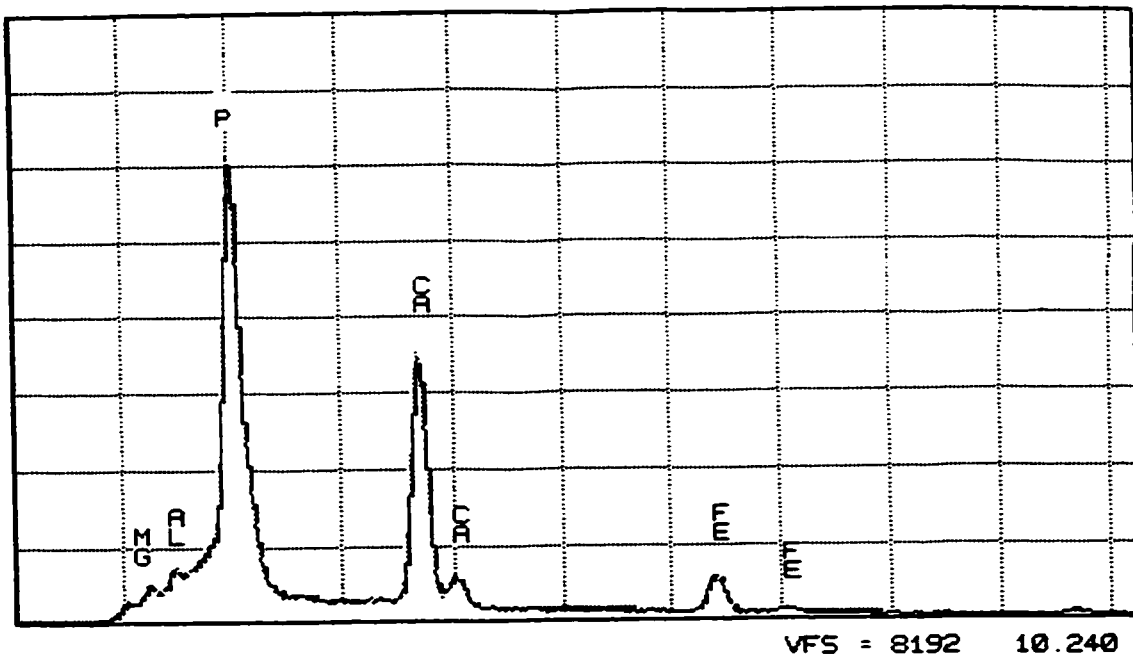

Figure 5.6: EDX Output of Vacuum Filtered Sample 1
Peak intensity is proportional to the number of atoms present on the filte surface.

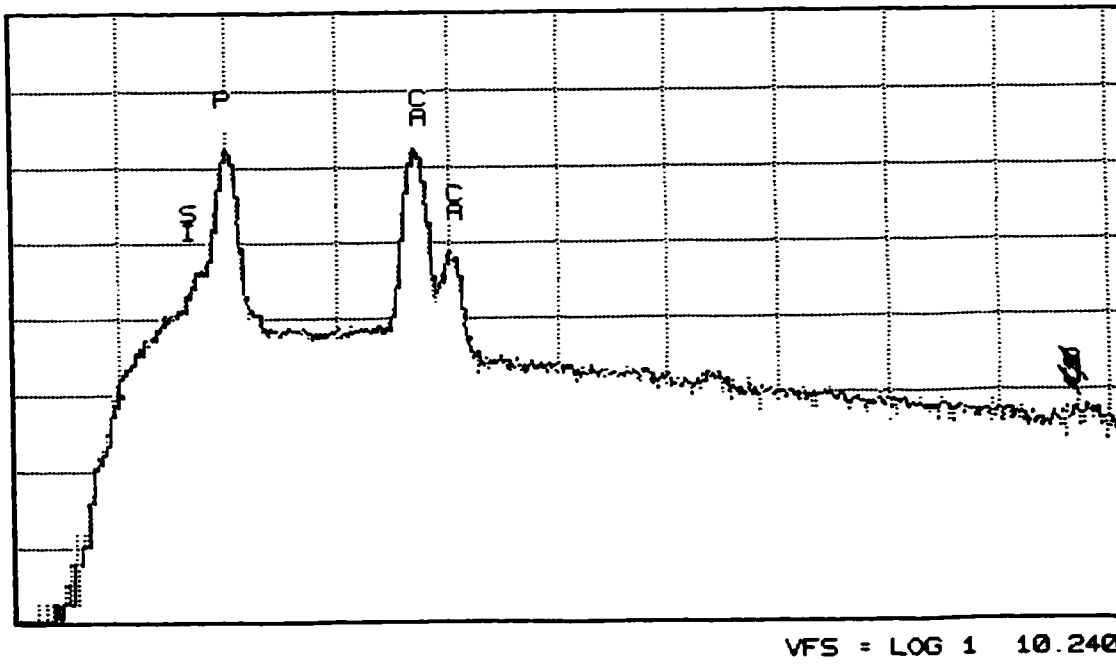

Figure 5.7: EDX Output of Vacuum Filtered Sample 2
Peak intensity is proportional to the number of atoms present on the fil surface.

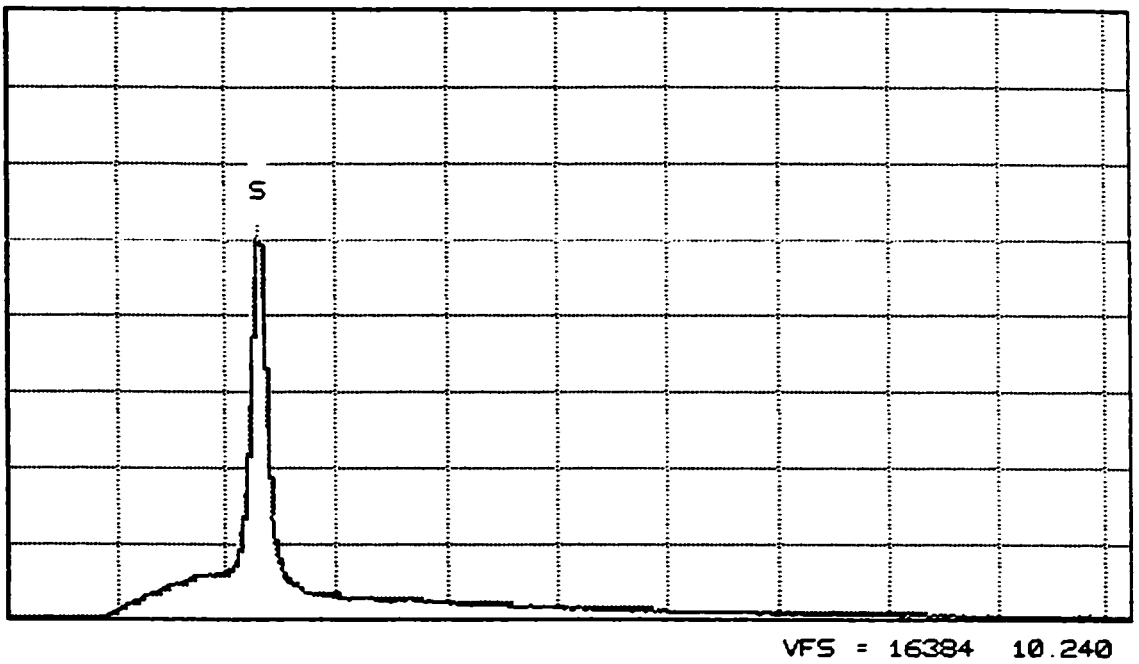

Figure 5.8: EDX Output of Clean, Unused Membrane

Peak intensity is proportional to the number of atoms present on the membrane surface.

Determining the origin of the sodium peak in figure 5.3 is more difficult. It is thought to be attributable to the abundant presence of the sodium cation in the AD/DC waste stream. Of the species present in the AD/DC waste, Na^+ makes up 48 mole percent. The high sodium concentration originates primarily from the detergent used by the DC and from the pH adjustment of the raw feed by sodium hydroxide before microfiltration. Of all the detergents and cleaners used by the DC, Decon 4324NP makes up the largest percentage (by volume) of the DC waste steam sent to the WTC for processing. The weekly production of DC waste is 40 000 litres. The volumes and percentages of the detergents and cleaners used by the DC are tabulated in table 5.2. The DC waste is made up mostly of Decon 4324NP. Various components make up the Decon 4324NP including some sodium salts, one of which is sodium citrate (Deane and Company, 1996). The high concentrations of sodium found in the AD/DC wastes most likely originate from the Decon 4324NP detergent and from the NaOH added for pH adjustment.

The membranes were not rinsed prior to being autopsied so many of the species present in the AD/DC waste crystallize onto the membrane surface which would leave large amounts of sodium on its surface as it dries. This is illustrated by the precipitation of sodium chloride crystals onto the membrane surface shown in figure 5.9. Nevertheless, sodium completely disassociates from any complex in water at near neutral pH values (Snoeyink and Jenkins, 1980). Therefore, any sodium complex should be removed from the membrane easily by rinsing with water. Thus, sodium is not suspected to cause the irreversible fouling of the plant-scale membranes. The focus will remain on the calcium, phosphate and iron precipitates.

Thus, the major potential fouling species in the AD/DC waste that will be dealt with in this report are phosphate and calcium in the form of $Ca_5(PO_4)_3OH$ and iron in the form of Fe_2O_3. These are the suspected compounds that are causing the irreversible fouling of the plant-scale SWRO membranes.

Table 5.2: Estimated Weekly Amounts of Detergents and Cleaners Used by the Decontamination Centre

Detergents/ Cleaners	Amount per Week	units
Decon 4324NP	100	litres
Swish Toilet Bowl Cleaner	24	litres
Phosphoric acid	18	litres
Fantastic	12	litres
Saniflush	12	litres
Spic and Span	500	grams
Nitric Acid	80	millliliters
Antifoam A	30	millliliters
Savlon	30	millliliters

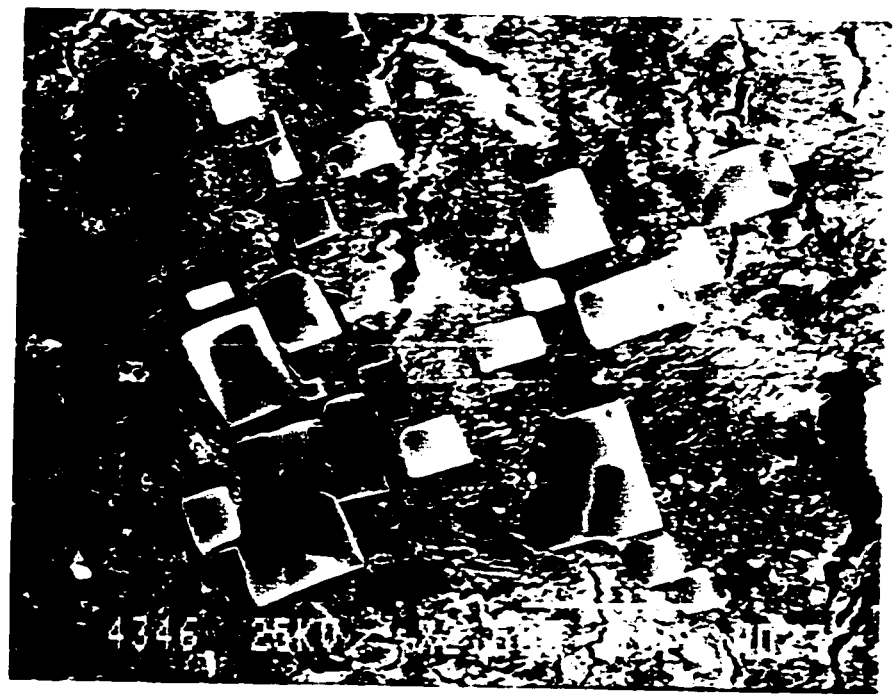

Figure 5.9: SEM Photograph of Sodium Chloride Crystals

5.2 Membrane Performance Characterization by Pure Water Permeability and Salt Solution Tests

The AD/DC waste test runs were performed at various crossflows ranging from 30 L/min to 60 L/min. Before and after each AD/DC waste test run, PWP and salt solution tests were performed to determine if any change in the membrane performance had taken place after processing 400 litre batches of waste at a particular velocity. To produce unbiased results, the crossflow experiments on the AD/DC wastes were performed at random crossflows in the order of 30, 60, 45, 52.5, and 37.5 L/min.

PWP were performed after each run to determine if any irreversible fouling had taken place during any of the AD/DC waste runs. From figure 5.10, it can be seen that no significant decrease in the pure water permeability occurred as a result of the volumetric reductions of the AD/DC waste at the different crossflows. Thus, processing the AD/DC waste had not caused any irreversible fouling. The PWP tests are also helpful in determining if any entrance effects, such as jetting or channeling of flow through the membrane module, was occurring at the higher crossflows. In the absence of dissolved solids, the crossflow is not expected to affect the PWP. Thus, any change in the PWP at different crossflows would be caused by entrance effects. Since the PWP is generally constant for all of the crossflows studied, it can be determined that entrance effects are negligible or are not taking place at all.

Table 5.3 shows the rejection efficiency of the membrane during NaCl tests that were performed in between the AD/DC waste tests. NaCl test 1 was performed before any volumetric reduction of the AD/DC waste occurred. NaCl tests 2, 3 and 4 were performed after three, four, and five 400 litre batches of AD/DC waste were treated respectively.

During NaCl tests 1, 2, and 3, the permeate line was not directed back to the feed tank. This process configuration led to increased salt concentrations in the feed over the course of the run since only the concentrate was being returned to the feed tank. Since the rejection efficiency is highly dependent on the concentration of the bulk feed solution and the concentration was

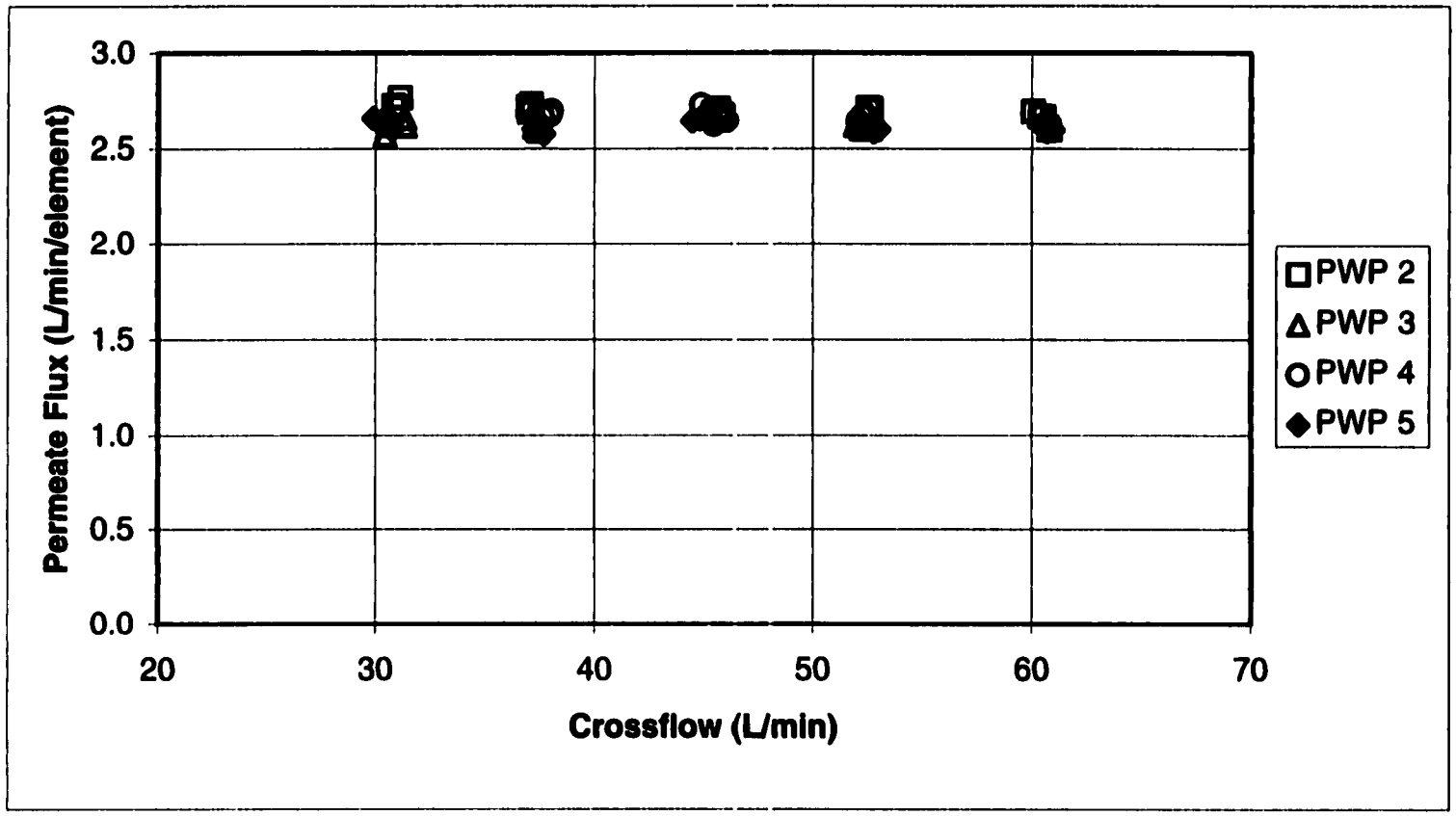

Figure 5.10: Pure Water Permeability Tests at Various Crossflows
(Raw Data Included in Tables C1 to C4)
1 L/min/element=2.65×10^{-6} $m^3/m^2/s$

Table 5.3: Rejection Efficiency of NaCl after Volumetric Reductions of AD/DC Waste
(Raw Data Included in Tables C5 to C8)

NaCl Test 1 Before AD/DC tests			NaCl Test 2 After 3 batches of AD/DC waste processed			NaCl Test 3 After 4 batches of AD/DC waste processed			NaCl Test 4 After 5 batches of AD/DC waste processed		
Crossflow (LPM)	Feed Concentration (wt%)	Rejection Efficiency (%±1%)	Crossflow (LPM)	Feed Concentration (wt%)	Rejection Efficiency (%±1%)	Crossflow (LPM)	Feed Concentration (wt%)	Rejection Efficiency (%±1%)	Crossflow (LPM)	Feed Concentration (wt%)	Rejection Efficiency (%±1%)
29.3	2.8	99	30.4	2.4	99	31.0	2.6	99	29.8	3.1	98
						31.2	2.6	99	29.7	3.1	97
						31.1	2.6	99	29.6	3.1	97
37.8	2.9	98	37.6	2.6	99	37.6	2.7	98	37.5	3.1	97
						37.7	2.8	98	37.6	3.1	98
						37.8	2.8	N/A	37.6	3.1	97
45.7	3.0	98	45.1	2.8	98	45.5	3.0	98	45.2	3.1	98
						45.5	3.0	98	45.2	3.1	98
						45.5	3.0	98	45.2	3.1	98
52.7	3.0	98	52.5	2.9	98	52.5	3.0	97	52.6	3.1	97
						52.5	3.1	97	52.6	3.1	97
						52.4	3.1	N/A	52.7	3.1	97
60.7	3.1	98	60.5	3.0	97	60.4	3.2	97	60.6	3.1	97
						60.4	3.2	97	60.6	3.1	97
						60.2	3.2	N/A	60.5	3.1	97

increasing with time, the rejection efficiency decreased from 99 to 98 percent during NaCl test 1 and 99 to 97 percent during NaCl tests 2 and 3.

An attempt to eliminate this increase in feed concentration was made during NaCl test 4. During NaCl test 4, the pilot-scale system was operated in full recirculation mode. Both the permeate and retentate lines were sent back to the feed tank in an attempt to maintain a relatively constant NaCl feed concentration. Unfortunately, it was necessary for samples to be taken for conductivity and this requirement would produce a slight increase in salt concentration over the duration of the run. However, the increase in concentration during test 4 was not as drastic as the increases seen in NaCl tests 1, 2, and 3. Again, with a slight increase in salt concentration over the duration of NaCl test 4, the rejection efficiency decreased from 98 to 97 percent.

Thus, it can be concluded that no significant change in the rejection efficiency of salt had taken place as a result of the volumetric reductions of AD/DC waste batches.

5.3 Determination of the Sodium Chloride Mass Transfer Coefficient

The mass transfer coefficient of the membrane with respect to sodium chloride was determined for crossflows of 30 L/min, 37.5 L/min, 45 L/min, 52.5 L/min and 60 L/min. It is possible to determine the mass transfer coefficient of salt (k_{NaCl}) by measuring the permeate flux during runs with a NaCl solution and with a pure water solution at each crossflow. Sample calculations are included in example A.3 of Appendix A.

Table 5.4 shows the values of the mass transfer coefficients for NaCl at each crossflow for two different trials. The k_{NaCl} was found after the volumetric reduction of 400 litres of AD/DC waste at a crossflow of 52.5 L/min and after the volumetric reduction at a crossflow of 37.5 L/min. Measurements at each crossflow velocity were taken in triplicate to determine reproducibility. The anticipated result of the mass transfer coefficient experiments was k_{NaCl} would increase with an increase in crossflow. This was not the case. A maximum k_{NaCl} is reached at a crossflow of 45 L/min in both cases. Although, figure 5.10 does not suggest that

Table 5.4: Mass Transfer Coefficient of NaCl at Various Crossflows

Crossflow (LPM)	k_{NaCl} 1 (m/s)	k_{NaCl} 2 (m/s)	Average (m/s)
30	1.89E-05	2.70E-05	3.20E-05
30	3.23E-05	3.76E-05	
30	4.40E-05	3.21E-05	
37.5	5.48E-05	3.28E-05	4.07E-05
37.5	4.14E-05	4.29E-05	
37.5	3.35E-05	3.86E-05	
45	4.74E-05	4.79E-05	5.42E-05
45	5.44E-05	4.95E-05	
45	4.59E-05	8.00E-05	
52.5	2.05E-05	4.08E-05	3.35E-05
52.5	2.41E-05	4.27E-05	
52.5	2.78E-05	4.50E-05	
60	1.57E-05	3.19E-05	2.40E-05
60	1.98E-05	2.85E-05	
60	2.34E-05	2.47E-05	

entrance effects are evident at the higher crossflows of 52.5 L/min and 60 L/min, entrance effects may be taking place to some extent. The PWP measurements taken are most likely not sensitive enough to detect any entrance effects but the mass transfer coefficient is quite sensitive to changes in permeate flux.

The FILMTEC® TFC membrane modules are rated at a maximum feed flow of 60 L/min (Dow Chemical Company, 1994). This value is the maximum allowable crossflow recommended by the manufacturer to prevent telescoping of the modules. Telescoping takes place when the crossflow is sufficiently high enough to damage the internal support of the spiral wound membrane module. This causes the spiral wound module to elongate in a similar fashion to an extended telescope. The maximum crossflow does not necessarily indicate the optimum operating conditions for the membrane module.

Figure 5.11 shows the average of all six k_{NaCl} values shown in table 5.4 with a confidence level of 95 percent. Figure 5.11 shows an optimum k_{NaCl} at a crossflow of 45 L/min. Using the average k_{NaCl} found at each crossflow, the boundary layer concentrations of the potential fouling species identified in section 5.1 can be predicted during the volumetric reduction of the AD/DC waste at all the various crossflows.

At the different crossflows of 30, 37.5, 45, 52.5, and 60 L/min, the boundary layer concentrations of calcium, phosphate and iron were predicted. The mass transfer coefficient of the ions of interest (Ca^{2+}, PO_4^{3-}, and Fe^{3+}) were calculated by the two-thirds rule (equation 5) using the average k_{NaCl} found at each crossflow. The mass transfer coefficient (k_{ion}) was used to find the mole fraction of the ion at the membrane surface (x_{A2}) using equation 3. Sample calculations are provided in example A.4 in Appendix A.

Figure 5.12 shows the predicted concentration of calcium ions fully dissolved at the membrane surface at the various crossflows. An average concentration of the initial bulk solutions (see table 5.1) was taken so that the effect of crossflow on the boundary layer

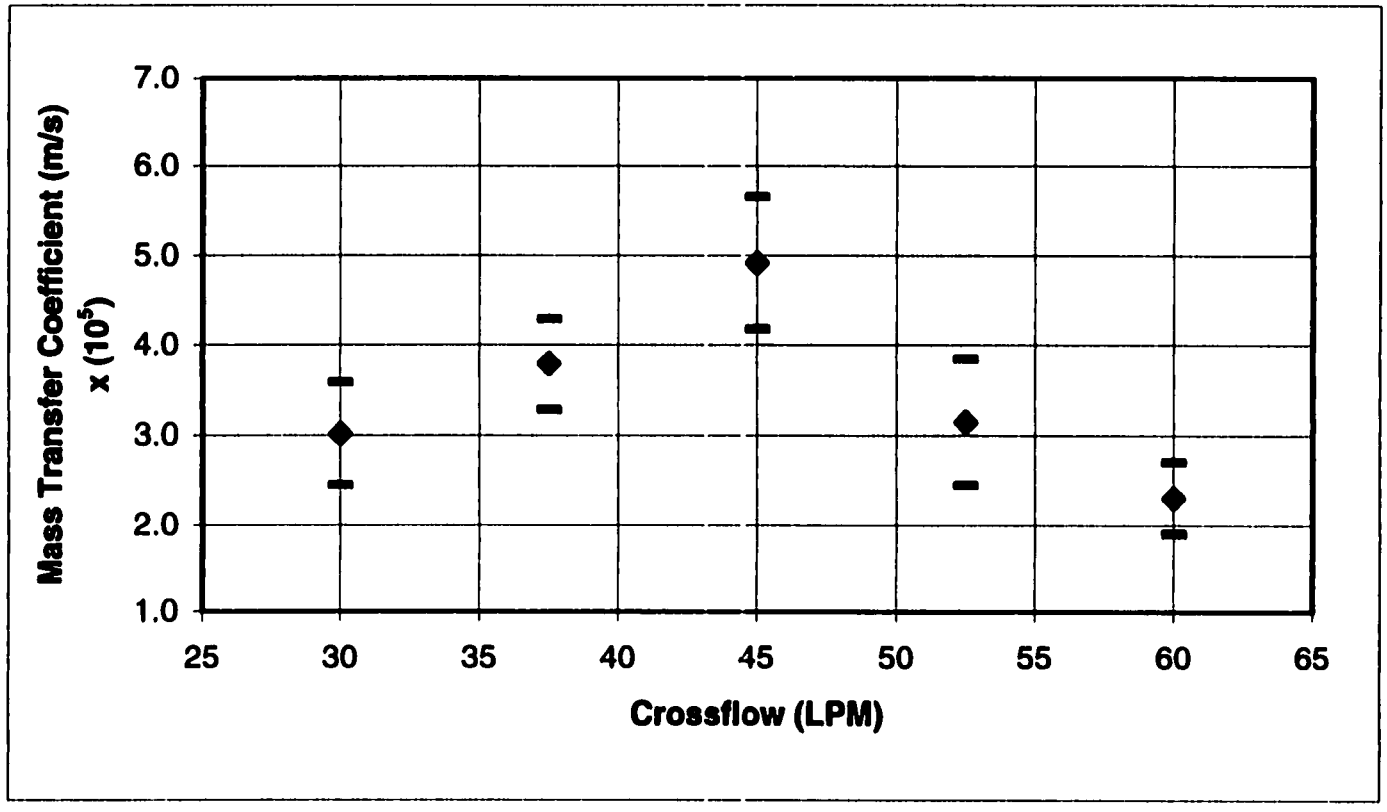

Figure 5.11: Average k_{NaCl} values with 95% Confidence Level

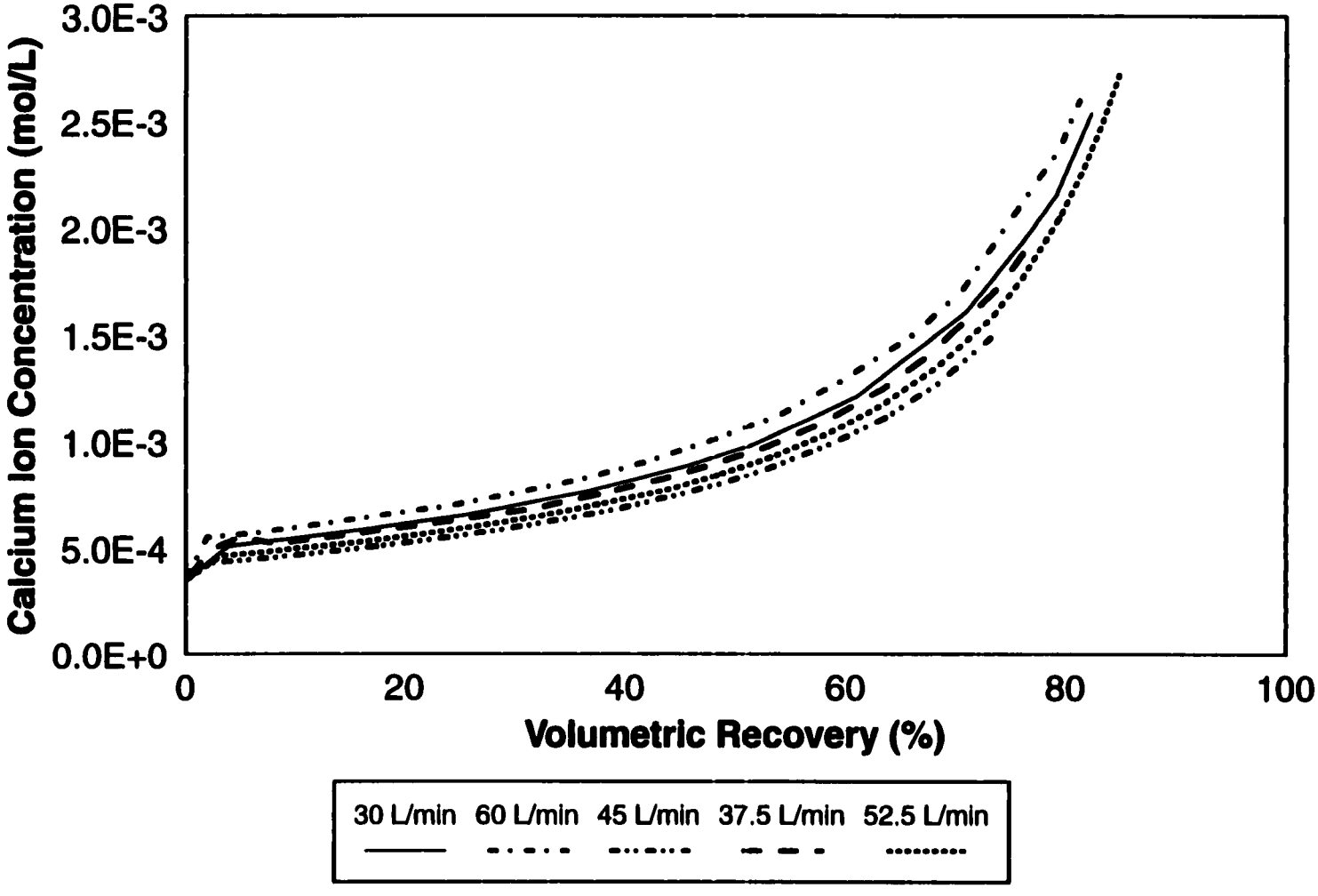

Figure 5.12: Boundary Layer Calcium Ion Concentration at Various Crossflows

concentration could be illustrated. Figure 5.12 shows that a crossflow of 45 L/min gives the lowest boundary layer concentration and crossflows of 30 L/min and 60 L/min tend to cause higher boundary layer concentrations which in turn creates a greater potential for fouling. This indicates that a moderate crossflow velocity should be utilized to minimize the concentration polarization effects that cause the higher boundary layer concentrations. The same trend occurs with fully dissolved Fe^{3+} ions as shown in figure 5.13. Crossflows of 30 L/min and 60 L/min tend to maximize the effects of concentration polarization and a crossflow velocity of 45 L/min tends to minimize the effects of concentration polarization.

Figure 5.14 shows the effect of crossflow velocity on the boundary layer concentration of PO_4^{3-}. The PO_4^{3-} concentration was determined by chemical equilibrium calculations involving the total phosphate concentration discussed in section 3.3. Unfortunately, it is not possible to measure the concentration of PO_4^{3-} directly. Only the total free phosphate in the forms of H_3PO_4, $H_2PO_4^-$, HPO_4^{2-}, and PO_4^{3-} can be measured by ion liquid chromatography. The concentration of PO_4^{3-} can be determined from the chemical equilibria with respect to the total free phosphate. This calculation is highly dependent on pH. The pH of the AD/DC waste increases as the waste is volumetrically reduced. As the pH increases, the more the equilibria shifts to the form of PO_4^{3-}. The combination of the increasing volumetric reduction and the increasing pH magnifies the increase in the PO_4^{3-} concentration. This can be seen by the sharp increase in PO_4^{3-} concentration at approximately 80% volumetric recovery in figure 5.14.

It has been shown that the crossflow velocity does play a role in the membrane performance when processing sodium chloride solutions by spiral-wound reverse osmosis. The next section evaluates the extent to which crossflow velocity does play a role when processing the AD/DC waste.

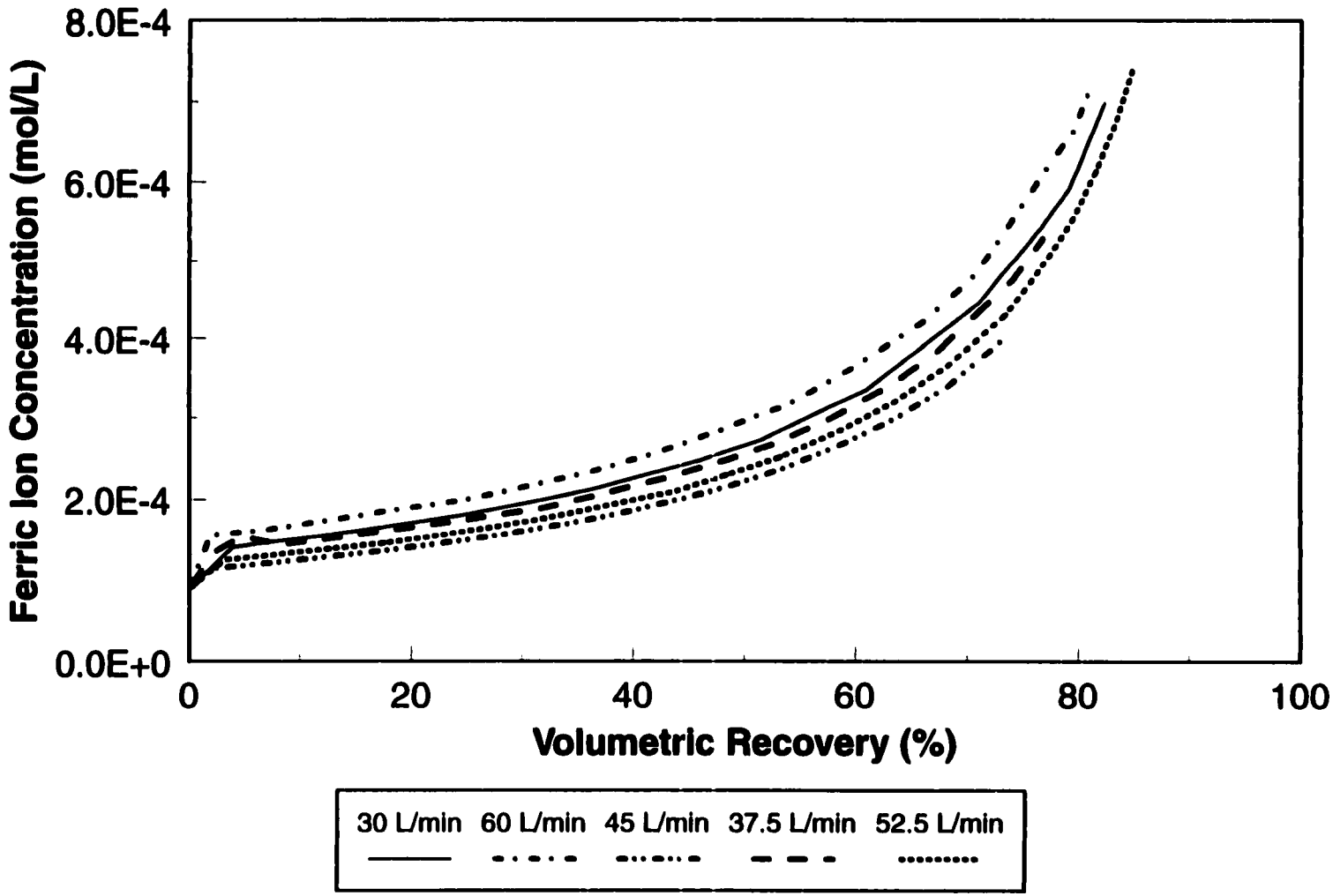

Figure 5.13: Boundary Layer Concentration of Ferric Ion at Various Crossflows

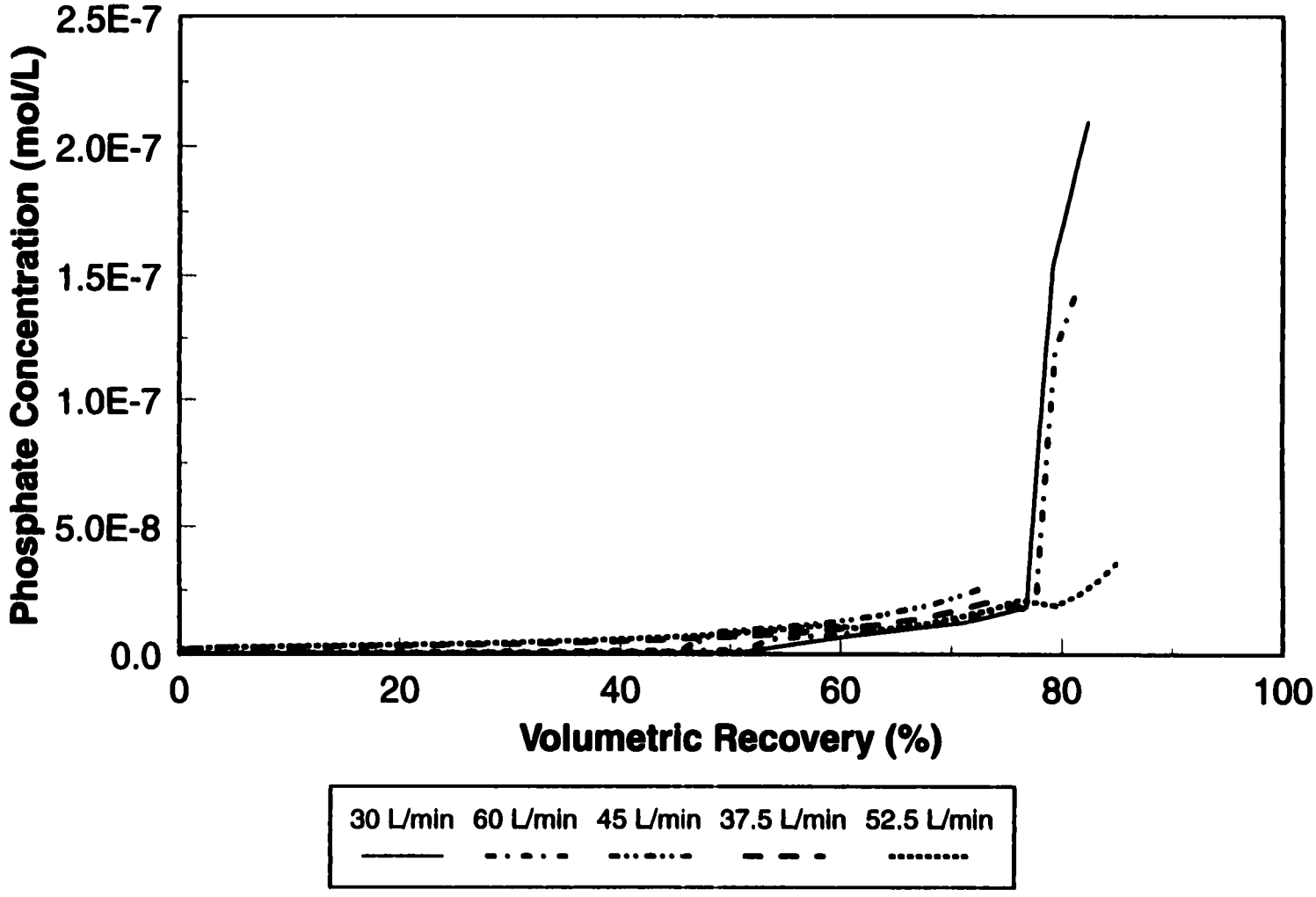

Figure 5.14: Boundary Layer Concentration of Phosphate at Various Crossflows

5.4 Extent of Crossflow Velocity Effects on Permeate Flux

In this section, the extent to which crossflow plays a role in improving the permeate flux during the volumetric reduction of the AD/DC runs is evaluated and discussed.

The volumetric reduction of the AD/DC waste at each crossflow velocity of 30, 37.5, 45, 52.5, and 60 L/min is plotted in figure 5.15. Based on figure 5.15, there is no advantage to using a crossflow of 45 L/min. This contradicts the findings of an optimum crossflow of 45 L/min in section 5.3. If the permeate flux of the AD/DC waste were primarily dependent on boundary layer concentrations, it should be possible to predict the permeate flux by osmotic pressure calculations based on the boundary layer concentrations. If this were true, then the permeate flux of the AD/DC waste would be dependent on the crossflow velocity just as the salt solution permeate fluxes. If the permeate flux, when processing the AD/DC waste, is dependent primarily on the osmotic pressure caused by boundary layer concentrations, the actual permeate flux and the permeate flux predicted from osmotic pressure calculations should be the same.

The predicted permeate fluxes at each crossflow were calculated from the bulk solution concentration of each of the ionic species present in the AD/DC waste at several volumetric recoveries found in table 5.5. The VRF can be calculated from volumetric recovery using equation 23. A sample calculation is shown in example A.5 of Appendix A. The concentrations of each ion at each volumetric recovery were found in the same manner as the values for the 85 percent volumetric recovery found in table 5.1. (Refer to example A.2 of Appendix A). The bulk solution concentrations of each ion at each VRF in table 5.5 were inputted into the MINTEQA2 equilibrium solution program. The output data give the concentration of the species precipitated and dissolved. The estimated concentration of the precipitated species are given in table 5.5. The significance of the precipitated species will be discussed later. A sample output of the MINTEQA2 compilation at 85 percent volumetric recovery is shown in Appendix D.

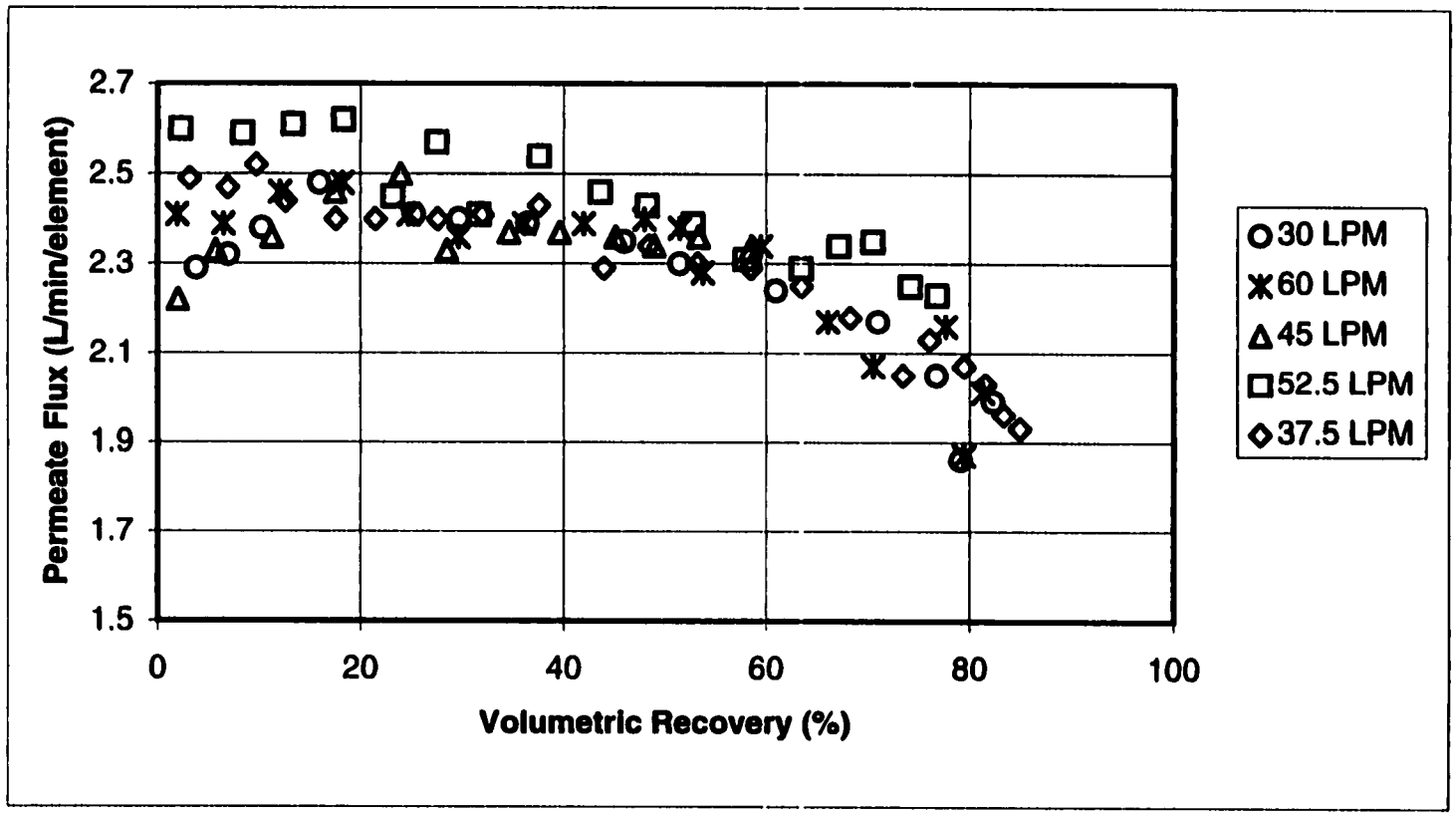

Figure 5.15: Actual Permeate Flux of AD/DC Waste at the Various Crossflows

1 L/min/element=2.65×10^{-6} $m^3/m^2/s$

Table 5.5: Estimated Concentrations at Various Volumetric Recoveries

Volumetric Recovery		0%	20%	40%	50%	60%	65%	70%	75%	80%	85%
VRF		1.0	1.3	1.7	2.0	2.5	2.9	3.3	4.0	5.0	6.7
MINTEQA2 Input											
pH		6.4	6.4	6.4	6.4	6.4	6.4	6.4	6.4	6.4	6.4
Iron	(mg/L)	5	6	8	10	13	14	17	20	25	33
Sodium	(mg/L)	263	328	438	526	657	751	876	1051	1314	1752
Magnesium	(mg/L)	3.4	4	6	7	8	10	11	13	17	22
Calcium	(mg/L)	14.1	18	24	28	35	40	47	57	71	94
Aluminum	(mg/L)	<1.1	NA	NA	NA	NA	NA	NA	NA	NA	NA
Chloride	(mg/L)	130	163	217	260	325	372	433	520	650	867
Nitrate	(mg/L)	104	130	173	208	260	297	347	416	520	693
Phosphate	(mg/L)	481	601	801	961	1202	1373	1602	1923	2403	3204
Sulfate	(mg/L)	62	77	103	123	154	176	205	246	308	410
Bicarbonate	(mg/L)	50	63	83	100	125	143	167	200	250	333
Citrate	(mg/L)	88	109	146	175	219	250	292	350	438	583
MINTEQA2 Output											
$Ca_5(PO_4)_3OH$	(mg/L)	19	30	41	53	70	83	99	123	159	192
Fe_2O_3	(mg/L)	7	10	12	14	18	21	24	29	36	48
Total Solids	(mg/L)	26	39	53	67	88	103	123	152	195	240

The boundary layer concentration and the osmotic pressure of each of the dissolved species in the MINTEQA2 output data is calculated simultaneously by solving equation 21. Once again, the value of k_{ion} is calculated by equation 5 using the average k_{NaCl} at each crossflow in table 5.4. The membrane constant, A, is calculated by taking the average of all of the pure water permeabilities at each crossflow in figure 5.10. The values of k_{NaCl} and A used in the prediction of the permeate flux at each crossflow is summarized in table 5.6:

Table 5.6: Values of k_{NaCl} and A for Permeate Flux Predictions

Crossflow (L/min)	k_{NaCl} (m/s)	A (m/atm/s)
30	3.20×10^{-5}	2.63×10^{-7}
37.5	4.07×10^{-5}	2.55×10^{-7}
45	5.42×10^{-5}	2.57×10^{-7}
52.5	3.35×10^{-5}	2.63×10^{-7}
60	2.40×10^{-5}	2.63×10^{-7}

The predicted permeate flux was calculated using equations 18 to 21 based on osmotic pressure and boundary layer concentrations calculated from the concentrations of ions predicted to be in solution by MINTEQA2. Since osmotic pressure is a colligative property, it can be assumed that all ions that MINTEQA2 predicts to be in solution behave independently of each other. Thus, the osmotic pressure can be calculated as the sum of all contributions of individual ions present in solution. Detailed sample calculations (example A.6) can be found in Appendix A.

If the osmotic pressure from boundary layer concentrations caused by concentration polarization were the only factor influencing the decline in permeate flux, the actual flux curve should be superimposed on the predicted flux curve. As shown in figures 5.16 to 5.20, this is not the case with any of the crossflows studied. Thus, another factor is playing a role in the permeate flux decline that was not present with the salt solution tests; particulate loading. The

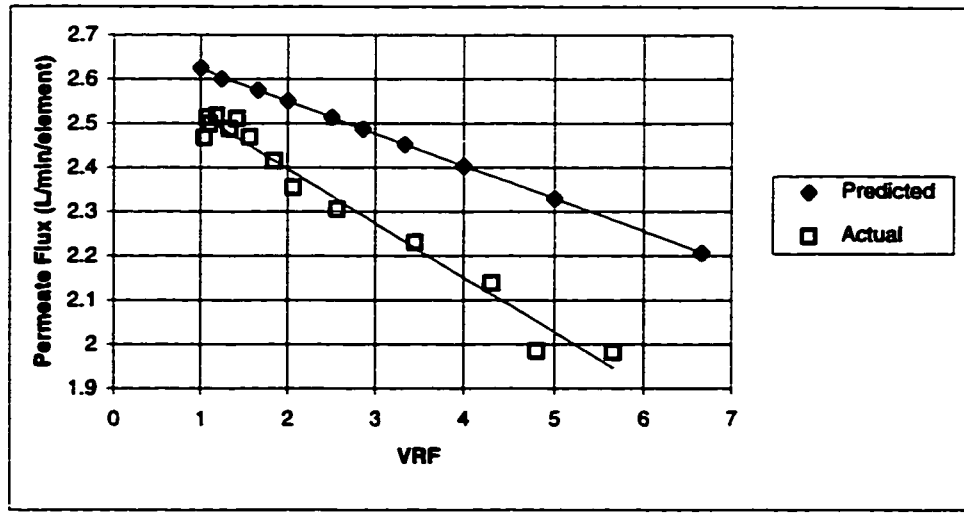

Figure 5.16: Predicted and Actual Permeate Fluxes at 30 L/min Crossflow
1 L/min/element=2.65×10^{-6} $m^3/m^2/s$

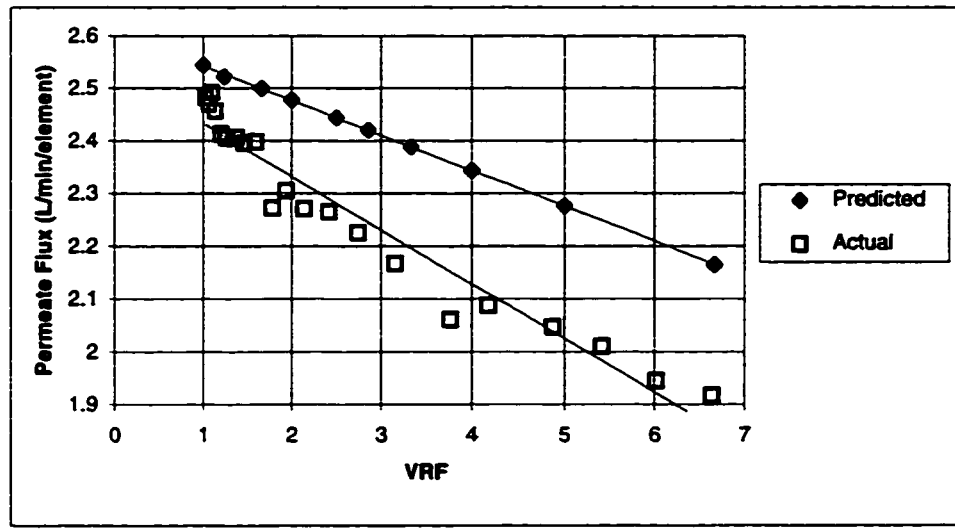

Figure 5.17: Predicted and Actual Permeate Fluxes at 37.5 L/min Crossflow
1 L/min/element=2.65×10^{-6} $m^3/m^2/s$

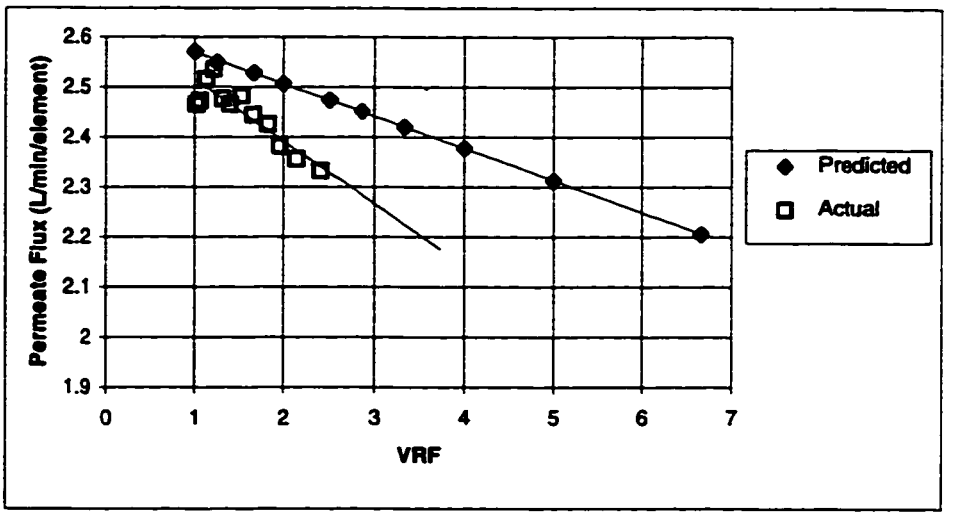

Figure 5.18: Predicted and Actual Permeate Fluxes at 45 L/min Crossflow
1 L/min/element=2.65×10^{-6} $m^3/m^2/s$

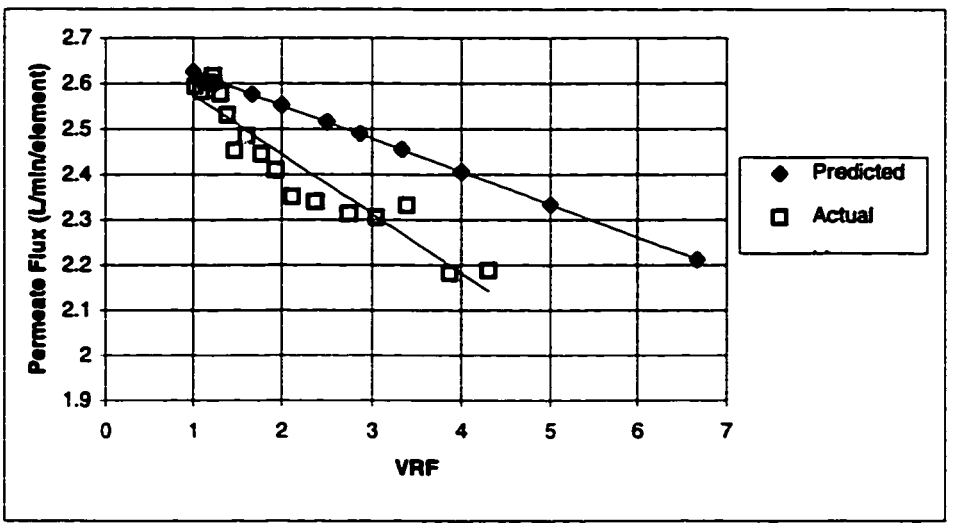

Figure 5.19: Predicted and Actual Permeate Fluxes at 52.5 L/min Crossflow
1 L/min/element=2.65×10^{-6} $m^3/m^2/s$

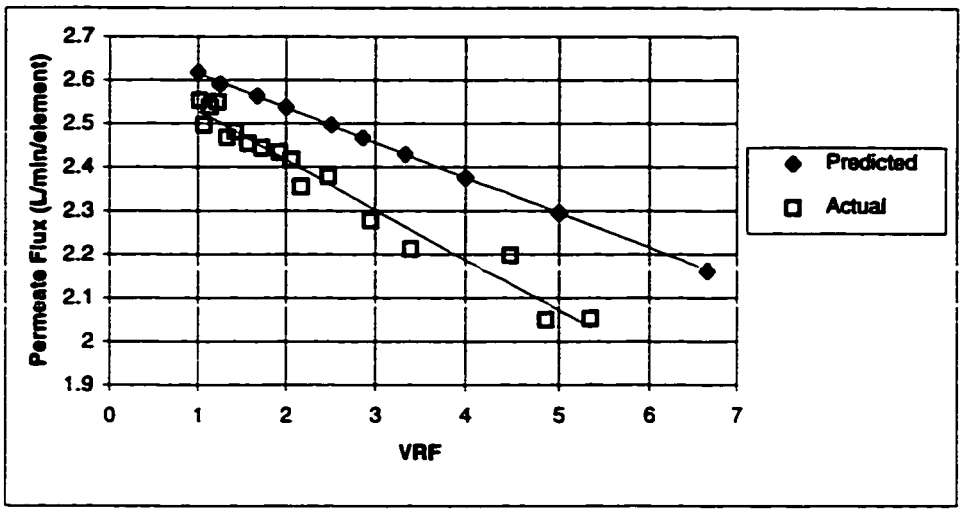

Figure 5.20: Predicted and Actual Permeate Fluxes at 60 L/min Crossflow
1 L/min/element=2.65×10^{-6} $m^3/m^2/s$

influence of particulate loading on the membrane performance increases as the VRF increases. Figures 5.16 to 5.20 show the difference between the predicted and actual permeate fluxes is greatest at the higher VRFs.

The mass transfer coefficients found in section 5.2 suggest that a crossflow of 45 L/min should give the best membrane performance. The slopes, intercepts, and sums of the squares of the residuals of the predicted and actual permeate fluxes are shown in table 5.7 and 5.8 respectively. The predicted flux slopes indicate how quickly the permeate flux should decline when processing the AD/DC waste if the permeate flux was dependent primarily on boundary layer concentrations. The better predicted membrane performance is indicated by the lowest negative slope of the predicted flux curve at a 45 L/min crossflow in table 5.7. It can be seen that a greater decline in flux is predicted when processing the waste at 30 L/min and 60 L/min. The slopes of the actual flux, found in table 5.8, do not support this. The lowest negative slope of the actual flux curves was found for a crossflow of 37.5 L/min and the highest negative slope was found for a 52.5 L/min crossflow. Thus, it can be concluded that the membrane performance is not dependent mainly on boundary layer concentrations but on particulate concentrations during the processing of the AD/DC waste. Hence, the permeate flux cannot be improved significantly by changing the crossflow velocity because of the overriding influence of the particulates in the AD/DC waste stream. This is in agreement with work performed by Sethi and Wiesner (1995) which was discussed in section 2.6.

The next step was to evaluate particulate loading and its affect on flux decline. The difference between the predicted flux, based on osmotic pressure considerations, and the actual flux at each crossflow velocity was plotted against the total precipitated solids as shown in figure 5.21. The total precipitated solids were estimated using the MINTEQA2 equilibrium solution program and are listed in table 5.5 for each VRF. It can be seen in figure 5.21 that at higher total precipitated solids concentrations, the difference between the predicted and actual permeate flux levels off. This suggests that at the higher precipitated solids concentrations a

Table 5.7: Slope, y-Intercept, and R^2 of Best Fit Line of Predicted Permeate Flux Data

Crossflow (L/min)	Slope	y-Intercept	R^2
30	-0.0735	2.6965	0.9998
37.5	-0.0668	2.6100	0.9998
45	-0.0643	2.6339	0.9998
52.5	-0.0727	2.6966	0.9998
60	-0.0801	2.6957	0.9998

Table 5.8: Slope, y-Intercept, and R^2 of Best Fit Line of Actual Permeate Flux Data

Crossflow (L/min)	Slope	y-Intercept	R^2
30	-0.1231	2.6427	0.9722
37.5	-0.1020	2.5353	0.9442
45	-0.1250	2.6408	0.8162
52.5	-0.1313	2.7067	0.8951
60	-0.1146	2.6449	0.9622

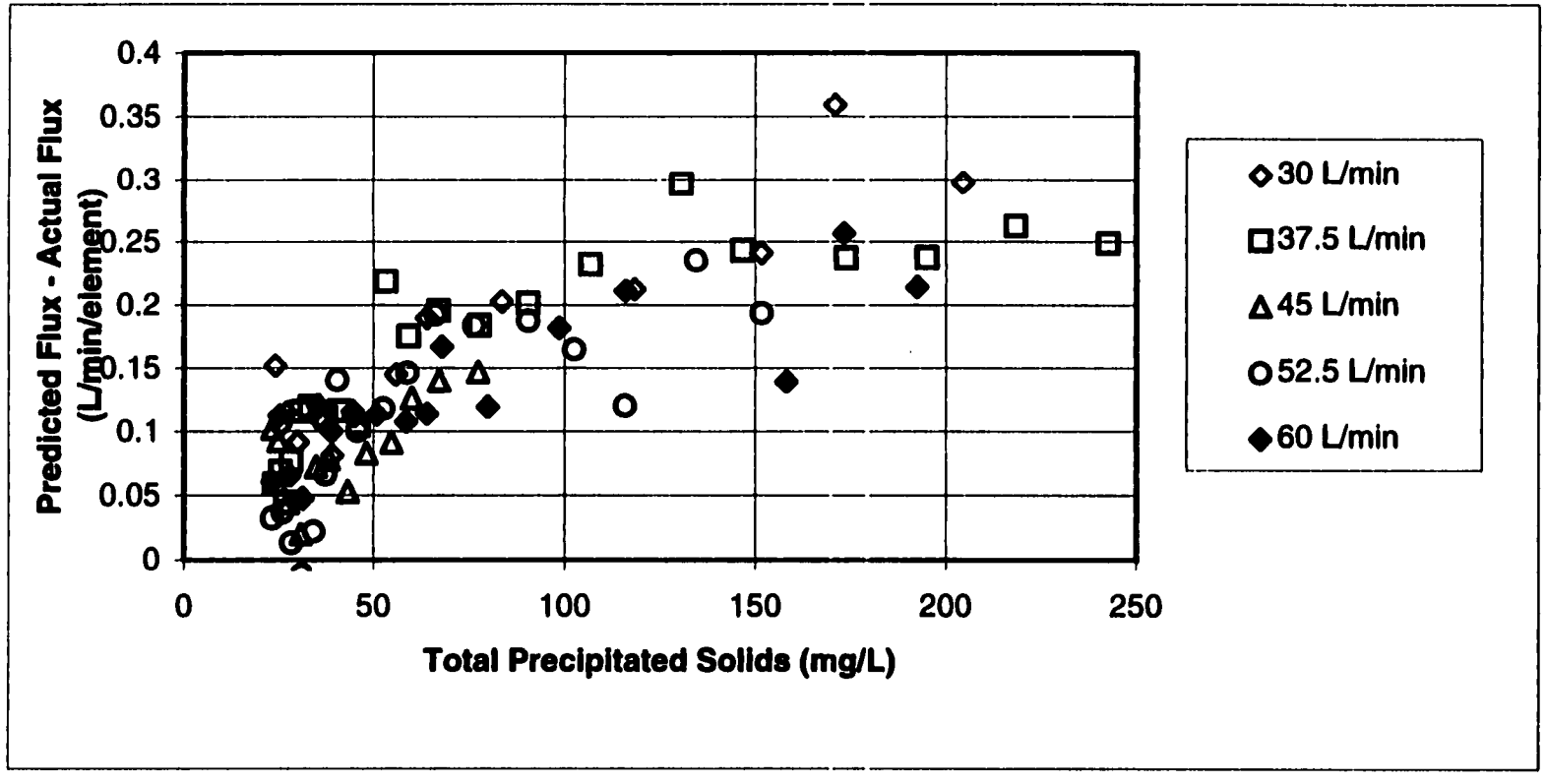

Figure 5.21: Difference Between Predicted and Actual Permeate Flux at the Various Crossflows versus Total Precipitated Solids
1 L/min/element=2.65×10^{-6} $m^3/m^2/s$

fouling layer or cake forms on the surface of the membrane. The presence of the cake limits the mass transfer through the membrane. The presence of particles in the AD/DC waste produces a greater than expected reduction in permeate flux at all crossflows, especially at the higher VRFs as seen in figures 5.16 to 5.20. This supports the observation that crossflow has no effect when particulates are present in solution.

The pilot-scale system, which operates in batch mode, processes waste at high VRFs only near the end of the run. The plant-scale SWRO system operates in feed-and-bleed mode which processes the AD/DC waste at high VRFs throughout the entire run. The discrepancies in the predicted permeate flux and actual permeate flux is greatest at the higher VRFs. This indicates that operating in batch mode may help prevent the severe permeate flux declines that the plant-scale SWRO system has been experiencing.

Unfortunately, due to the radioactive nature of the AD/DC waste, no particulate size analysis could be conducted. Analysis of the AD/DC waste would have contaminated the size analysis equipment. However, SEM photographs were taken of the fouled membranes taken from the plant-scale SWRO system. Figure 5.22 shows a deposit on the membrane, 300 μm across at its widest point. It would not be possible to determine the particulate size during the runs since the particulates would have grown in size as the run proceeded.

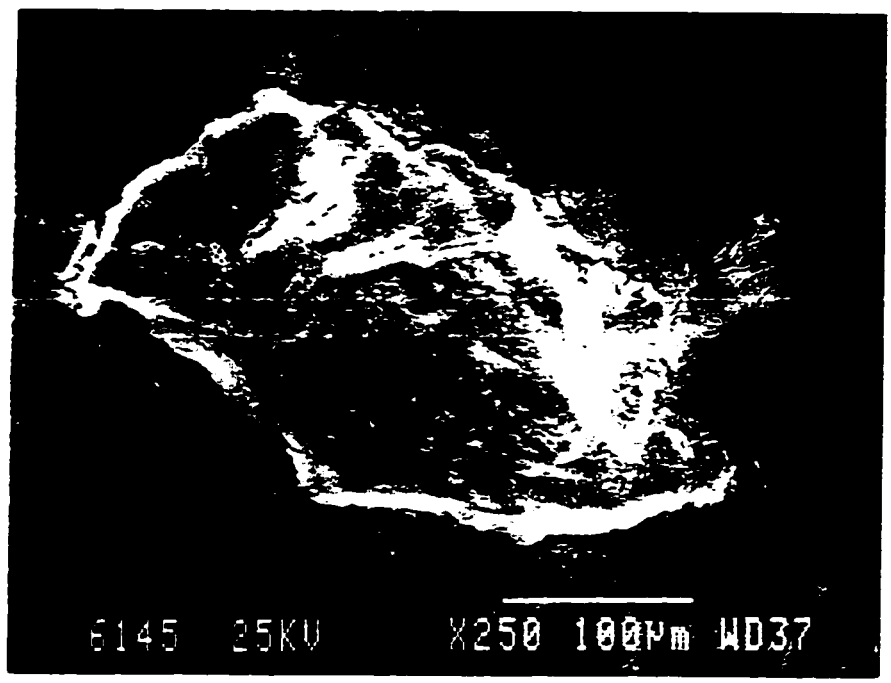

Figure 5.22: SEM Photograph of Membrane Deposit

Chapter 6

Evaluation of Three-Step Cleaning Procedure for Improving Membrane Performance

The pilot-scale SWRO membranes have experienced severe fouling over their operational lifetime at the CRL site (see section 2.9.3). In an attempt to remove deposits from the membrane surface and improve the permeate flux, a three-step cleaning procedure has been developed. The performance of the three-step cleaning procedure with respect to permeate flux improvement is discussed in section 6.1. To determine if the improved permeate flux resulting from the cleaning could be maintained, batches of AD/DC waste were processed and the permeate flux measured. In section 6.2, the effect of the aggressive cleaning procedure on the rejection efficiency of the membrane for cesium and strontium is discussed. The raw data for the work conducted for chapter 6 can be found in Appendix E.

6.1 Effect of Cleaning on Permeate Flux

In this section, the results of the cleaning procedure performed on the fouled reverse osmosis membranes taken from the plant-scale system are given and discussed. The cleaning procedure and the tests performed to measure the performance of the cleaning are given in section 4.4.

6.1.1 Effect of the Three-Step Cleaning Procedure on Overall Membrane Performance

Two modules were removed from the head of two different pressure vessels in the first stage of the plant-scale spiral wound reverse osmosis system. The first step was to determine the extent of the fouling on the membranes. It would be expected that both modules would be fouled to the same extent but the pure water flux observed before cleaning for module 1 was 0.480 L/min/element (table 6.1) and the pure water flux observed before cleaning for module 2 was 0.693 L/min/element (table 6.2). The before cleaning permeate flux of module 2 is almost 50 percent higher than that of module 1 indicating that module 1 was fouled to a greater extent than module 2. This suggests that the feed flow in the plant-scale spiral wound reverse osmosis system is not being divided amongst the five pressure vessels equally. Module 1 may have been situated in a pressure vessel that had a much lower crossflow velocity than the pressure vessel module 2 was placed. Unfortunately, this is impossible to determine as the pressure vessels do not have individual flowmeters.

Steps 1 and 2 were identical for both modules cleaned. In step 3, module 1 was cleaned with an EDTA solution and module 2 was cleaned with a NTA solution. The improvement in permeate flux for each individual cleaning step is summarized in table 6.1 for module 1 and in table 6.2. for module 2.

Table 6.1 shows the pure water permeability of module 1 at 2760 kPa before cleaning and after each cleaning step. It can be seen from table 6.1 that after the final cleaning step, the pure water permeability of module 1 at 2760 kPa more than doubled. After the cleaning procedure, the permeate flux improved by almost 140 percent when compared to the before cleaning flux.

Table 6.2 shows the pure water permeability of module 2 at 2760 kPa before and after each cleaning step. Module 2 showed dramatic improvements in the permeate flux as well, although not quite as great as for module 1. Module 2 showed an improvement of approximately 70 percent at 2760 kPa after the final cleaning step.

Table 6.1: Permeate Flux Improvements of Module 1 at 2760 kPa

	Pure Water Permeability Test		
	Permeate Flux (L/min/element)*	Overall Improvement (%)	Improvement After Each Cleaning Step (%)
Before Cleaning	0.480	--	--
After Triton-X	0.834	73.5	73.5
After HCl	0.951	97.9	14.0
After NaOH and EDTA	1.140	137.4	19.9

*1 L/min/element = 2.65×10^{-6} $m^3/m^2/s$

Table 6.2: Permeate Flux Improvements of Module 2 at 2760 kPa

	Pure Water Permeability Test		
	Permeate Flux (L/min/element)*	Overall Improvement (%)	Improvement After Each Cleaning Step (%)
Before Cleaning	0.693	--	--
After Triton-X	1.021	47.3	47.3
After HCl	0.970	40.0	none
After NaOH and EDTA	1.164	68.0	20.0

*1 L/min/element = 2.65×10^{-6} $m^3/m^2/s$

Figure 6.1 shows the improvement in the permeate flux after the three-step cleaning procedure for both modules at all the pressures tested. The pure water permeability of module 1 before cleaning varied from 0.25 to 0.9 L/min from 1400 kPa to 5500 kPa. After cleaning, the range in the pure water permeability increased from 0.6 to 2.3 L/min over the pressure range tested. As mentioned previously, module 2 appeared less fouled than module 1. This is indicated by the higher pure water flux of module 2 before cleaning than the pure water permeability of module 1 before cleaning. Despite the difference in the initial pure water flux between the two modules, the pure water flux of both elements is approximately the same at all the pressures tested after cleaning. The pure water permeability after cleaning ranged from just over 0.5 L/min to approximately 2.3 L/min. The nearly identical permeate flux of both of these modules after cleaning would suggest that the membranes were cleaned to the maximum possible extent that they could by the three-step cleaning procedure. The flux after cleaning is approximately 50 percent of a new membrane module's performance. According to the manufacturer's membrane performance data, module 1 displayed a permeate flux of 3.11 L/min when processing a salt solution of 3.2 wt% and module 2 displayed a permeate flux of 3.06 L/min for the same feed stream when they were new (Zenon Environmental Systems Inc., 1993).

6.1.2 Improvement Observed After Each Individual Cleaning Step

Looking at the efficiency of each individual cleaning step, it appears that Triton X-100 gave the best permeate flux improvement in comparison to the other two cleaning steps for both modules. It can be seen from tables 6.1 and 6.2 that module 1 resulted in an improved flux of 73.5 percent at the pressure tested (2760 kPa) after cleaning with Triton X-100 and module 2 gave an improved flux of 47.3 percent. The HCl cleaning resulted in the least improvement in the permeate flux; approximately 14 percent for module 1 and no improvement for module 2. The cleaning with NaOH and EDTA on module 1 resulted in an improvement of 19.9 percent; and the cleaning with NaOH and NTA on module 2 resulted in an improvement of 20.0 percent.

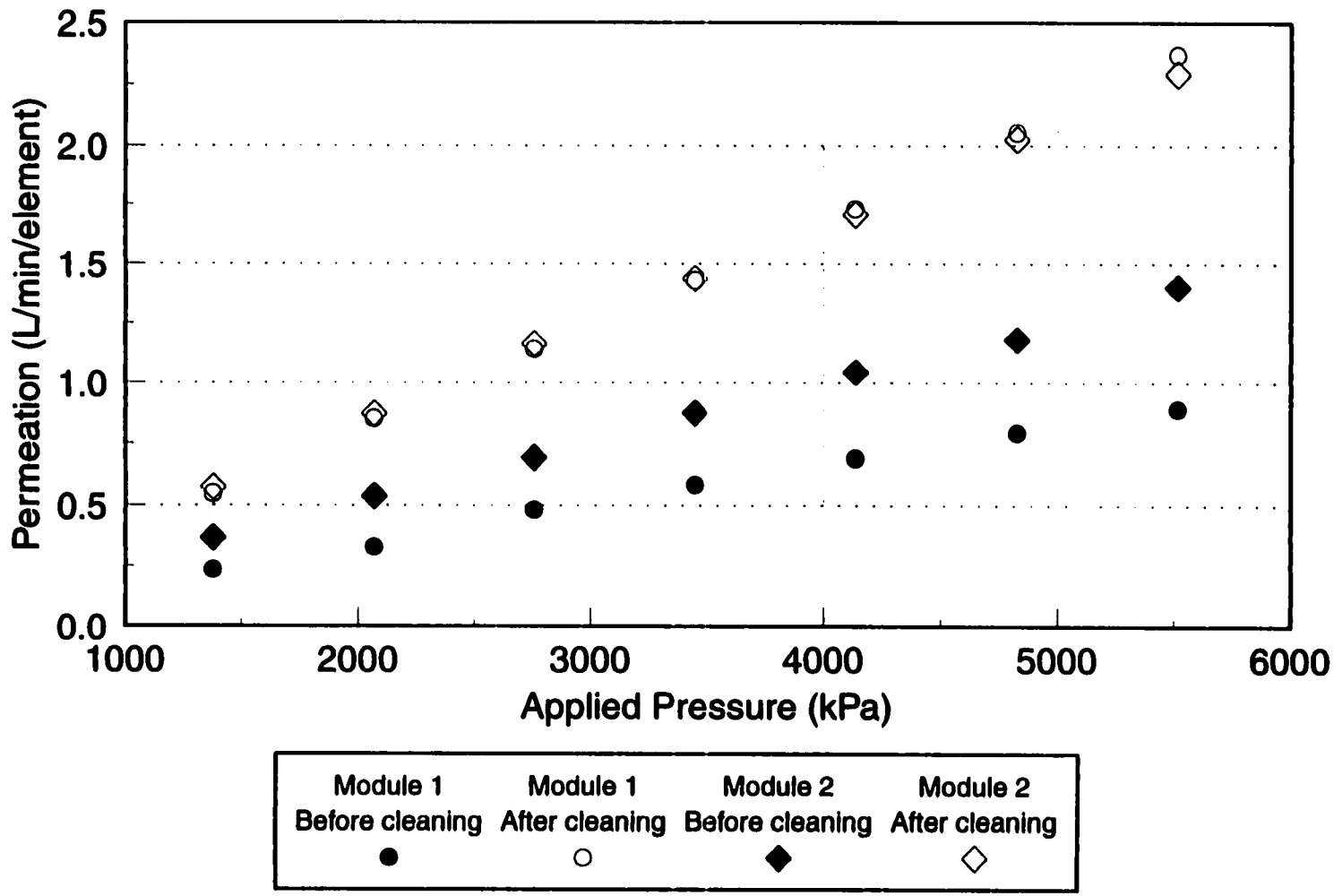

Figure 6.1: Pure Water Permeability Tests Performed Before and After Cleaning
(1 L/min/element = 2.65×10^{-6} $m^3/m^2/s$)

The large improvement in the permeate flux to the Triton X-100 treatment was the result of a removal of a large amount of oil from the surface of the membrane. It was suspected that the membranes may have become coated with a film of oil from waste originating from a pilot-project being conducted elsewhere on the CRL site. Sampling and analysis of the spent detergent solution, Triton X-100, verified that fouling by oil did take place. A total of 0.8 kg of oil was removed from module 1.

Triton X-100 is a non-ionic detergent soluble in water and is produced from octylphenol polymerized with ethylene oxide. The Triton X-100 molecule has 5 to 15 ethylene oxide units and has an average molecular weight of 647. The straight aliphatic chain is linked to the hydrophilic ethylene oxide end by an aromatic ring (Merck Index, 1989):

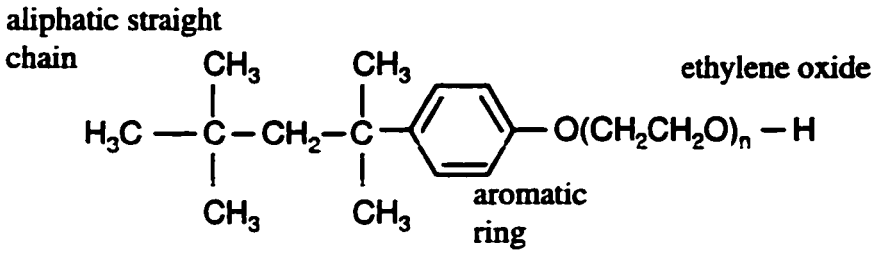

The aliphatic end of the Triton X-100 molecule is attracted by the oil which is also a hydrocarbon. Since "like dissolves like" the hydrophobic aliphatic chain would solubilize the oil present on the membrane surface. The ethylene oxide end is hydrophilic and attracts water, forming an oil emulsion. The oil is then carried away from the surface of the membrane by the flow of the water.

The hydrochloric acid treatment at pH 2 was employed for the dissolution of metals. There was little response by the membrane to this second cleaning step. As discussed in chapter 5, the primary foulants are believed to be calcium hydroxyapatite, $Ca_5(PO_4)_3OH$, and ferric oxide, Fe_2O_3. The solubility constant of calcium hydroxyapatite is $10^{-44.2}$ or, expressed in other terms, the pK_{sp} is +44.2 (see section 3.5). This value is quite large and indicates the insolubility of the precipitate. Ferric oxide is more soluble with a solubility constant of 10^{-4}. The contact

time of one hour between the HCl solution at a pH 2 and the fouled membrane was not sufficient for significant disassociation to take place.

The substances, EDTA and NTA, are chelating agents that bring metals into solution freeing them from the membrane surface.

EDTA is a reagent with carboxymethyl groups bound to two nitrogen atoms (Pribil, 1972):

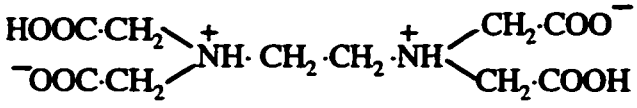

NTA belongs to a group of chelating agents with the carboxymethyl groups bound to a single nitrogen atom (Pribil, 1972):

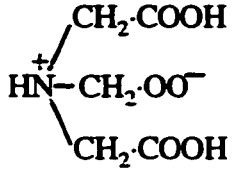

Increasing the pH to 12 with sodium hydroxide would completely disassociate the carboxyl groups of EDTA:

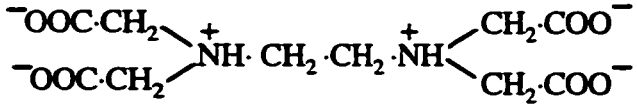

and NTA would be in the form;

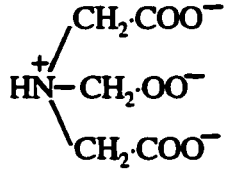

At this high pH, the number of attachment sites is maximized.

The stability of the metal complex with a chelating agent is dependent on the number of sites of attachment between the metal ion and the chelating agent. A monovalent metal ion can attach at each of the acetate groups and nitrogen sites for a total of six attachment sites on EDTA (Snoeyink and Jenkins, 1980). These six attachment sites give rise to five chelating rings. It is the number and size of the chelate rings that help determine the stability of the complex (Pribil, 1972). NTA has only four sites for attachment which give rise to only three chelating rings. Thus, the membrane cleaning capabilities of EDTA would be expected to be far superior to that of NTA. This can be illustrated by considering the stability constants of EDTA and NTA with Ca^{2+}. The stability constant for the $(Ca\text{-}EDTA)^{2-}$ complex is $10^{10.7}$; where the stability constant of the $(Ca\text{-}NTA)^{-}$ complex is $10^{6.4}$ (Snoeyink and Jenkins, 1980). The higher the stability constant, the more stable the complex is in solution.

Unfortunately the main purpose of the chelating agents, the complexation of metals, leads to major problems in disposal sites. The remobilization of heavy metals and radionuclides in radioactive disposal sites is a real concern (see section 2.7). At CRL, the chelating agents would be solidified during the evaporation and bituminization of the liquid waste and ultimately disposed as radioactive waste.

Several factors must be considered when determining the suitability of a chelating agent in the cleaning of membrane systems that are used to process radioactive liquid wastes. The factors that must be considered are the binding capabilities of each of the chelates to the metals to be removed from the foulant layer (i.e. membrane cleaning effectiveness); their possible enhancement to the mobility of radionuclides leached from solidified waste forms; and their degradation. These factors must be fully investigated to determine the suitability of any chelating agent as a possible cleaning agent of membranes used for radioactive liquid wastes.

The literature surveyed in section 2.7 indicated that NTA is more easily degradable than EDTA, whether it is by chemical or biological means. The chelating agent, EDTA, was found to be slightly more susceptible to radiological degradation. The complete degradation of chelating agents that will ultimately end up in radioactive disposal sites is very important so that

remobilization and migration of heavy metals and radionuclides do not take place. The fragments of partially degraded chelating agents may also have remobilizing capabilities which are sometimes greater than their parent compounds (Toste, 1991). Means and Alexander (1981) suggest degrading the chelating agents either chemically or thermally prior to disposal.

EDTA is a stronger complexing agent than NTA which should result in greater cleaning capabilities of the former. From the work performed with the membranes taken from CRL's plant-scale reverse osmosis membrane system, there appears to be no significant advantage of using EDTA over NTA. Using the pure water permeate flux at the normal operating pressure of 2760 kPa as a reference, EDTA resulted in an improvement of 19.9 percent (table 6.1) and cleaning with NTA gave an improvement of 20.0 percent (table 6.2).

6.1.3 Effect of AD/DC Waste Processing on Overall Improvement

After the final cleaning step, both modules treated approximately 1200 liters of AD/DC waste, 400 liters at a time. Module 2 treated an additional 400 liters before any cleaning, pure water permeability or rejection efficiency tests of the module. The 400 liters of AD/DC waste was reduced at 2760 kPa and system temperatures between 22-27°C to approximately 10 percent of the original volume of waste, giving an approximate volumetric recovery of 90 percent. After the three-step cleaning procedure, the first AD/DC test was performed with the five micron filter installed for both modules. The test was then repeated and a third test was performed without the five micron filter. The AD/DC test performed on module 2 before cleaning was performed with the five micron filter installed. Figure 6.2 shows the permeate flux curves during the volumetric reduction of three different batches of AD/DC waste using module 1 with and without the use of a five micron filter. A gradual decrease in the permeate flux during the volumetric reduction of each batch of AD/DC waste by module 1 is evident until a volumetric recovery of approximately 80 percent. After 80 percent recovery is reached, the permeate flux declines more rapidly. The initial permeate fluxes with the AD/DC waste are between 1.02 and 1.08 L/min/element for module 1.

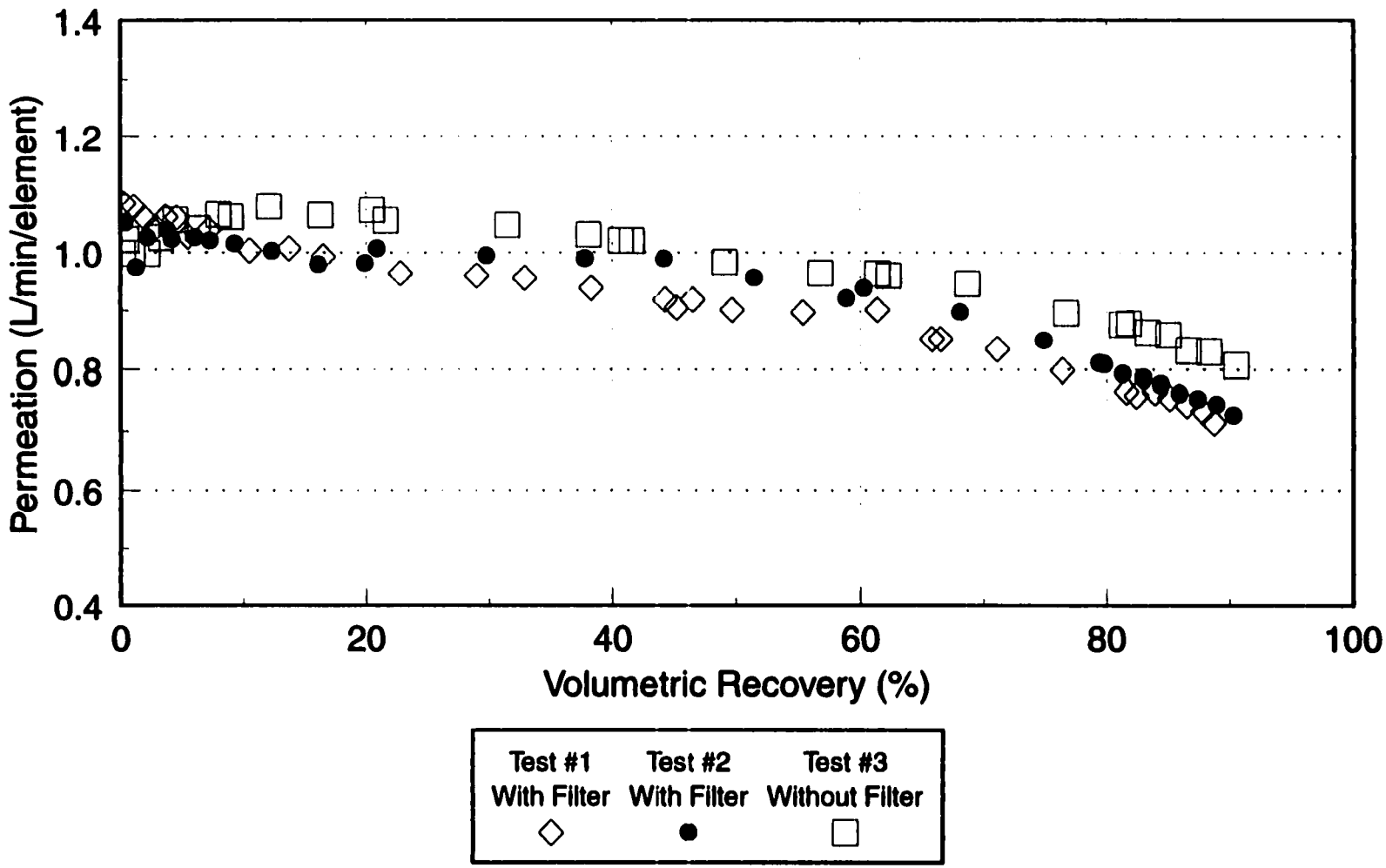

Figure 6.2: Permeate Flux with AD/DC Waste using Module 1
(1 L/min/element = 2.65×10^{-6} $m^3/m^2/s$)

Figure 6.3 shows the permeate flux curves during the volumetric reduction of four different batches of AD/DC waste using module 2 with and without the use of a five micron filter. With module 2, a volumetric reduction of 400 litres of AD/DC waste was performed to determine the improvement made by the three-step cleaning procedure on the permeate flux when treating the waste. The same flux curve observed during the AD/DC waste tests with module 1 is found with module 2 after cleaning. After the cleaning procedure, the initial flux was between 1.1 and 1.2 L/min/element. This is an improvement of almost 120 percent over the initial flux of 0.5 L/min/element found before cleaning.

As stated in section 2.92, the filtrate rate of the microfiltration unit is approximately 42 L/min which is sent to the plant-scale SWRO system for further processing. If the permeate rate of the entire SWRO system is less than 42 L/min, a backlog of wastes is produced. The microfiltration system would have to be put in recirculation mode or shut down completely in order for the SWRO system to be able to keep up with the filtrate production rate. With a permeate flux over 1 L/min per membrane element, the permeate flux for the entire SWRO system would exceed that 42 L/min filtrate rate and a backlog of waste would not be produced.

The relative flux, defined as the flux at time t divided by the initial flux, of each subsequent test at 80 percent recovery is 0.75, 0.82, and 0.90 for module 1 (figure 6.2) and 0.90, 0.91, and 0.85 for module 2 (figure 6.3). The initial flux values and the relative flux values at 80 percent recovery are very close in value for each test indicating that no permanent fouling is taking place after each 400 liter batch volumetric reduction. It can be ascertained, given the relatively low volume of waste treated, the principal cause of the permeate flux decline observed while processing the batches of AD/DC waste with increasing volumetric recovery is caused by concentration polarization and not by irreversible fouling. No flux decline can be attributed to membrane compaction since any membrane compaction would have only occurred during the first few runs in the plant system.

In both cases shown in figures 6.2 and 6.3, the permeate flux did not change significantly with each subsequent volumetric reduction of the AD/DC waste after cleaning. This was even

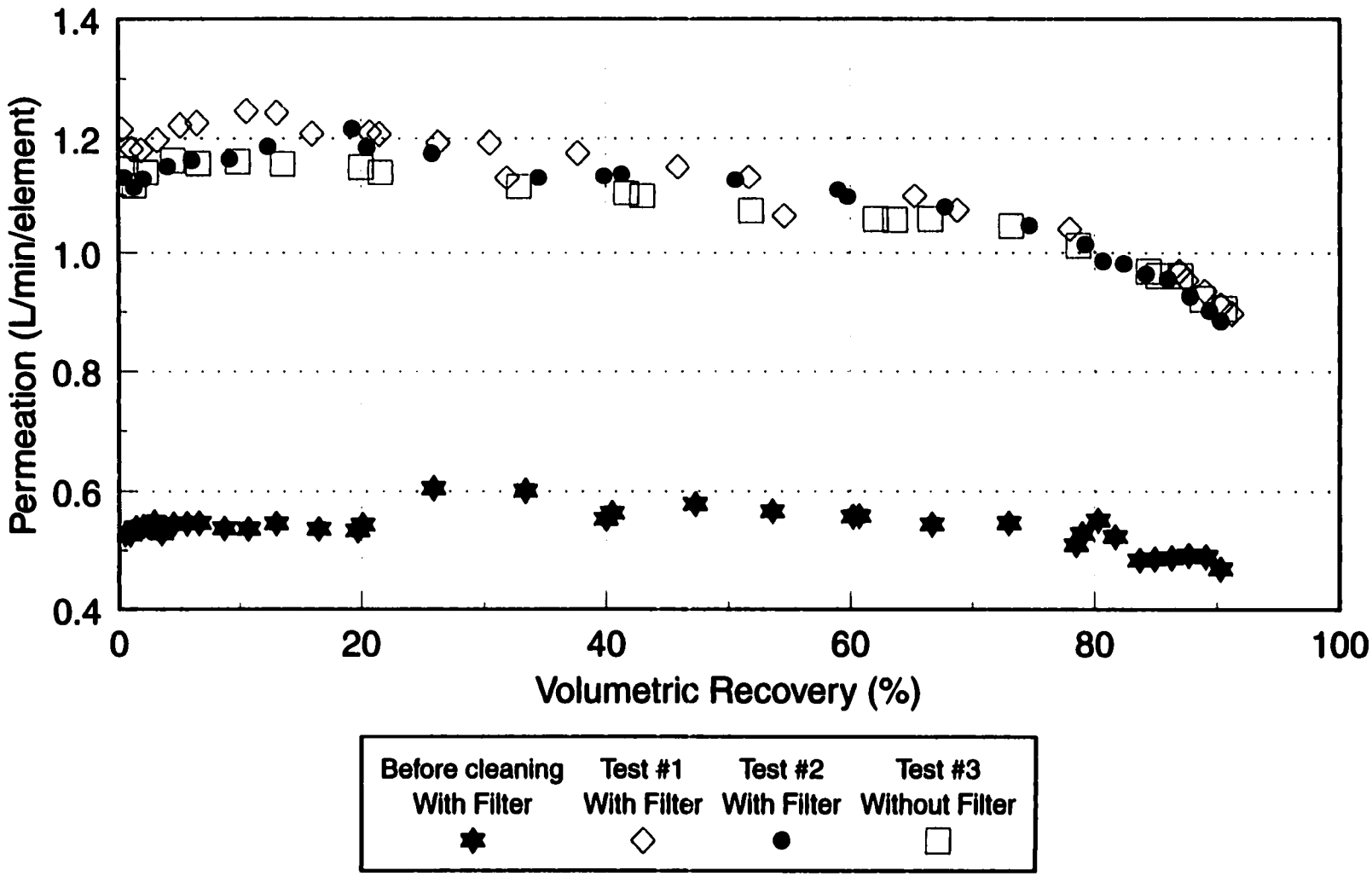

Figure 6.3: Permeate Flux with AD/DC Waste using Module 2
(1 L/min/element = 2.65×10^{-6} $m^3/m^2/s$)

true of the third AD/DC test without the five micron filter for both cleaned modules. These observations suggest that a five micron filter is unnecessary to maintain higher permeate fluxes in the pilot-scale system. As Sethi and Wiesner (1995) discussed (see section 2.5), a filter removing particles larger than 5 μm would not assist in maintaining increased permeate fluxes.

6.2 Effect of Cleaning on Rejection Efficiency of Cesium and Strontium

Although the main focus of the experimental work was on improving the permeate flux, some work was conducted in an attempt to determine the effect of the cleaning procedure on the rejection efficiency of the membrane. This was measured using the stable isotopes cesium 133 and strontium 88. The effect of applied pressure on the rejection efficiency of both species was also studied. The results of the rejection efficiency tests were found using module 2 since the permeate samples obtained using module 1 were below detection limits. A more concentrated solution of cesium and strontium was used for the experiments using module 2.

Table 6.3 shows the rejection efficiency of cesium and strontium at 2760 kPa using module 2 before and after each cleaning step. As seen in table 6.3, the rejection efficiency did not change significantly with cleaning:

Table 6.3: Rejection Efficiencies of ^{133}Cs and ^{88}Sr using Module 2 Before and After Each Cleaning Step at 2760 kPa

	Rejection of ^{133}Cs	Rejection of ^{88}Sr	DF of ^{133}Cs	DF of ^{88}Sr
Before Cleaning	97.94	99.98	48.5	5000
After Triton X-100	98.30	99.98	58.8	5000
After HCl	97.39	99.97	38.3	3333
After NaOH and EDTA	97.39	99.99	38.3	10 000

The rejection of cesium before cleaning is 97.94 percent at 2760 kPa and after cleaning it is 97.93 percent at 2760 kPa. The rejection of strontium increased slightly from 99.98 percent to 99.99 percent after cleaning. After each individual cleaning step, the rejection efficiency varied

only slightly. In general, the cleaning did not have any significant effect on the rejection efficiency of the membrane modules. The decontamination factors (DF) are listed in table 6.3 as well.

Tests were also conducted at various pressures from 1380 kPa to 5500 kPa to study the effect of applied pressure on both species. Figure 6.4 shows the decontamination factor (DF) for cesium and strontium using module 2 at various applied pressures.

As expected, the DF for cesium does improve from 30 to 50 (96.7 to 98.0 percent) with increasing applied pressures. This is because the solvent flux, in this case, water is more dependent on the applied pressure than the solute (cesium or strontium) flux. The driving force of the solute is generally the concentration gradient across the membrane; not the applied pressure. Hence, while more solvent passes through the membrane at higher applied pressures, less solute is able to pass through depending on the concentration gradient. The DF for strontium is at least 4000 for all of the applied pressures tested. This DF relates to a rejection efficiency of 99.975 percent; therefore, has little room for improvement even at the higher applied pressures.

These rejection results for the used membrane modules are different from the rejection efficiencies of new membrane modules. The DF for cesium using new membranes is approximately 100 at an applied pressure of 2760 kPa (Sen Gupta et al., 1996) and for used membranes (both before and after cleaning), the DF is approximately 50 at 2760 kPa (figure 6.4). The DF for strontium using new membrane modules is approximately 1000 at 2760 kPa (Sen Gupta et al., 1996). In comparison, the DF for strontium using a fouled membrane, again both before and after cleaning, is at least 4000.

The used membranes show a loss in cesium rejection and an increase in strontium rejection. The loss in cesium rejection efficiency from 99 to 98 percent (DF 100 to 50) may have been the result of a loss in membrane integrity caused by the numerous chemical cleanings conducted. Although, it is apparent from figure 6.4 that no further loss in rejection efficiency was experienced after the aggressive three-step cleaning procedure was conducted. The increase

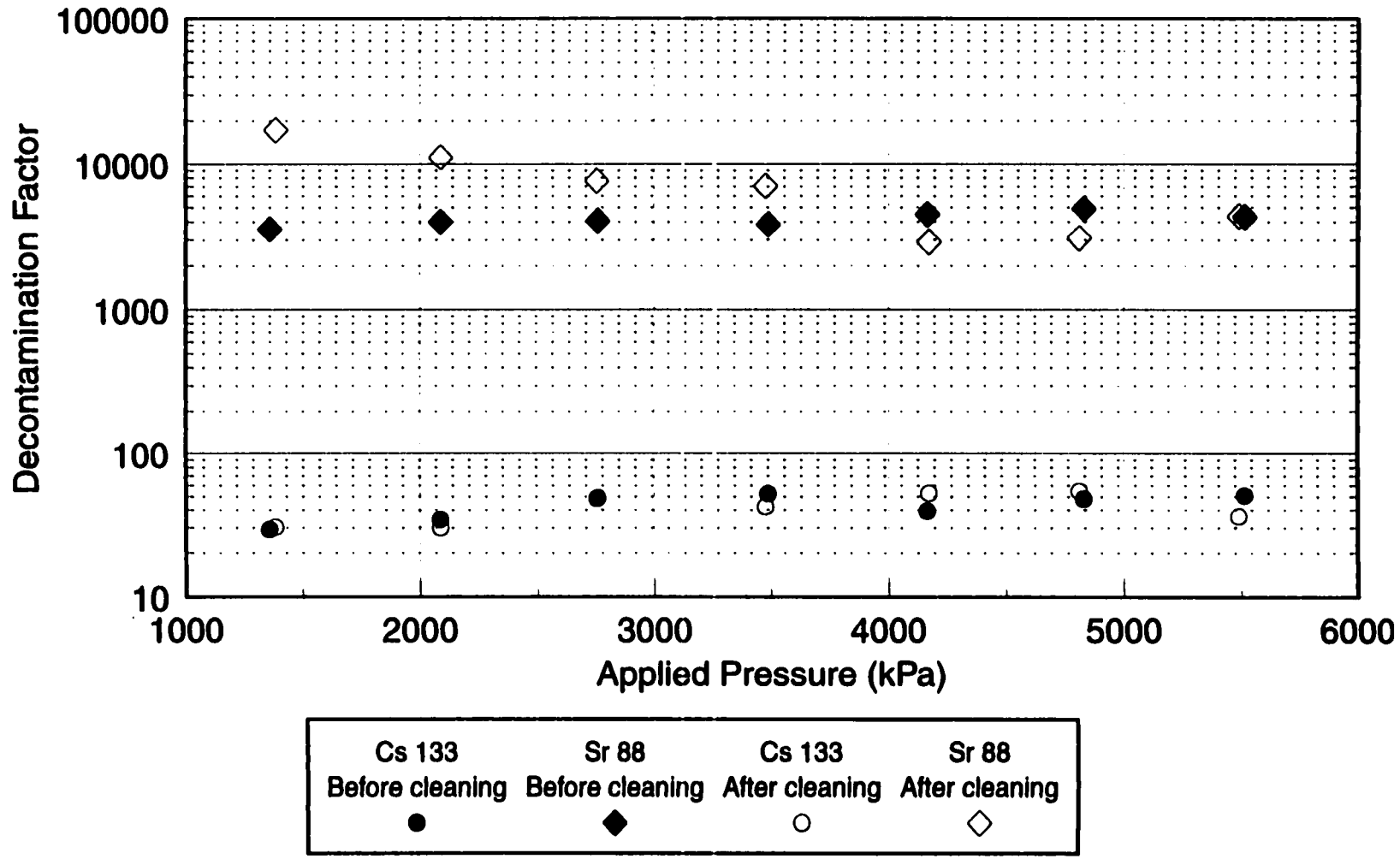

Figure 6.4: DF of Cesium and Strontium versus Applied Pressure

in the rejection efficiency of strontium from 99.9 for a new membrane to 99.975 percent for a fouled membrane (DF 1000 to 4000) can be explained by noting that a dominant scale on the membrane is calcium hydroxyapatite (as determined in chapter 5). It is suspected that strontium may be replacing the calcium in the calcium hydroxyapatite precipitate. Although, no solubility constants for $Sr_nCa_m(PO_4)OH$ where (n+m=5) can be found in the literature, very high beta fields have been found on the used membrane modules taken from the plant-scale SWRO system. No abundant beta emitters other than strontium are present in the CRL waste (Sen Gupta, 1996) which supports the Ca^{2+} and ^{90}Sr exchange theory.

Chapter 7

Conclusions

Conclusions Obtained from Work Discussed in Chapter 5

1. The major foulants of the plant-scale SWRO membranes are precipitates of calcium, phosphorus and iron. These foulants are most likely calcium hydroxyapatite, $Ca_5(PO_4)_3OH$, and ferric oxide, Fe_2O_3.

2. An optimum crossflow of 45 L/min was found for a 3 weight percent sodium chloride solution.

3. Processing the AD/DC waste at the various crossflow velocities studied did not affect the pure water permeability or rejection efficiency of the membrane.

4. The permeate flux of a sodium chloride solution is dependent on boundary layer concentrations which are dependent on the degree of concentration polarization observed. In turn, the degree of concentration polarization is dependent on the crossflow velocity. Hence, the permeate flux of a sodium chloride solution is dependent on crossflow velocity.

5. No optimum crossflow velocity was found when processing the AD/DC waste due to the presence of particulates in the waste.

6. Actual permeate fluxes observed during the processing of the AD/DC waste were well below the permeate flux predictions based on boundary layer concentration and osmotic pressure calculations.

7. The particulate present in the AD/DC waste stream (which is not present in the sodium chloride solutions) is responsible for the permeate flux declines observed while processing the waste stream.

8. At higher volumetric recoveries, the particulate loading increases considerably which causes a greater decline in permeate flux. Since the discrepancy in the permeate flux while processing the AD/DC waste is greatest at the higher volumetric recoveries, operating in feed-and-bleed mode is not ideal.

Conclusions Obtained from Work Discussed in Chapter 6

9. The pure water flux of two different fouled reverse osmosis membranes more than doubled after using the three-step cleaning procedure.

10. The three-step cleaning procedure does provide an acceptable means of restoring permeate flux to a level of 1 L/min/element which is sufficient to directly treat the filtrate from the microfiltration system.

11. During pilot-scale studies, processing the relatively small batches of AD/DC waste had no significant effect on the permeate flux of the membrane. The initial flux value was restored to the same approximate value with each batch of waste processed.

12. The rejection efficiency of the fouled membrane was not affected by the aggressive three-step cleaning procedure.

13. Using a fouled membrane, the DF for cesium was found to be dependent on applied pressure. A DF of 30 (96.7 % rejection) at 1380 kPa increased to a DF of 50 (98.0 % rejection) at 5500 kPa. The DF of cesium using a new membrane is approximately 100 (99.0 % rejection).

14. The DF for strontium using the fouled membrane appeared independent of applied pressure with a DF of at least 4000 (99.975 % rejection). Fouled membranes have a higher DF for strontium than do new membranes. The DF for strontium using a new membrane is approximately 1000 (99.9 % rejection). The higher rejection using fouled membranes is associated with strontium exchanging with calcium in the calcium hydroxyapatite precipitate.

Chapter 8

Recommendations

Eliminating the Fouling Species at the Source

It was determined that the major fouling species are Ca^{2+}, PO_4^{3-}, and Fe^{3+}. The source of these contaminants should be identified and eliminated if possible. Water used at the CRL site originates from the Ottawa River and is not extensively treated. Sampling of the tap water and the intake from the Ottawa River should be conducted to test for calcium and iron content. Given the high volumetric recoveries in the SWRO system, even minute concentrations of Ca^{2+} forms insoluble calcium hydroxyapatite scale. Any Fe^{3+} present in the water will react to form ferric oxide, Fe_2O_3, upon contact with air. If the fouling species can be removed at the source, it would provide the WTC with vast cost savings. It would minimize costs associated with purchasing cleaning solutions and downtime during cleanings. It would also reduce energy costs associated with treating the spent cleaning solutions by the thin-film evaporators. The volume of solidified waste sent to storage and disposal would be reduced. As the operational lifetime of the membranes increase, the membrane replacement costs decrease as do the costs associated with the storage and disposal of the spent membranes.

A mass balance on calcium and iron content should be initiated. If the Ottawa River is found to be the primary source of the fouling species, then an RO unit could be installed after the water intake.

Suggested Improvements to Plant-Scale SWRO Mode of Operations

Currently the plant-scale SWRO system is operated in feed-and-bleed mode at an volumetric recovery of 80 to 85 percent. The continual high total solids content of the feed stream to the SWRO system is promoting premature fouling of the membranes. Operating in feed-and-bleed mode versus batch mode may save on pumping energy costs but the costs associated with membrane replacement may be much higher than any energy savings incurred.

The microfiltration and SWRO system could be operated in batch mode minimizing the time the membranes are treating highly concentrated AD/DC wastes. Figure 8.1 shows a simplified schematic of a possible MFU and SWRO batch system. The MFU treats the AD/DC waste and the filtrate is stored in tank A. Once full, the MFU system is shut down and the SWRO system begins processing the waste. When the waste stream reaches a volumetric recovery between 55 to 70 percent which corresponds to a total precipitated solids content of 75 mg/L to 120 mg/L, the concentrated waste is transferred to another tank, tank B. The waste in tank B would be agitated to promote aggregation of the particulates (a chemical coagulant could be added at this stage) and allowed to settle. The supernatant from tank B would be combined with fresh feed and pretreated by the MFU where the process would begin again.

A cost analysis of the operational scheme discussed above compared to the current operating costs of the WTC should be performed to determine the feasibility of operating the MFU and SWRO systems in batch mode.

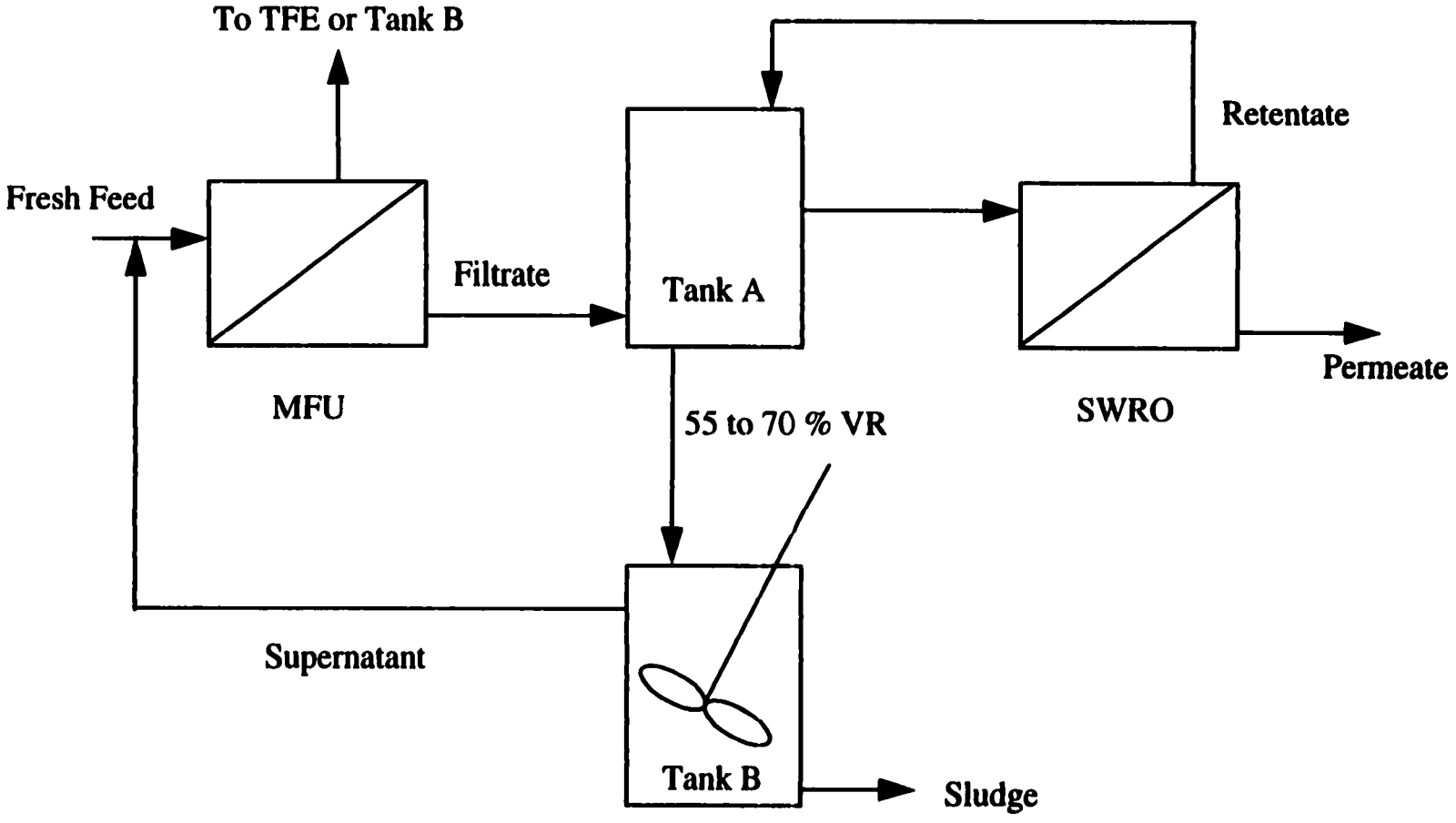

Figure 8.1: Simplified Schematic of Proposed Batch MFU and SWRO System

MFU - Microfiltration Unit SWRO - Spiral Wound Reverse Osmosis

TFE - Thin Film Evaporator VR - Volumetric Recovery

References

Amirtharajah, A., and C. R. O'Melia, "Coagulation Processes: Destabilization, Mixing, and Flocculation", in "Water Quality and Treatment: A Handbook of Community Water Supplies", 4th ed., F. W. Pontius, Ed., McGraw-Hill, Inc., Toronto, Ontario, pp. 269-273, (1990).

Amjad, Z., "Advanced in Membrane Cleaners for Reverse Osmosis Systems", Ultrapure Water, 6(6), pp. 38-42 (1989).

Amjad, Z., J. Hooley, and J. Pugh, "Reverse Osmosis Failures: Causes, Cases, and Prevention", Ultrapure Water, 1(1), pp. 14-21 (1991).

Amjad, Z., "Mechanistic Aspects of Reverse Osmosis Mineral Scale Formation and Inhibition", Ultrapure Water, 5(6), pp. 23-28 (1988).

Bader, M. S. H., and J. N. Veenstra, "Analysis of Concentration Polarization Phenomenon in Ultrafiltration Under Turbulent Flow Conditions", J. Membrane Sci., 114, pp. 139-148 (1996).

Barger, M., and R. P. Carnahan, "Fouling Prediction in Reverse Osmosis Systems", Desalination, 83, pp. 3-33 (1991).

Berry, J. B., C. H. Brown, Jr., V. L. Fowler, and S. M. Robinson, "Treatment of ORNL Process Waste", Proceedings of the International Topical Meeting on Nuclear and Hazardous Waste Management, Spectrum '88, Pasco, WA, pp. 416-420 (1988).

Bhattacharyya, D., and M. E. Williams, "Reverse Omosis: Theory" in "Membrane Handbook", W. S. Winston and K. K. Sirkar, Eds., Van Nostrand Reinhold, Scarborough, Ontario, p. 269-277, (1992).

Bodzek, M., and K. Konieczny, "Optimization of the Ultrafiltration of Latex Wastewaters", Desalination, 94, pp. 289-306 (1994).

Bolton, H., S. W. Li, J. Workman, and D. C. Girvin, "Biodegradation of Synthetic Chelates in Subsurface Sediments from the Southeast Coastal Plain", J. Environ. Qual., 22, pp. 12-132, (1993).

Buckley, C. A., A. Bindoff, C. A. Kerr, A. Kerr, A. E. Simpson, and D. W. Cohen, "The Use of Speciation and X-Ray Techniques for Determining Pretreatment Steps for Desalination", Desalination, 66, pp. 327-337 (1987).

Bukay, M. "How to Monitor a Reverse Osmosis System", Ultrapure Water, 1(1), pp. 32-36 (1984).

Chauvet, P., and T. Dippel, "Chemical Precipitation" in "Radioactive Waste: Advanced Management Methods for Medium Active Liquid Waste", K. W. Carley-Macauly, R. G. Gutman, E. W. Hooper, J. A. Jenkins, A. D. Turner, P. F. Wace, P. Chauvet, J. P. Gauchon, and T. Dippel, Eds., Harwood Academic Publishers, New York, N.Y., (1981), pp. 3-40.

Chauvet, P., and K. W. Carley-Macauly, "Origin and Characteristics of Medium and Low Activity Liquid Wastes" in "Radioactive Waste: Advanced Management Methods for Medium Active Liquid Waste", K. W. Carley-Macauly, R. G. Gutman, E. W. Hooper, J. A. Jenkins, A. D. Turner, P. F. Wace, P. Chauvet, J. P. Gauchon, and T. Dippel, Eds., Harwood Academic Publishers, New York, N.Y., (1981), pp. 299-315.

Chmielewski, A. G., and M. Harasimowicz, "Application of Ultrafiltration and Complexation to the Treatment of Low-level Radioactive Effluents", 8th Symposium on Separation Science and Technology for Energy Applications, Gatlinburg, Tenn., pp. 1779-1789 (1995).

Cohen, R. D., and R. F. Probstein, "Colloidal Fouling of Reveres Osmosis Membranes", J. Colloid and Interface Sci., **114**(1), pp. 194-207 (1986).

Comstock, D. L., L. A. Durham, and D. W. Walker & Associates, U.S. Patent 5,198,116, Mar. 30 (1993).

Deane and Company, Div. Groulx Robertson Ltd., personal communication with technical support, Point Claire, Quebec, (1996).

Del Debbio, J. A., R. I. Donovan, and J. E. Lundstrom, "Treatment of Low-level Liquid Radioactive Wastes by Electrodialysis", Chemical Separations: Developed from Selected Papers Presented at the First International Conference on Separations Science and Technology, New York, N.Y., pp. 111-122 (1986).

Dow Chemical Company, Technical Bulletin: FILMTEC® Membranes, Form No. 609-07050-393AMS, Minneapolis, Minnesota, (1994).

Ebrahim, S., "Cleaning and Regeneration of Membranes in Desalination and Wastewater Applications: State-of-the-Art", Desalination, **96**, pp. 225-238 (1994).

Ebrahim, S., and H. El-Dessouky, "Evaluation of Commercial Cleaning Agents for Seawater Reverse Osmosis", Desalination, **99**, pp. 169-188 (1994).

Egli, T., "Biodegradation of Synthetic Chelating Agents with Special Reference to Nitrilotriacetic Acid (NTA)", J. Chem. Technology and Biotechnology, **55**(4), pp. 404-406 (1992).

Elimelech, M., and X. Zhu, "Colloidal Fouling of Reverse Osmosis Membranes", Critical Issues in Water and Wastewater Treatment, Proceedings of the 1994 National Conference on Environmental Engineering, Boulder, Colorado, pp. 329-335 (1994).

Field, R. W., and P. Aimar, "Ideal Limiting Fluxes in Ultrafiltration: Comparison of Various Theoretical Relationships", J. Membrane Sci., **80**, pp. 107-115 (1993).

Freer, J., S. Hanson, A. Bond, E. Freer, and A. Collery, "Pilot Studies to Achieve Waste Minimization and Enhance Radioactive Liquid Waste Treatment at The Los Alamos National Laboratory Radioactive Liquid Waste Treatment Facility", LA-UR-96-2274, Doe Pollution Prevention Conference XII, Chicago, Illinois, (1996).

Gaddis, J. L., "Effects of Pressure and Crossflow Velocity on Ultrafiltration Flux", Chem. Eng. Comm., **116**, pp. 153-169 (1992).

Gauchon, J. P., E. W. Hooper, and J. A. Jenkins, "Ion Exchange", in "Radioactive Waste: Advanced Management Methods for Medium Active Liquid Waste", K. W. Carley-Macauly, R. G. Gutman, E. W. Hooper, J. A. Jenkins, A. D. Turner, P. F. Wace, P. Chauvet, J. P. Gauchon, and T. Dippel, Eds., Harwood Academic Publishers, New York, N.Y., pp. 41-130. (1981).

Gutman, R. G., and R. H. Knibbs, "Review of Nuclear and Non-Nuclear Applications of Membrane Processes - Present Problems and Future R & D Work" in "Future Industrial Prospects of Membrane Processes", L. Cecille and J. C. Toussaint, Eds., Elsevier Science Publishing Co., Inc., New York, N.Y., pp. 16-30, (1989).

Gutman, R. G., "Membrane Processes", in "Radioactive Waste: Advanced Management Methods for Medium Active Liquid Waste", K. W. Carley-Macauly, R. G. Gutman, E. W. Hooper, J. A. Jenkins, A. D. Turner, P. F. Wace, P. Chauvet, J. P. Gauchon, and T. Dippel, Eds., Harwood Academic Publishers, New York, N.Y., pp. 159-229, (1981).

Hickman, C. E., "Membrane Cleaning Techniques", Memb. Technol. Water Ind., AWWA Membr. Processes Conference, Denver, CO, pp. 329-344 (1991).

Ho, W. S. W., and K. K. Sirkar, Eds., "Membrane Handbook", Von Nostrand Reinhold, New York, N.Y. (1992).

International Atomic Energy Agency, "Advances in Technologies for the Treatment of Low and Intermediate Level Radioactive Liquid Wastes", Technical Report Series No. 370, IAEA, Vienna (1994).

International Atomic Energy Agency, "Chemical Treatment of Radioactive Wastes", Technical Report Series No. 89, IAEA, Vienna (1968).

International Atomic Energy Agency, "Treatment of Low-and Intermediate-Level Liquid Radioactive Wastes", Technical Report Series No. 236, IAEA, Vienna (1984).

Jonsson, A-S., and G. Tragardh, "Fundamental Principles of Ultrafiltration", Chem. Eng. Process., **27**, pp. 67-81 (1990).

Kennedy, T. J., R. L. Merson, and B. J. McCoy, "Improving Permeation Flux by Pulsed Reverse Osmosis", Chem. Eng. Sci., **29**, pp. 1927-1931 (1974).

Knibbs, R. H., "The Decontamination of Alpha Bearing Waste Streams Using Coprecipitation with Ferric Hydroxide in Conjunction with Ultrafiltration", AERE-R-10269, EDB8502, HMSO, London, United Kingdom, pp. 1-29 (1984).

Koenst, J. W., and R. C. Roberts, "Evaluation of Ultrafiltration Membranes for Treating Low-Level Radioactive Contaminated Liquid Waste", MLM-2448, U. S. Department of Energy, Miamisburg, Ohio, pp. 2-10, (1978).

Kronmiller, D., "RO Permeate Water Flux Enhancement", Ultrapure Water, **10**(2), pp. 37-40 (1993).

Kruss, P., "Liquid and Solutions, Structure and Dynamics", Marcel Dekker Inc., New York, N.Y. (1977).

Kulkarni, A., D. Mukherjee, and W. N. Gill, "Enhanced Transport Properties of Reverse Osmosis Membranes by Chemical Treatment", J. Appl. Polym. Sci., **60**, pp. 483-492 (1996).

Kulkarni, S. S., E. W. Funk, and N. N. Li, "Ultrafiltration: Introduction and Definitions", in "Membrane Handbook", W. S. Winston and K. K. Sirkar, Eds., Van Nostrand Reinhold, Scarborough, Ontario, (1992), pp. 393-397.

Kutscher, U., G. Holker, A. Chrubasik, P. L. Ipatov, and V. I. Ignatov, "Radioactive Waste Treatment in Nuclear Power Plants with VVER Reactors Using Balakovo NPP(Russia) as an Example", Low and Intermediate Level Radioactive Waste Management: Proceedings, 1993 International Conference on Nuclear Waste Management and Enviromental Remediation, Prague, Czech Repulic, pp. 623-632 (1993).

Laidler, K. J., and J. H. Meiser, "Physical Chemistry", The Benjamin/Cummings Publishing Company, Inc., Don Mills, Ontario, (1982), pp. 770-771.

Leger, J. P., and L. C. Hawker, "The Composition and Structure of Reverse Osmosis Foulant Deposits Formed from Rand Water Board Water: A Preliminary Investigation", Desalination, **61**, pp. 137-158, (1987).

Levy, P. F., and R. S. Earle, "The Effect of Channel Height and Channel Spacers on Flux and Energy Requirements in Crossflow Filtration", J. Membrane Sci., **91**, pp. 135-143 (1994).

Lide, D. R., Ed., "CRC Handbook of Chemistry and Physics", 76th ed., CRC Press Inc., Boca Raton, Florida, (1995), pp. 5-90, 5-91.

Lindau, J., and A-S. Jonsson, "Cleaning of Ultrafiltration Membranes after Treatment of Oily Waste Water", J. Membrane Sci., **87**, pp. 71-78 (1994).

Longfield, J. D., private communication (1997).

Luek, S., "Membranes: Reverse Osmosis Treatment of Oil- and Gas-Produced Water", Industrial Water Treatment, **27:4**, p. 25 (1995).

Luu, C. A., "Improved Chelators and Sequestrants for Army Reverse Osmosis Water Purification Units (ROWPUs)", Desalination, **97**, pp. 165-170 (1994).

Matsuura, T., M. E. Bednas, and S. Sourirajan, "Reverse Osmosis Separation of Single and Mixed Alcohols in Aqueous Solutions Using Porous Cellulose Acetate Membranes", J. Applied Polymer Sci., **18**, pp. 567-588 (1974).

Means, J. L., and C. A. Alexander, "The Environmental Biogeochemistry of Chelating Agents and Recommendations for the Disposal of Chelated Radioactive Wastes", Nuclear and Chemical Waste Management, **2**, pp. 183-196 (1981).

Means, J. L., D. A. Crerar, and J. O. Duguid, "Migration of Radioactive Wastes: Radionuclide Mobilization by Complexing Agents", Science, **200**, pp. 1477-1486 (1978).

Mans, J. L., T. Kucak, and D. A. Crerar, "Relative Degration Rates of NTA, EDTA and DTPA and Environmental Implications", Environmental Pollution Ser. B, **1**, pp. 45-60 (1980).

Merck Index, 11th ed., Merck & Co., Inc., No. 6681 (1989).

Merten, U., "Desalination by Reverse Osmosis", U. Merten, Ed., M.I.T. Press, Cambridge, Mass., pp. 15-54 (1966).

Mukherjee, D., A. Kulkarni, and W. N. Gill, "Chemical Treatment for Improved Performance of Reverse Osmosis Membranes", Desalination, **104:3**, pp. 239-249 (1996).

Mukherjee, D., A. Kulkarni, and W. N. Gill, "Flux Enhancement of Reverse Osmosis Membranes by Chemical Surface Modification", J. Membrane Sci., **97**, pp. 231-249 (1994).

Mulder, M. H. V., "Basic Principles of Membrane Technology", Kluwer Acad., Dordrecht, Netherlands (1991).

Nilsson, J., and B. Hallstrom, "Deviations in the Fouling Resistance of UF Membranes due to Clean Membrane Permeability Variations", J. Membrane Sci., **67**, pp. 177-189 (1991).

Nobel, R. D., and S. A. Stern, Eds., "Membrane Separations Technology: Principles and Applications", Elsevier Science B.V., New York, N.Y. (1995).

Palmer, J. F., "Derived Release Limits (DRL's) for Airborne and Liquid Effluents from the Chalk River Nuclear Laboratories During Normal Operations", AECL - 7243, Atomic Energy of Canada Limited, Chalk River Laboratories, Chalk River, Ontario, pp. 1-3, 4-1, 5-27, 5-28, 6-19 (1981).

Panicker, S. T., S. Prabhakar, B. M. Misra, and M. P. S. Ramani, "Radioactive Liquid Effluent Management - State of Art and the Role of Membrane Processes", B.A.R.C. - 1534, Government of India Atomic Energy Commission, Bhabha Atomic Research Centre, Bombay, India (1990).

Pervov, A. G., "Scale Formation Prognosis and Cleaning Procedure Schedules in Reverse Osmosis Systems Operation", Desalination, **83**, pp. 77-118, (1991).

Polyakov, A. S., B. V. Martynov, V. V. Tugolukov, B. E. Ryabchikov, V. S. D'yakov, I. A. Sobolev, A. S. Dmitriev, Yu. V. Kuznetsov, N. A. Rakov, V. A. Kichik, A. P. Darienko, V. E. Vyatkin, N. F. Kuleshov, and A. A. Svittsov, "Problems of Improving Engineering Procedures and Processing Flow Diagrams for Low- and Medium-Level Liquid Wastes, Soviet-Atomic-Energy, **67**(1), pp. 507-515 (1990).

Pribil, R., "Analytical Applications of EDTA and Related Compounds", in "International Series of Monographs in Analytical Chemistry", R. Belcher and H. Freiser, Eds., 1st ed., vol. 52, Pergamon Press Ltd., Toronto, Ont., (1972), pp. 3-51.

Ramamurthy, P., R. Poole, and J. G. Dorica, "Fouling of Ultrafiltration Membranes During Treatment of CMTP Screw Press Filtrates", Proc. 1993 Environ. Conf., Canadian Pulp & Paper Assoc., Montreal, Que., pp. 67-71 (1993).

Reitz, R. L., "A Computer Program for Evaluation of Water Chemistry and Scale Prevention in RO Desalination Systems", Ultrapure Water, **6**(1), pp. 44-49 (1989).

Ryabchikov, B. E., D. I. Trofimov, E. I. Zakharov, A. S. Dudin, and L. K. Mikheev, "Purification of Liquid Radioactive Effluents by Continuous Ion Exchange", Atomnaya Energiya, **38**(4), pp. 284-287 (1975).

Ryabchikov, B. E., E. I. Zakharov, A. P. Darienko, A. V. Rakhchev, and M. C. Murabuldaev, "Treating Radioactive Waters with a Mixed Ion Exchange Bed in a Continuous Operation Plant", Atomnaya Energiya, **55**(6), pp. 373-376 (1983).

Sayed Razavi, S. K., J. L. Harris, and F. Sherkat, "Fouling and Cleaning of Membranes in the Ultrafiltration of the Aqueous Extract of Soy Flour", J. Membrane Sci., **114**, pp. 93-104 (1996).

Sebesta, F., A. Motl, J. John, M. Prazsky, and J. Binka, "Composite Ion Exchangers and Their Possible Use in Treatment of Low/Intermediate Level Liquid Radioactive Wastes", Low and Intermediate Level Radioactive Waste Management: Proceedings, 1993 International Conference on Nuclear Waste Management and Enviromental Remediation, Prague, Czech Repulic, pp. 871-878 (1993).

Sen Gupta, S. K., and J. A. Slade, "Membrane Treatment of Radioactive Waste Liquids", Ultrapure Water, **10**(8), pp. 12-22 (1993).

Sen Gupta, S. K., J. A. Slade, and W. S. Tulk, "Integrated Plant for Treatment of Liquid Radwaste", Proceedings: 1994 EPRI International Low Level Waste Conference, Norfolk, VA, pp. 16.1-16.26 (1994).

Sen Gupta, S. K., L. P. Buckley, S. J. Rimpelainen, and A. Y. Tremblay, "Liquid Radwaste Processing with Spiral Wound Reverse Osmosis", Session 36 - Improved Techniques for Liquid LLW, Paper 36-2, Waste Management 96 Conference, Tucson, Arizona (1996).

Sen Gupta, S. K. and S. Rimpelainen, "Liquid Radwaste Processing with Spiral-Wound Reverse Osmosis", Ultrapure Water, **14**(1), pp. 32-39 (1997).

Sen Gupta, S. K., "Radwaste Processing with Microfiltration and Reverse Osmosis", Industrial Water Treatment, **28**(4), pp. 22-24, 33-38 (1996).

Sethi, S., and M. R. Wiesner, "Performance and Cost Modeling of Ultrfiltration", J. of Environmental Engineering, **121**(12), pp. 874-883 (1995).

Siler, J. L., "A Comparison of Reverse Osmosis Membrane Cleaning Methods", WSRC-RP-92-056, U. S. Department of Energy, pp. 1-8 (1992).

Simon, R., and L. Cecille, "The C.E.C. Research Activities on Membrane Processes Dealing with Radioactive Waste Management" in "Future Industrial Prospects of Membrane Processes", Elsevier Science Publishing Co., Inc., New York, N.Y., (1989), pp. 8-14.

Slade, J. A., private communication (1996).

Small, H., "Ion Chromatography", Plenum Press, New York, N.Y., (1989), pp. 11-16, 74-75, 132.

Smith, B. R. and Y. Huilin, "Influence of Various Factors on the Performance of Gypsum Scaling Retardants", Water Treatment, **7**, pp. 51-66 (1992).

Snoeyink, V. L, and D. Jenkins, "Water Chemistry", John Wiley and Sons, Inc., Toronto, Ontario, (1980), pp.74-79, 111,130-132, 194-204, 226-240.

Toste, A. P., "Degradation of Chelating and Complexing Agents in an Irradiated, Simulated Mixed Waste", J. Radioanalytical and Nuclear Chem., **161**(2), pp. 549-559 (1992).

Tremblay, A.Y., "The Role of Structural Forces in Membrane Transport: Cellulose Acetate Membranes", University of Ottawa, Ph.D., Ottawa, Ontario, Canada, 1989.

Treybal, R. E., "Mass-Transfer Operations", 3rd ed., McGraw-Hill, Inc., Toronto, Ontario, (1980), p. 19.

Tunay, O., and N. I. Kabdasli, "Hydroxide Precipitation of Complexed Metals", Wat. Res. **28**(10), pp. 2117-2124 (1994).

U.S. Environmental Protection Agency, "MINTEQA2: Metal Speciation Equilibrium Model for Surface and Ground Water", Ver. 3.11, CEAM, Office of Research and Development, Environmental Research Laboratory, Athens, Georgia (1991).

Vandegrift, G. F., C. Conner, J. C. Hutter, R. A. Leonard, L. Nufiez, J. Sedlet, and D. G. Wygmans, "Preliminary Plan for Treating Mixed Waste", ANL-93/29, Defence Waste Management (UC-721), Argonne National Laboratory, Argonne, Illinois, pp. 1-16, 19-24 (1993).

Warren, M., and D. Comstock, "Techniques for RO Membrane Cleaning", Water, **18**(9), (1995).

Weast, R. C., Ed., "CRC Handbook of Chemistry and Physics", 66th ed., CRC Press Inc., Boca Raton, Florida, (1985), pp. D219-D254.

Weber, W. J., "Physicochemical Processes for Water Quality Control" in "Environmental Science and Technology", R. L. Metcalf and J. N. Pitts, Jr., Eds., John Wiley and Sons, Inc., Toronto, Ontario, (1972), pp. 310-311.

Wijmans, J. G., S. Nakao, J. W. A. Van Den Berg, F. R. Troelstra and C. A. Smolders, "Hydrodynamic Resistance of Concentration Polarization Boundary Layers in Ultrafiltration", J. Membrane Sci., **22**, pp. 117-135 (1985).

Winfield, B. A., "Waste Treatment with Reverse Osmosis Membranes", Bioprocess Technology, **1**, pp. 355-373 (1986).

Winzeler, H. B., and G. Belfort, "Enhanced Performance for Pressure-Driven Membrane Processes: The Argument for Fluid Instabilities", J. Membrane Sci., **80**, pp. 35-47 (1993).

Zeiher, E. H. K., "Reverse Osmosis Iron and Scale Control: Treatment, Development, and Testing", Ultrapure Water, **1**(1), pp. 36-41 (1996).

Zenon Environmental Systems Inc., technical information on Filmtec modules provided at the time of purchase, 1993.

Appendix A

Sample Calculations

A.1 Permeate Flux Correction

Permeate flux is a function of several variables including temperature and pressure. The permeate flux was corrected to a temperature of 25°C and an applied pressure of 2760 kPa using a method proposed by Bukay (1984). The formula for the corrected permeate flux is given below:

$$\text{Corrected Permeate Flux} = \frac{2760\ \text{kPa}}{\text{Measured Pressure kPa}} \times \frac{\text{Measured Permeate Flux}}{\text{TCF}};$$

where TCF is the temperature correction factor supplied by the membrane manufacturer. For example, the permeate flux was observed to be 2.10 L/min at 2700 kPa and 23°C. The corrected permeate flux can then be calculated:

$$\begin{aligned}\text{Corrected Permeate Flux} &= \frac{2760\ \text{kPa}}{2700\ \text{kPa}} \times \frac{2.10\ \text{L/min}}{0.948} \\ &= 2.26\ \text{L/min}\ .\end{aligned}$$

Therefore, the corrected permeate flux is 2.26 L/min.

A.2 Volumetric Recovery

The volumetric reduction of waste can be expressed as VR. For example, 100 L of waste that has been volumetrically reduced to 15 L has produced 85 L of permeate. The VR can be calculated by the following:

$$\begin{aligned}VR &= \frac{\text{Permeate Volume}}{\text{Initial Feed Volume}} \times 100\% \\ &= \frac{85\ \text{L}}{100\ \text{L}} \times 100\% \\ &= 85\%\end{aligned}$$

Therefore, the VR is 85 percent. Note: It is important not to neglect the volume of the piping in the pilot-scale system to obtain accurate volumetric recoveries. The volume of the piping was determined to be 28.5 L and was added to the initial feed volume in the VR calculations. The method and calculations performed to determine the piping volume is shown in appendix F.

The concentration can be calculated for any volumetric recovery from the initial concentrations. For example, the concentration of calcium at 85 percent volumetric recovery can be calculated from the following:

$$\begin{aligned}\left[Ca^{2+}\right]_{85\%} &= \frac{\left[Ca^{2+}\right]_{0\%}}{(1-0.85)} \\ &= \frac{14.1}{(1-0.85)} \\ &= 94\ (mg/L)\end{aligned}$$

The concentration of the calcium ion is 94 mg/L.

A.3 Mass Transfer Coefficient Calculations

For test 1, the calculation of the mass transfer coefficient of salt, (k_{NaCl}), at a crossflow of 30 L/min is the following.

Known: C_{A3} = 0.0805 wt%
C_{A1} = 3.181 wt%
P_g = 27.218 atm
SA = 6.2802 m^2

Extrapolating from table in the reference by Weast (1985) gives a freezing point depression of 0.05047 K for the permeate solution. Thus, the freezing point of the solution, T_{sol}, is 273.15 - 0.05047 K = 273.09953 K. Using equation 1,

$$\begin{aligned}\Pi(C_{A3}) &= 9.8286\times10^{5}\left(\frac{1}{273.009953}-\frac{1}{273.15}\right) \\ &= 0.6643 \text{ atm.}\end{aligned}$$

Plugging this into equation 2 gives,

$$\Pi(C_{A2}) = 0.6643 + 27.218\left(1 - \frac{0.189}{2.63}\right)$$
$$= 25.926 \text{ atm.}$$

The freezing point of the solution at the membrane surface can be found from equation 1.

$$25.926 = 9.8286 \times 10^5 \left(\frac{1}{T_{sol}} - \frac{1}{273.15}\right)$$
$$T_{sol} = 271.196 \text{ K.}$$

The freezing point depression for C_{A2} is 1.954 K. From the freezing point depression of the salt solution, the concentration of the solution can be found using the same table used above. Thus, C_{A2} is equal to 3.264 wt. %.

The mass transfer coefficient of the salt (k_{NaCl}) can be found using equation 3. First the mole flux of water must be determined using equation 4:

$$N_B = \frac{0.189 \times \frac{1}{60}}{6.2802} \times 55.6$$
$$= 0.02789 \ \frac{\text{mol}}{\text{m}^2 \cdot s};$$

and C_{A1}, C_{A2}, and C_{A3} must be converted to mole fractions:

$$C_{A1} = \frac{3.181\%}{100\%} \times 1.0231 \frac{g}{cm^3} \times 1000 \frac{cm^3}{L} \times \frac{1}{58.5} \frac{mol}{g}$$
$$= 0.55632 \frac{mol}{L}.$$

Thus,

$$x_{A1} = \frac{0.55632}{55.6 + 0.55632}$$
$$= 0.009907.$$

The mole fractions, x_{A2} and x_{A3},, can be found in a similar manner:

$$x_{A2} = 0.010168$$
$$x_{A3} = 2.474 \times 10^{-4}.$$

Finally,

$$k = \frac{0.02789}{55600 \ln\left(\frac{0.010168 - 2.474 \times 10^{-4}}{0.009907 - 2.474 \times 10^{-4}}\right)}$$
$$= 1.881 \times 10^{-5} \frac{m}{s}.$$

Therefore, the mass transfer coefficient of salt (k_{NaCl}) at a crossflow of 30 L/min is 1.881×10^{-5} m/s.

A.4 Boundary Layer Concentration Calculations

The boundary layer concentration of specific ions can be calculated using the mass transfer coefficient of salt found at each crossflow velocity. The mass transfer coefficient of the suspected fouling species can be found by the two-thirds rule (equation 5). The diffusion coefficient of calcium (D_{Ca+}) is 7.920×10^{-6} cm^2/s and the diffusion coefficient of salt (D_{NaCl}) is 1.611×10^{-5} cm^2/s. Therefore,

$$k_{Ca^{2+}} = 1.881 \times 10^{-5}\left(\frac{7.920 \times 10^{-6}}{1.611 \times 10^{-5}}\right)^{2/3}$$
$$= 1.171 \times 10^{-5} m/s.$$

Knowing the feed and permeate concentrations of calcium, the mole fraction of calcium at the membrane surface (x_{A2}) can be determined from equation 3 similar to example A.2. The mole fraction can then be converted to mol/L giving C_{A2}.

A.5 Volumetric Recovery Factor

The VRF can be calculated from the VR expressed as a fraction. At a VR of 85 percent, the VRF can be calculated from the following:

$$VRF = \frac{1}{1 - VR}$$
$$= \frac{1}{1 - 0.85}$$
$$= 6.67$$

Therefore, the VRF is 6.67 for a VR of 85 percent.

A.6 Predicted Permeate Fluxes

The predicted permeate flux is based on the total osmotic pressure created by the boundary layer concentrations of the species present in solution. The C_{A1} values are obtained from the dissolved concentrations in the MINTEQA2 output. The boundary layer concentrations, C_{A2}, of each of the species present in the AD/DC waste and their associated osmotic pressure, $\Pi(C_{A2})$, must be found.

The following example illustrates the steps required to find the boundary layer concentration and osmotic pressure of the sodium ion at 85 percent volumetric recovery during the AD/DC waste batch run at a crossflow of 52.5 L/min.

In order to solve equation 18, the following values must be known: $[Na^+]$, k_{Na^+} and A. From MINTEQA2 output (sample shown in appendix D), $[Na^+] = 7.682 \times 10^{-2}$ mol/L at 85 percent volumetric recovery. At 52.5 L/min crossflow, the mass transfer coefficient of the sodium ion, k_{Na^+}, is calculated from equation 5 using the appropriate value of k_{NaCl}. The value of k_{Na^+} is found to be 2.77×10^{-5} m/s. The membrane constant, A, is determined from the average of the pure water permeabilities (PWP_{avg}) obtained prior to the AD/DC test:

$$A = \frac{PWP_{avg}}{\Delta p \cdot SA}$$

$$= \frac{2.70 \frac{L}{\min}}{27.2\ atm \cdot 6.28\ m^2} \times \frac{1}{1000} \frac{m^3}{L} \times \frac{1}{60} \frac{\min}{s}$$

$$= 2.632 \times 10^{-7} \frac{m}{atm \cdot s}$$

Solving equation 21, the boundary layer concentration of Na^+ and its related osmotic pressure can be found. Again, the osmotic pressure due to the permeate is considered negligible; therefore, $\Delta\Pi \equiv \Pi(C_{A2})$.

$$\ln\left(\frac{C_{A2}}{C_{A1}}\right) - \frac{A}{k_{Na^+}}\left(\Delta p - \Pi(C_{A2})_{Na^+}\right) = 0$$

$$\ln\left(\frac{C_{A2}}{7.682 \times 10^{-2}}\right) - \frac{2.632 \times 10^{-7}}{2.77 \times 10^{-5}}\left(27.2 - \Pi(C_{A2})_{Na^+}\right) = 0$$

We find C_{A2} of sodium equals 9.73×10^{-2} mol/L and $\Pi(C_{A2})_{Na^+}$ equals 2.328 atm.

The sum of all of the osmotic pressures due to the boundary layer concentrations of all of the dissolved species is used to predict the permeate flux. At 85 percent volumetric recovery, $\Pi(C_{A2})$ is 4.92 atm. Using equation 18 and assuming the total osmotic pressure of the permeate is negligible,

$$N_B = A\left(\Delta p - \Pi(C_{A2})\right)$$

$$= 2.632 \times 10^{-7}(27.2 - 4.92)$$

$$= 5.86 \times 10^{-6} \frac{m^3}{m^2 \cdot s}.$$

Converting to L/min for one membrane element,

$$N_B = 5.86 \times 10^{-6} \times 1000 \frac{L}{m^3} \times 60 \frac{s}{\text{min}} \times 6.28\ m^2$$

$$= 2.21 \frac{L}{\text{min}} .$$

Therefore, the predicted permeate flux for the membrane element at 85 percent volumetric recovery at a crossflow velocity of 52.5 L/min is 2.21 L/min.

Appendix B

Computer Program to Calculate Osmotic Pressures and Boundary Layer Concentrations

The following computer program was written in Microsoft® QuickBASIC™ for easy transfer of data to Lotus 1-2-3.

Given the permeate concentration in weight percent, the freezing point depression of the permeate (T_{sol}) is calculated by linear interpolation between the given set of data points. The osmotic pressure of the permeate, $\prod(C_{A1})$, can then be calculated using equation 1.

Given the osmotic pressure of the boundary layer concentration ($\prod(C_{A2})$), the boundary layer concentration is calculated by linear interpolation between the given set of data points. The output of the program can be inputted into a spreadsheet for further calculations.

```
OPEN "ospress.out" FOR APPEND AS #1
OPEN "ospress2.out" FOR APPEND AS #2
OPEN "conc.out" FOR APPEND AS #3
OPEN "conc2.out" FOR APPEND AS #4

'  Output #1 and #3 creates output with easy to read headings
'  Output #2 and #4 creates output for easy transfer to Lotus 123

CLS

DIM a(42)
DIM b(42)

' tb = freezing point of pure water (K)
tb = 273.15

' salt solution concentrations (wt%)
FOR j = 1 TO 41
a(j) = .1# + a
a = a + .1
NEXT j

' freezing point depressions of the salt solutions wrt concentration (K)
b(1) = .062
b(2) = .121
b(3) = .181
b(4) = .24
b(5) = .299
b(6) = .358
b(7) = .417
b(8) = .475
b(9) = .534
b(10) = .593
b(11) = .652
b(12) = .711
b(13) = .77
b(14) = .829
b(15) = .888
b(16) = .948
b(17) = 1.007
b(18) = 1.067
b(19) = 1.126
b(20) = 1.186
b(21) = 1.246
b(22) = 1.306
b(23) = 1.366
b(24) = 1.426
b(25) = 1.486
b(26) = 1.547
b(27) = 1.607
b(28) = 1.668
b(29) = 1.729
b(30) = 1.79
b(31) = 1.851
b(32) = 1.913
b(33) = 1.974
b(34) = 2.036
b(35) = 2.098
b(36) = 2.16
b(37) = 2.222
```

```
b(38) = 2.284
b(39) = 2.347
b(40) = 2.409

' Choice between determining the osmotic pressure of the permeate knowing
' the permeate concentration or determining the boundary layer concentration
' knowing the osmotic pressure of Ca2

INPUT "Type 1 if permeate conc. known or type 2 if osmotic pressure known"; x
IF x <> 1 AND x <> 2 THEN 30
IF x = 1 THEN 5
IF x = 2 THEN 15

' THIS SECTION CALCULATES THE OSMOTIC PRESSURE OF THE PERMEATE

5 INPUT "Type in file name"; z$
PRINT #1, z$
PRINT #1, "Permeate Conc       Freezing Point Depression     Osmotic Pressure"
PRINT #2, z$
10 INPUT "Input concentration in wt% or zero to exit"; conc

IF conc = 0 THEN 30

' the freezing point depression is found by linear interpolation between two
' permeate concentration points

IF conc < a(1) THEN
conc1 = 0
conc2 = a(1)
fpd1 = 0
fpd2 = b(1)
END IF

FOR i = 1 TO 41
IF conc >= a(i) AND conc < a(i + 1) THEN
conc1 = a(i)
conc2 = a(i + 1)
fpd1 = b(i)
fpd2 = b(i + 1)
END IF
NEXT i

PRINT , "Permeate Concentration (wt%)      ", conc
' freezing point depression is calculated by linear interpolation
fpd = (fpd2 - fpd1) * (conc - conc1) / (conc2 - conc1) + fpd1
PRINT , "Freezing pt depression (K)         ", fpd
' osmotic pressure calculation
pi = 982860 * (1 / (tb - fpd) - 1 / tb)
PRINT , "Osmotic pressure of permeate (atm)", pi
PRINT #1, TAB(5); conc; TAB(30); fpd; TAB(53); pi
PRINT #2, conc; fpd; pi
GOTO 10

' THIS SECTION CALCULATES THE BOUNDARY LAYER CONCENTRATION FROM THE
' OSMOTIC PRESSURE OF Ca2.

15 INPUT "Type in file name"; z$
PRINT #3, z$
PRINT #3, "Osmotic Pressure   Freezing Point Depression  Boundary Layer Conc'
PRINT #4, z$
```

```
20 INPUT "Input osmotic pressure of the boundary layer or zero to exit"; p

IF pi = 0 THEN 30

' the freezing point of the solution (tsol) is calculated
tsol = 1 / (pi / 982860 + 1 / tb)
' the freezing point depression calculation
fpd = tb - tsol

' the concentration of the boundary layer is found by linear interpolation
' between two freezing point depressions

FOR m = 1 TO 41
IF fpd = b(m) THEN
fpd1 = b(m)
fpd2 = b(m + 1)
conc1 = a(m)
conc2 = a(m + 1)
END IF
NEXT m

FOR n = 1 TO 41
IF fpd > b(n) AND fpd < b(n + 1) THEN
fpd1 = b(n)
fpd2 = b(n + 1)
conc1 = a(n)
conc2 = a(n + 1)
END IF
NEXT n

PRINT , "Boundary layer osmotic pressure (atm)", pi
PRINT , "Freezing point depression (K)        ", fpd
' the boundary layer concentration calculation
conc = conc1 + (fpd - fpd1) * ((conc2 - conc1) / (fpd2 - fpd1))
PRINT , "Boundary layer concentration (wt%)   ", conc
PRINT #3, TAB(5); pi; TAB(30); fpd; TAB(53); conc
PRINT #4, pi, fpd, conc
GOTO 20

30 END
```

Appendix C

Raw Data for Work Discussed in Chapter 5

Table C1: Raw PWP Data for PWP 2 Run

Date: Mar. 26/96

Time (min.sec)	Total permeate Weight (kg)	Crossflow (LPM)	Accumulated Flow (L)	Low pre-mem. press. reading (psi)	High pre-mem. press. reading (psi)	Post-membrane pressure (psi)	Initial Permeate weight (kg)	Final Permeate weight (kg)	Suction press. to HP pump (psi)	Feed flowrate (LPM)	Recirculation flowrate	System temperature (deg. C)	pH meter temperature (deg. C)
2.00	8.04	30.9	62052	390	394	387.5	9.9	12.42	16.5	N/A	19.5	23	N/A
9.00	25.91	30.83	62263	390	396	388.5	27.2	29.92	15.5	N/A	19	26	25.6
14.00	39.39	31.13	62420	393	400	392.5	40.2	42.92	15.5	N/A	19	25	24.7
										N/A			
2.00	13.15	37.1	62813	386	392	383.5	14.2	16.87	19	N/A	24	25	25.2
4.30	19.69	36.95	62905	386	392	383.5	20.4	23.07	19	N/A	24	25	25.4
7.15	27	37	63009	388	393	384.5	28.6	31.43	19	N/A	24	25	25.1
										N/A			
3.00	41.57	45.89	63266	386	392	382	42.6	45.17	22.5	N/A	31.75	24	24.4
5.30	47.87	45.64	63383	386	393	382	48.7	51.24	22.5	N/A	31.75	23	24.3
9.15	57.38	45.68	63558	386	391	380.5	58.3	60.96	22.5	N/A	31.75	25	25.7
										N/A			
2.30	17.19	52.51	64040	386	390	380	18.5	21.15	25	N/A	37.5	25	25.3
5.00	23.73	52.64	64174	386	391	380.5	24.8	27.45	25	N/A	37.5	25	25.3
7.30	30.21	52.54	64304	385	390	379.5	31	33.64	25	N/A	37.5	25	25.4
										N/A			
2.00	42.66	60.06	64589	386	393	378.5	44.2	46.85	26.5	N/A	45	25	25.4
4.45	50.03	60.36	64754	388	395	379.5	50.8	53.43	26.5	N/A	45	25	25.3
7.15	58.52	60.53	64909	389	394	378.5	57.4	60.03	26.5	N/A	45	25	25.3

Table C2: Raw PWP Data for PWP 3 Run

Date: Mar. 27/96

Time (min.sec)	Total permeate Weight (kg)	Crossflow (LPM)	Accumulated Flow (L)	Low pre-mem. press. reading (psi)	High pre-mem. press. reading (psi)	Post-membrane pressure (psi)	Initial Permeate weight (kg)	Final Permeate weight (kg)	Suction press. to HP pump (psi)	Feed flowrate (LPM)	Recirculation flowrate (LPM)	System temperature (deg. C)	pH meter temperature (deg. C)
3.30	15.29	30.42	80799	389	401	389.5	16.1	16.47	16	N/A	19	22	22.5
7.30	24.74	31.35	80925	386	392	384	25.4	27.87	16	N/A	19	24	23.9
10.00	30.83	31.33	81003	386	393	383.5	31.4	33.96	15.5	N/A	20	25	24.6
1.00	41.86	37.24	81162	386	394	382	43.4	46.07	18.5	N/A	25	26	25.4
3.30	48.4	37.23	81255	387	397	385.5	49.5	52.03	18.5	N/A	25	24	24.5
6.00	54.63	37.39	81350	388	396	385.5	55.3	57.79	18.5	N/A	25	24	24.2
1.00	7.69	45.35	81587	388	392	381.5	9	11.64	23	N/A	31.75	25	25.3
4.00	15.55	45.02	81724	385	391	379.5	16.2	18.89	22.5	N/A	31.75	26	26.1
6.00	20.87	45.23	81814	385	390	378	21.6	24.34	22.5	N/A	31.75	26	26.6
1.00	31.34	52.16	82015	387	396	379.5	35.3	37.84	24.5	N/A	37.5	25	24.9
4.00	38.94	52.17	82171	388	395	380.5	39.7	42.24	24.5	N/A	37.5	24	24.4
7.00	46.39	51.91	82330	388	394	380.5	47.5	50.01	24.5	N/A	37.5	24	24.2
1.00	55.39	60.84	82541	384	391	374.5	56.7	59.19	26.5	9.4	46	24	24.5
3.30	61.5	60.75	82685	382	391	373.5	62.3	64.84	26.5	9.4	46	24.5	24.6
6.00	67.64	60.76	82843	383	391	372.5	67.9	70.39	26.5	9.4	46	25	24.6

Table C3: Raw PWP Data for PWP 4 Run

Date: Apr. 1/96

Time (min.sec)	Total permeate Weight (kg)	Crossflow (LPM)	Accumulated Flow (L)	Low pre-mem. press. reading (psi)	High pre-mem. press. reading (psi)	Post-membrane pressure (psi)	Initial Permeate weight (kg)	Final Permeate weight (kg)	Suction press. to HP pump (psi)	Feed flowrate (LPM)	Recirculation flowrate (LPM)	System temperature (deg. C)	pH meter temperature (deg. C)
2.30	11.96	30.5	96307	388	396	386.5	13.4	15.97	16	N/A	18.75	24	25
5.30	19.62	30.59	96396	389	400	387.5	20.5	23.06	15.5	N/A	18.75	24	24.7
8.00	25.99	30.52	96476	389	396	387	26.6	29.21	15.5	N/A	18.75	25	25.1
2.00	11.83	37.65	96764	386	396	382.5	13	15.65	19	N/A	25	25	25.6
4.30	18.41	37.96	96859	385	394	381.5	19.2	21.86	19	N/A	25	26	26
7.00	25.02	38.05	96953	386	393	381.5	25.7	28.41	19	N/A	25	26	26.1
2.15	41.21	46.07	97228	387	394	380.5	42.4	44.97	22.5	N/A	32.5	25	24.8
4.45	47.52	45.47	97344	388	396	381.5	48.7	51.24	22.5	N/A	32	24	24.5
7.15	53.73	44.91	97456	387	395	382.5	54.4	57.01	22.5	N/A	32	23	24.2
2.00	9.22	52.06	97769	386	392	378	10.4	13.01	25	N/A	37.5	25	25.6
4.30	15.69	52.25	97926	384	392	377.5	16.7	19.34	25	N/A	37.5	26	25.7
7.00	22.15	52.38	98050	385	392	378.5	22.8	25.42	25	N/A	37.5	25	25.3
2.15	34.23	60.55	98324	386	396	377.5	35.5	38.06	26.5	9.5	45	25	25
4.45	40.53	60.83	98474	387	394	379.5	41.1	43.65	26.5	9.5	45	24	24.8
7.15	46.79	60.78	98629	386	397	377.5	47.5	50.04	26.5	9.5	45	24	24.8

Table C4: Raw PWP Data for PWP 5 Run

Date: May 7/96

Time (min.sec)	Total permeate Weight (kg)	Crossflow (LPM)	Accumulated Flow (L)	Low pre-mem. press. reading (psi)	High pre-mem. press. reading (psi)	Post-membrane pressure (psi)	Initial Permeate weight (kg)	Final Permeate weight (kg)	Suction press. to HP pump (psi)	Feed flowrate (LPM)	Recirculation flowrate (LPM)	System temperature (deg. C)	pH meter temperature (deg. C)
2.00	10.63	30.75	112870	405	407	402	16.6	19.16	16	N/A	19	24	23.9
8.00	25.79	30.36	113060	396	400	394.5	26.8	29.46	15	N/A	19	25	25.3
11.00	33.69	29.9	113149	394	398	391.5	34.3	37	15	N/A	19	26	25.9
0.30	45.72	37.55	113315	402	404	396.5	46.5	49.11	18.5	N/A	25	24	24.6
3.00	52.06	37.66	113406	401	405	396.5	52.7	55.31	18.5	N/A	25	25	25.2
5.00	57.36	37.22	113487	392	396	386	58	60.62	18.5	N/A	25	25	25.8
1.00	11.09	44.83	113864	398	400	390.5	12.1	14.84	22.5	N/A	31	26	26.2
4.00	19.18	44.46	113969	397	400	390.5	19.9	22.61	22.5	N/A	31	26	26
6.30	25.88	44.41	114110	396	400	390	26.4	N/A	22.5	N/A	31	25.5	25.7
1.00	42.69	52.77	114444	396	404	387	46.8	49.43	24.5	N/A	37.5	25	25.6
4.00	50.5	53.01	114613	395	401	387.5	51.7	54.33	24.5	N/A	37.5	25	25.6
6.30	56.96	52.75	114734	395	400	386	57.7	60.34	24.5	N/A	37.5	25	25.6
1.00	65.71	60.97	114928	398	402	387	67.9	70.54	26.5	9.75	45	25	25.6
4.00	73.49	60.97	115110	397	401	387	74.2	76.84	26.5	9.75	45	25	25.7
6.30	79.99	60.69	115264	396	402	387	80.6	83.19	26.5	9.75	45	25	25.1

Table C5: Raw NaCl Data for Test 1

Date: Mar. 21/96

Time (min.sec)	Conductivity Feed (uS/cm)	Permeate (uS/cm)	Total permeate Weight (kg)	Crossflow (LPM)	Accumulated Flow (L)	Low pre-mem. press. reading (psi)	High pre-mem. press. reading (psi)	Post-membrane pressure (psi)	Initial Permeate weight (kg)	Final Permeate weight (kg)	Suction press. to HP pump (psi)	Feed flowrate (LPM)	Recirculation flowrate (LPM)	System temperature (deg. C)	pH meter temperature (deg. C)
1.00	43900	591	7.63	29.32	51971	390	393	382.5	7.66	8.25	17	N/A	20	25	N/A
4.15			8.60	29.47	52068	386	393	383.5	8.9	9.28	17	N/A	20	25	N/A
6.00			9.46	29.61	52120	386	390	383.5	9.6	9.97	17	N/A	20	25	N/A
2.00	45200	695	11.33	37.79	52344	390	394	385.5	11.5	11.86	21	N/A	27.5	25	N/A
4.30			12.13	37.67	52439	390	394	385.5	12.23	12.56	21	N/A	27.5	25	N/A
6.00			12.66	37.7	52494	390	393	385.5	12.74	13.09	21	N/A	27.5	25	N/A
1.00	46000	732	13.85	45.65	52667	389	393	382.5	13.97	14.29	24.5	N/A	35	25	N/A
4.00			14.71	45.94	52805	390	394	382.5	14.83	15.14	24.5	N/A	35	24	N/A
6.00			15.33	45.68	52894	389	393	382.5	15.43	15.73	24.5	N/A	35	25	N/A
1.00	46900	1000	16.03	52.7	53145	388	392	379	16.19	16.48	26	N/A	40	25	N/A
4.00			16.81	52.51	53300	388	391	379.5	16.9	17.19	26	N/A	40	26	N/A
6.00			17.38	52.64	53405	388	392	379.5	17.46	17.74	26	N/A	40	26	N/A
1.00	48000	1015	18.16	60.67	53576	388	392	376.5	18.33	18.59	28	7.5	48.75	26	N/A
4.00			18.82	60.94	53759	388	392	376.5	18.94	19.18	28	7.5	48.75	26	N/A
6.00			19.31	60.75	53880	388	392	376	19.4	19.64	28	7.5	48.75	26	N/A

Table C6: Raw NaCl Data for Test 2

Date: Apr. 1/96

Time (min.sec)	Conductivity Feed (uS/cm)	Permeate (uS/cm)	Total permeate Weight (kg)	Crossflow (LPM)	Accumulated Flow (L)	Low pre-mem. press. reading (psi)	High pre-mem. press. reading (psi)	Post-membrane pressure (psi)	Initial Permeate weight (kg)	Final Permeate weight (kg)	Suction press. to HP pump (psi)	Feed flowrate (LPM)	Recirculation flowrate (LPM)	System temperature (deg. C)	pH meter temperature (deg. C)
7.00	38700	478	3.73	30.36	99818	387	392	384.5	4.00	4.52	17	N/A	21	23	24
10.00	N/A	N/A	5.28	30.47	99910	386	393	384.5	5.40	5.92	17	N/A	21	24	24.7
13.30	N/A	N/A	7.08	30.37	100016	387	392	384.5	7.21	7.72	17	N/A	21	25	N/A
6.00	41200	556	11.55	37.64	100357	388	395	384.5	11.77	12.22	21	N/A	27.5	25	25.1
10.00	N/A	N/A	13.23	37.51	100507	390	395	385.5	13.36	13.78	21	N/A	27.5	23	24.3
12.30	N/A	N/A	14.28	37.68	100602	390	396	386	14.36	14.77	21	N/A	27.5	23	24.1
6.00	43700	730	17.91	45.06	101050	388	394	382.5	18.05	18.41	24	N/A	35	25	25.5
9.00	N/A	N/A	18.88	44.88	101184	388	395	382.5	18.96	19.31	24	N/A	35	25.5	26
11.30	N/A	N/A	19.74	45	101296	389	394	382.5	19.84	20.17	24	N/A	35	24	24.9
6.00	45700	909	22.35	52.5	101796	386	394	378.5	22.55	22.82	26	14.2	40	24	24.3
9.30	N/A	N/A	23.19	52.34	101979	388	396	380.5	23.29	23.56	26	14.2	40	24	24.1
12.00	N/A	N/A	23.84	52.19	102112	387	394	380.5	23.91	24.16	26	14.2	40	23	24
6.00	47200	1246	25.79	60.46	102620	386	392	376.5	25.970	26.185	27.5	7.2	48	24	24.2
10.00	N/A	N/A	26.52	60.65	102864	388	393	377	26.570	26.773	27.5	7.2	48	23	23.4
12.30	N/A	N/A	27.00	60.33	103013	389	394	377.5	27.040	27.237	27.5	7.2	48	24	24.7

Table C7: Raw NaCl Data for Test 3

Date: May 14/96

Time (min.sec)	Conductivity Feed (uS/cm)	Permeate (uS/cm)	Rejection Efficiency	otal permeat Weight (kg)	Crossflow (LPM)	Accumulated Flow (L)	Low pre-mem ɔress. reading (psi)	High pre-mem. press. reading (psi)	Post-membrane pressure (psi)	Initial Permeate weight (kg)	Final Permeate weight (kg)	Suction press. to HP pump (psi)	Feed flowrate (LPM)	Recirculation flowrate (LPM)	System temperature (deg. C)	pH meter temperature (deg. C)
6.00	40600	480	0.988177	3.11	30.97	116705	399	407	401	3.55	4.07	17	N/A	22	24	24.9
9.30	41100	490	0.988078	4.79	31.19	116817	405	408	401.5	4.94	5.44	17	N/A	22	25	25.2
12.00	41600	522	0.987452	5.94	31.14	116895	403	406	399.5	6.06	6.53	17	N/A	22	25	25.3
5.00	42600	643	0.984977	9.29	37.61	117192	402	403	396.5	9.47	9.88	20	N/A	27.5	25	25.7
8.00	43600	670	0.984633	10.43	37.67	117306	402	404	396.5	10.52	10.92	20	N/A	27.5	26	25.9
11.00	44100	N/A	N/A	11.51	37.75	117420	402	404	397	11.63	12.01	20	N/A	27.5	26	26.1
2.00	46000	1005	0.978152	16.06	45.53	118097	399	400	391	16.25	16.53	24	N/A	34.5	26	25.9
5.00	46700	1035	0.977837	16.82	45.51	118235	399	401	391.5	16.93	17.20	24	N/A	34.5	26	25.7
8.30	46700	1060	0.977302	17.64	45.52	118394	400	402	392.5	17.71	17.96	24	N/A	34.5	23	24
2.00	47200	1293	0.972606	18.57	52.45	118672	398	400	387.5	18.690	18.914	26	N/A	40	26	25.6
5.30	47600	1340	0.971849	19.24	52.45	118854	397	400	387.5	19.30	19.51	26	N/A	40	26	26
8.30	N/A	N/A	N/A	19.76	52.35	119015	396	399	387.5	19.840	20.040	26	N/A	40	26	26
3.00	48900	1600	0.96728	20.799	60.40	119316	401	404	388.5	20.900	21.060	27.5	7.8	N/A	25	25.9
6.00	49100	1670	0.965968	21.323	60.36	119497	400	403	389	21.460	21.629	27.5	7.2	48	25	25.4
10.00	49100	N/A	N/A	21.847	60.22	119740	400	402	389	21.900	22.061	27.5	7.2	48	25	N/A

Table C8: Raw NaCl Data for Test 4

Date: June 18/96

Time (min.sec)	Conductivity Feed (uS/cm)	Permeate (uS/cm)	Total permeate Weight (kg)	Crossflow (LPM)	Low pre-mem. press. reading (psi)	High pre-mem. press. reading (psi)	Post-membrane pressure (psi)	Suction press. to HP pump (psi)	Feed flowrate (LPM)	Recirculation flowrate (LPM)	System temperature (deg. C)	pH meter temperature (deg. C)	Permeate weight (kg)	Time (min)
42.30	47800	1170	N/A	29.78	393	405	394.3	16.5	N/A	21	26	25.4	0.497	118.65
56.00	47800	1218	N/A	29.70	389	404	395.5	16.5	N/A	21	25	25.1	0.506	119.09
66.00	47800	1239	N/A	29.55	396	402	394.0	17.5	N/A	21	25	25.1	0.505	121.32
11.00	47900	1215	N/A	37.48	398	402	393.0	21.0	N/A	28	25	24.7	0.525	132.25
21.00	47900	1189	N/A	37.57	398	402	393.8	21.0	N/A	28	25	24.9	0.525	126.92
31.00	47900	1208	N/A	37.55	398	401	393.0	21.0	N/A	28	25	25.3	0.500	122.06
11.00	47800	1186	N/A	45.21	401	403	393.0	24.0	N/A	34	25	24.6	0.511	123.13
20.00	47900	1162	N/A	45.23	401	403	393.5	24.0	N/A	34	25	24.9	0.518	125.91
29.30	47900	1172	N/A	45.23	401	403	393.5	24.0	N/A	34	25	25.1	0.514	118.53
13.00	48000	1269	N/A	52.61	400	402	390.3	26.5	N/A	40	25	25.5	0.509	127.8
22.30	48300	1256	N/A	52.59	400	402	390.5	26.5	N/A	40	25	25.6	0.498	124.19
36.00	48300	1231	N/A	52.68	400	402	390.5	26.5	N/A	40	25	25.0	0.507	124.99
25.00	48600	1300	N/A	60.57	400	403	388.3	28.0	7.5	48	25	24.7	0.512	134.77
40.15	48600	1370	N/A	60.59	400	402	387.5	28.0	7.5	48	25	25.7	0.514	139.52
49.30	48500	1350	N/A	60.53	400	402	388.0	28.0	7.5	48	25	25.1	0.499	135.36

Table C9: Raw NaCl Run Data for k_{NaCl} /

Date: June 12/96

Time (min.sec)	Conductivity Feed (uS/cm)	Conductivity Permeate (uS/cm)	Crossflow (LPM)	Low pre-mem. press. reading (psi)	High pre-mem. press. reading (psi)	Post-membrane pressure (psi)	Permeate weight (kg)	Time (min)	Suction press. to HP pump (psi)	Recirculation flowrate (LPM)	System temperature (deg. C)	pH meter temperature (deg. C)
15	49200	1560	29.64	397	403	397.5	0.988	5.23	16.5	21	25	24.9
26	49200	1570	29.24	398	404	396	0.484	2.26	16.5	21	25	25.2
34	49300	1570	29.66	397	405	396.5	0.495	2.26	16.5	21	25	25.2
13	49400	1530	37.24	398	402	394.5	0.496	2.31	21	27.5	25	25.2
20.3	49300	1560	37.25	398	402	394.5	0.496	2.32	21	27.5	25	25.3
27	49300	1560	37.41	398	402	394.5	0.495	2.38	21	27.5	25	25.3
10	49400	1540	45.35	401	404	394.5	0.49	2.26	24	34	25	25.3
18	49400	1520	45.24	401	403	394	0.491	2.24	24	34	25	25.2
24	49400	1530	45.53	401	404	394.5	0.488	2.27	24	34	25	25.2
55.3	49400	1690	52.4	396	400	387.5	0.496	2.68	26.5	40	25	24.9
64	49500	1700	52.58	396	400	387.5	0.486	2.56	26.5	40	25	25.2
74	49500	1700	52.51	396	400	387.5	0.494	2.6	26.5	40	25	24.2
29	49900	1830	60.33	397	402	387	0.485	3.11	28	47.5	25	24.7
41	49900	1850	60.31	397	401	386.5	0.492	2.94	28	47.5	25	24.9
50	49900	1870	60.35	397	402	387	0.492	2.8	28	47.5	25	25.1

Table C10: Raw NaCl Run Data for k_{NaCl} 2

Date: June 18/96

Time (min.sec)	Conductivity Feed (uS/cm)	Permeate (uS/cm)	Crossflow (LPM)	Low pre-mem. press. reading (psi)	High pre-mem. press. reading (psi)	Post-membrane pressure (psi)	Permeate weight (kg)	Time (sec)	Suction press. to HP pump (psi)	Recirculation flowrate (LPM)	System temperature (deg. C)	pH meter temperature (deg. C)
13.3	48000	1250	30.3	397	401	394.5	0.497	119	17	21	25	25.9
25.3	48000	1206	30.17	397	400	394.8	0.506	119	17	21	25	24.7
41	48200	1196	30.29	398	401	394.3	0.505	121	17	21	25	24.9
18	48300	1237	37.55	400	403	394.8	0.525	132	21	28	25	25.1
25.45	48300	1246	37.51	400	404	395.5	0.525	129	21	28	25	24.5
35	48300	1239	37.59	400	402	395	0.5	122	21	28	25	25.4
12	48800	1320	45.07	398	401	391.3	0.511	123	24	34	26	25.6
21.15	48700	1350	44.77	398	401	391	0.518	126	24.3	34	25	25
30.3	48100	1380	45.05	398	401	391	0.514	119	24	34	25	25.2
11	48400	1197	52.41	399	402	391	0.509	128	26	40	25	24.9
19	48400	1177	52.6	400	402	391.8	0.498	124	26.3	40	25	25
27.3	48400	1177	52.6	400	404	392.8	0.507	125	26	40	25	25.1
14	48600	1234	60.66	400	402	388.5	0.512	135	28	48	25	25.3
23.3	48500	1243	60.72	400	402	387.8	0.514	140	28	48	25	24.9
33	48600	1272	60.7	399	402	388	0.499	135	28	48	26	25.7

Table C11: Raw Data for AD/DC Test at 30 L/min Crossflow

Date: Mar. 25/96
Test #1 - 30 L/min crossflow

Time (min.sec)	Permeate Weight (kg)	Total permeate Weight (kg)	Crossflow (LPM)	Accumulated Flow (L)	Low pre-mem. press. reading (psi)	High pre-mem. press. reading (psi)	Post-membrane pressure (psi)	Initial Permeate weight (kg)	Final Permeate weight (kg)	Suction press. to HP pump (psi)	Feed flowrate (LPM)	Recirculation flowrate (LPM)	System temperature (deg. C)	pH meter temperature (deg. C)
0.00														
4.15	16.25	16.25	30.97	56262	389	394	384	17.3	19.59	15.5	N/A	20	23	N/A
10.00	29.21	29.21	30.93	56440	386	393	385	29.8	32.12	15.5	N/A	20	23	N/A
16.00	43.02	43.02	30.74	56627	389	393	386	43.6	45.96	15.5	N/A	20	24	N/A
26.00	66.95	66.95	30.91	56939	393	395	389.5	67.6	70.26	15.5	N/A	20	25	N/A
42.00	105.91	105.91	31.1	57438	390	394	387	106.8	109.21	15.5	N/A	20	24.5	N/A
44.50	109.659	109.659												
51.00	14.81	124.469	31.32	57760	388	397	387.5	15.8	18.2	15.5	N/A	20	24	N/A
63.00	42.63	152.489	29.81	58123	394	401	392	43.7	46.09	15.5	N/A	18.75	24	N/A
80.00	82.76	192.419	30.13	58691	389	393	388.5	83.6	85.95	15.5	N/A	19	25	24.8
90.00	105.82	215.479	30.32	58996	390	393	387	106.8	109.1	15.5	N/A	19	25	24.9
92.22	110.743	220.402												
108.00	34.67	255.072	30.18	59595	388	391	385.5	36.3	38.54	15.5	N/A	19	25	24.9
127.00	76.7	297.102	30.27	60166	390	392	386.5	80.3	82.47	15.5	N/A	19	25	24.8
78.30	100.74	321.142	30.36	60520	388	392	385.5	101.4	103.45	15.5	N/A	19	24	24.3
81.00	105.414	325.816												
144.00	5.33	331.146	30.64	60617	386	390	382.5	6.3	8.16	15.5	N/A	20	23	23.7
151.00	18.58	344.396	30.77	61032	385	390	383	19.3	21.29	15.5	N/A	20	26	26.2
N/A	22.776	348.592	30.77	61032	385	390	383	19.3	21.29	15.5	N/A	20	26	26.2

Table C12: Raw Data for AD/DC Test at 60 L/min Crossflow

Date: Mar. 25/96
Test #2-60 L/min crossflow

Time (min.sec)	Permeate Weight (kg)	Total permeate Weight (kg)	Crossflow (LPM)	Accumulated Flow (L)	Low pre-mem. press. reading (psi)	High pre-mem. press. reading (psi)	Post-membrane pressure (psi)	Initial Permeate weight (kg)	Final Permeate weight (kg)	Suction press. to HP pump (psi)	Feed flowrate (LPM)	Feed flowrate (LPM)	Recirculation flowrate (LPM)	System temperature (deg. C)	pH meter temperature (deg. C)
0.00	0	0													
3.00	7.71	7.71	60.41	69944	376	379	364.5	9.4	11.81	26.5	N/A	9.25	45	25	24.90
10.30	25.86	25.86	60.17	70400	390	396	379.5	27.2	29.59	26.5	N/A	9.5	46	24	23.80
20.00	48.18	48.18	60.84	70976	383	392	374	49.5	51.96	26.5	N/A	9.5	46	25	25.30
30.00	72.69	72.69	60.76	71587	386	392	375.5	73.4	75.88	26.5	N/A	9.5	46	25	25.50
41.00	98.75	98.75	60.92	72261	387	394	376.5	99.9	102.31	26.5	N/A	9.6	45	25	N/A
44.27	104.496	104.496													
49.00	13.78	118.278	60.84	73102	387	394	378.5	15.7	18.08	26.5	N/A	9.7	45.5	24	24.30
60.00	39.49	143.968	60.68	73787	386	393	377	40.5	42.89	26.5	N/A	9.7	45.5	25	24.80
70.00	62.97	167.468	60.7	74373	386	394	376.5	63.7	66.09	26.5	N/A	9.7	45.5	25	25.10
80.00	86.79	191.288	60.66	74967	386	394	375.5	87.8	90.2	26.5	N/A	9.7	45.5	25	25.40
88.00	100.77	205.268	60.81	75345	386	393	376	101.6	103.98	26.5		9.7	45.5	25	25.40
88.41	106.725	211.223									N/A				
90.00	3.14	214.363	60.55	75655	386	392	377.5	4.6	6.88	26.5	N/A	9.6	46	24	24.80
100.00	26.03	237.253	60.64	76259	384	392	375	27.1	29.44	26.5	N/A	9.7	45.5	25	25.50
111.30	52.22	263.443	60.74	76958	385	395	376.5	53.3	55.47	26.5		9.6	45.5	23	24.10
120.00	70.02	281.243	60.62	77477	386	396	379.5	70.8	72.87	26.5	N/A	9.6	45.5	23	23.30
133.30	98.44	309.663	60.15	78296	382	391	374.5	99.6	101.76	26.5	N/A	9.4	46	26	25.60
136.18	104.071	315.294									N/A				
137	1.44	316.734	59.6	78845	380	385	370	2.5	4.37	27		9.4	45	23	23.2
141	8.95	324.244	58.7	79081	391	394	381.5	9.9	11.91	26.5		9.4	45	25	24.9
140.3	13.963	329.257													

Table C13: Raw Data for AD/DC Test at 45 L/min Crossflow

Date: Mar. 28/96
Test #3 - 45 L/min crossflow

Time (min.sec)	Permeate Weight (kg)	Total permeate Weight (kg)	Crossflow (LPM)	Accumulated Flow (L)	Low pre-mem. press. reading (psi)	High pre-mem. press. reading (psi)	Post-membrane pressure (psi)	Initial Permeate weight (kg)	Final Permeate weight (kg)	Suction press. to HP pump (psi)	Feed flowrate (LPM)	Recirculation flowrate (LPM)	System temperature (deg. C)	pH meter temperature (deg. C)
0.00														
3.00	8.52	8.52	45.57	89094	388	393	382	9.6	11.82	23	N/A	31.75	22	22.6
10.00	24.02	24.02	45.46	89418	393	402	388.5	24.8	27.13	22.5	N/A	31.75	23	23.2
20.00	47.11	47.11	46.53	89890	386	394	380.5	48.2	50.56	22.5	N/A	32.5	23.5	24.1
31.00	73.19	73.19	46.77	90403	384	392	378.5	74.1	76.56	22.5	N/A	32.5	25	25.2
42.00	100.26	100.26	46.76	90917	387	397	383.5	101.3	103.6	22.5	N/A	32.5	26	25.6
45.52	108.785	108.785												
50.00	10.53	119.315	46.18	91374	390	396	385.5	12.9	15.23	22.5	N/A	32.5	23.5	24.1
64.00	35.98	144.765	46.37	91886	388	396	384.5	38.7	39.07	22.5	N/A	32.5	24	24.6
70.00	56.88	165.665	46.63	92304	387	394	382	57.5	59.87	22.5	N/A	32.5	25	24.7
80.00	79.98	188.765	46.38	92770	387	395	382.5	80.6	82.96	22.5	N/A	32.5	25	24.8
87.00	96.04	204.825	46.6	93095	389	397	384.5	97.3	99.64	22.5	N/A	32.5	25	N/A
90.43	104.031	212.816												
95.00	10.26	223.096	45.59	93558	389	394	384.5	11.1	13.46	22.5	N/A	32.5	26	25.8
104.00	31.45	244.286	45.92	93969	390	396	385.5	32.3	34.63	22.5	N/A	32.5	25	25.5
115.30	53.45	266.266	45.58	94470	391	396	385.5	54.1	56.26	22.5	N/A	32.5	24	24.8
128.00	73.08	285.876	45.75	95086	389	396	384	73.7	75.76	22.5	N/A	32.5	24	24.6
138.00	93.42	306.236	45.96	95547	388	396	385.5	94	96.04	22.5	N/A	32.5	26	25.8
142.13	101.139	313.955												

Table C14: Raw Data for AD/DC Test at 52.5 L/min Crossflow

Date: May 6/96
Test #4 - 52.5 L/min crossflow

Time (min.sec)	Permeate Weight (kg)	Total permeate Weight (kg)	Crossflow (LPM)	Accumulated Flow (L)	Low pre-mem. press. reading (psi)	High pre-mem. press. reading (psi)	Post-membrane pressure (psi)	Initial Permeate weight (kg)	Final Permeate weight (kg)	Suction press. to HP pump (psi)	Feed flowrate (LPM)	Recirculation flowrate (LPM)	System temperature (deg. C)	pH meter temperature (deg. C)
0.00														
2.00	9.34	9.34	52.42	105320	400	402	391.5	11.9	14.5	25	N/A	37.5	25	N/A
6.00	19.57	19.57	52.65	105532	402	403	393	20.08	23.39	25	N/A	37.5	25	N/A
12.00	34.56	34.56	52.8	105852	400	402	390.5	35.5	38.09	24.5	N/A	37.5	25	N/A
20.00	54.88	54.88	53.02	106277	400	402	391	55.7	58.31	24.5	N/A	37.5	25	N/A
28.00	75.29	75.29	52.9	106700	399	402	391	75.9	78.52	24.5	N/A	37.5	25	N/A
36.00	95.31	95.31	52.54	107124	399	403	391.5	95.9	98.35	24.5	N/A	37.5	23	N/A
40.31	105.575	105.575												
43.00	7.56	113.135	52.57	107584	395	401	386.5	9	11.57	24.5	N/A	37.5	26	25.7
50.00	24.7	130.275	52.69	107958	398	404	390.5	25.4	27.81	24.5	N/A	37.5	24	24.2
60.00	49.05	154.625	53.06	108492	397	402	389.5	50	52.54	24.5	N/A	37.5	25	25.8
70.00	73.67	179.245	52.94	109019	398	402	390.5	74.3	76.76	24.5	N/A	37.5	25	25.2
78.00	92.74	198.315	52.94	109444	400	402	391.5	93.5	95.93	24.5	N/A	37.5	25	25.2
80.24	97.637	203.212												
86.00	13.81	217.022	52.59	109923	397	400	389.5	21.3	23.69	24.5	N/A	37.5	25.5	25.7
95.00	34.82	238.032	52.19	110398	398	401	390	35.5	37.81	24.5	N/A	37.5	24	24.5
105.00	57.67	260.882	52.65	110930	398	401	390	58.2	60.49	24.5	N/A	37.5	24	24.6
112.00	72.92	276.132	52.35	111294	401	404	392.5	74.2	76.54	24.5	N/A	37.5	25	25.3
118.00	86.66	289.892	52.62	111609	402	404	392.5	87.1	89.45	24.5	N/A	37.5	25	N/A
122.10	95.379	298.591												
140.30	6.34	304.931	52.27	112159	403	403	389	7	9.25	25	N/A	37.5	25	25.8
130.00	17.06	315.651	52.15	112419	402	402	388.5	17.5	19.73	24.5	N/A	37.5	25.5	N/A

Table C15: Raw Data for AD/DC Test at 37.5 L/min Crossflow

Date: June 13/96
Test #5 - 37.5 L/min crossflow

Time (min.sec)	Permeate Weight (kg)	Total permeate Weight (kg)	Crossflow (LPM)	Accumulated Flow (L)	Low pre-mem. press. reading (psi)	High pre-mem. press. reading (psi)	Post-membrane pressure (psi)	Initial Permeate weight (kg)	Final Permeate weight (kg)	Suction press. to HP pump (psi)	Feed flowrate (LPM)	Recirculation flowrate (LPM)	System temperature (deg. C)	pH meter temperature (deg. C)
0.00	N/A	N/A	N/A	N/A	N/A	N/A	N/A	N/A	N/A	N/A	N/A	N/A	N/A	N/A
3.30	13.57	13.57	38.02	148767	402	406	398.5	16	18.49	19	N/A	25	24	24.6
10.00	29.52	29.52	37.75	149017	397	403	393.5	30.3	32.77	18.5	N/A	25	25	25
15.00	41.72	41.72	37.36	149203	398	402	393.5	42.3	44.82	18.5	N/A	25	25	25.4
20.00	54	54	37.62	149395	399	405	395.5	54.7	57.14	18.5	N/A	25	25	24.5
29.00	75.06	75.06	37.42	149732	399	406	395.5	75.6	78	18.5	N/A	25	24	24.5
36.00	91.66	91.66	37.56	149997	398	404	394.5	92.3	94.7	18.5	N/A	25	25	24.6
38.34	97.6	97.6												
47.00	20.32	117.92	37.33	150612	396	402	393.5	23.9	26.3	18.5	N/A	25	25	25
55.00	39.11	136.71	37.28	150911	396	402	392	39.7	42.11	18.5	N/A	25	25	25.3
65.00	62.87	160.47	37.42	151286	395	402	392.5	63.6	66.03	18.5	N/A	25	25	25.6
77.30	90.17	187.77	37.62	151637	396	406	394.5	91.2	93.49	18.5	N/A	25	25	25.1
81.48	99.231	196.83												
86.00	9.85	206.68	37.2	152224	396	400	391.5	10.6	12.94	18.5	N/A	25	25	25.7
94.00	30.59	227.42	37.61	152561	398	403	394.5	31.2	33.5	18.5	N/A	25	25	25.4
105.00	53.1	249.93	37.54	152940	398	404	394.5	53.7	55.99	18.5	N/A	25	25	25.3
114.30	74.25	271.08	37.72	153297	398	404	394.5	75	77.25	18.5	N/A	25	25	25.3
124.00	94.83	291.66	37.62	153656	395	403	395.5	98.6	100.78	18.5	N/A	25	25	25.3
131.14	109.52	306.35												
135.00	7.33	313.68	37.85	154201	399	404	394.5	7.9	9.95	19.5	N/A	25	24	24.6
140.30	18.45	324.8	37.62	154410	397	403	392.5	21.6	23.73	19.5	N/A	25	26	25.7
147.30	33	339.35	37.76	154674	398	404	394.5	33.6	35.67	19	N/A	25	25	25.3
152.00	41.81	348.16	38.03	154849	399	404	395.5	42.4	44.43	19	N/A	25	25	25.2
156.00	49.67	356.02	38.09	154999	401	405	395.5	50.2	52.16	19	N/A	25	25	25
159.30	56.32	362.67	38.15	155132	401	406	396.5	56.7	58.63	19	N/A	25	25	24.9

Table C16: Temperature Correction Factors

Temperature (deg. C)	Temperature Correction Factor	Temperature (deg. C)	Temperature Correction Factor	Temperature (deg. C)	Temperature Correction Factor
15	0.74	21.1	0.899	27.2	1.068
15.1	0.7423	21.2	0.9013	27.3	1.0708
15.2	0.7447	21.3	0.9037	27.4	1.0737
15.3	0.747	21.4	0.906	27.5	1.0765
15.4	0.7493	21.5	0.9083	27.6	1.0793
15.5	0.7517	21.6	0.9107	27.7	1.0822
15.6	0.754	21.7	0.913	27.8	1.085
15.7	0.757	21.8	0.916	27.9	1.0886
15.8	0.76	21.9	0.919	28	1.0922
15.9	0.763	22	0.922	28.1	1.0958
16	0.766	22.1	0.925	28.2	1.0994
16.1	0.769	22.2	0.928	28.3	1.103
16.2	0.7712	22.3	0.9397	28.4	1.106
16.3	0.7733	22.4	0.9373	28.5	1.109
16.4	0.7755	22.5	0.935	28.6	1.112
16.5	0.7777	22.6	0.9327	28.7	1.115
16.6	0.7798	22.7	0.9303	28.8	1.118
16.7	0.783	22.8	0.942	28.9	1.121
16.8	0.786	22.9	0.945	29	1.1246
16.9	0.789	23	0.948	29.1	1.1282
17	0.792	23.1	0.951	29.2	1.1318
17.1	0.795	23.2	0.954	29.3	1.1354
17.2	0.798	23.3	0.957	29.4	1.139
17.3	0.8003	23.4	0.9593	29.5	1.142
17.4	0.8027	23.5	0.9617	29.6	1.145
17.5	0.805	23.6	0.964	29.7	1.148
17.6	0.8073	23.7	0.9663	29.8	1.151
17.7	0.8097	23.8	0.9687	29.9	1.154
17.8	0.812	23.9	0.971	30	1.157
17.9	0.815	24	0.974	30.1	1.1602
18	0.818	24.1	0.977	30.2	1.1633
18.1	0.821	24.2	0.98	30.3	1.1665
18.2	0.824	24.3	0.983	30.4	1.1697
18.3	0.827	24.4	0.986	30.5	1.1728
18.4	0.8293	24.5	0.9883	30.6	1.176
18.5	0.8317	24.6	0.9907	30.7	1.1798
18.6	0.834	24.7	0.993	30.8	1.1836
18.7	0.8363	24.8	0.9953	30.9	1.1874
18.8	0.8387	24.9	0.9977	31	1.1912
18.9	0.841	25	1	31.1	1.195
19	0.844	25.1	1.0028	31.2	1.1982
19.1	0.847	25.2	1.0057	31.3	1.2013
19.2	0.85	25.3	1.0085	31.4	1.2045
19.3	0.853	25.4	1.0113	31.5	1.2077
19.4	0.856	25.5	1.0142	31.6	1.2108
19.5	0.8583	25.6	1.017	31.7	1.214
19.6	0.8607	25.7	1.0202	31.8	1.2178
19.7	0.863	25.8	1.0234	31.9	1.2216
19.8	0.8653	25.9	1.0266	32	1.2254
19.9	0.8677	26	1.0298	32.1	1.2292
20	0.87	26.1	1.033	32.2	1.233
20.1	0.8723	26.2	1.036		
20.2	0.8747	26.3	1.039		
20.3	0.877	26.4	1.042		
20.4	0.8793	26.5	1.045		
20.5	0.8817	26.6	1.048		
20.6	0.884	26.7	1.051		
20.7	0.887	26.8	1.0544		
20.8	0.89	26.9	1.0578		
20.9	0.893	27	1.0612		
21	0.896	27.1	1.0646		

Appendix D

Sample Output from MINTEQA2

PART 1 of OUTPUT FILE

PC MINTEQA2 v3.10 DATE OF CALCULATIONS: 23-FEB-97 TIME: 10:34: 0

Testing for potential precipitates in AD/DC waste at 85% VR

Temperature (Celsius): 25.00
Units of concentration: MG/L
Ionic strength to be computed.
If specified, carbonate concentration represents total inorganic carbon.
Do not automatically terminate if charge imbalance exceeds 30%
Precipitation is allowed for all solids in the thermodynamic database and
the print option for solids is set to: 1
The maximum number of iterations is: 200
The method used to compute activity coefficients is: Debye-Huckel equation
Abbreviated output file

---

330 0.000E-01 -6.40 y
967 5.830E+02 -2.28 y
281 3.340E+01 -3.22 y
500 1.752E+03 -1.12 y
460 2.240E+01 -3.04 y
150 9.420E+01 -2.63 y
180 8.670E+02 -1.61 y
492 6.930E+02 -1.95 y
580 3.204E+03 -1.47 y
732 4.100E+02 -2.37 y
140 3.330E+02 -2.26 y

H2O has been inserted as a COMPONENT
3 1
330 6.4000 0.0000

Charge Balance: UNSPECIATED

Sum of CATIONS= 8.523E-02 Sum of ANIONS = 1.671E-01

PERCENT DIFFERENCE = 3.244E+01 (ANIONS - CATIONS)/(ANIONS + CATIONS)

| IMPROVED ACTIVITY GUESSES PRIOR TO FIRST ITERATION: |
| Fe+3 Log activity guess: -10.36 |
| PO4-3 Log activity guess: -8.28 |
| SO4-2 Log activity guess: -2.37 |
| CO3-2 Log activity guess: -6.46 |
| |

PART 3 of OUTPUT FILE

PC MINTEQA2 v3.10 DATE OF CALCULATIONS: 23-FEB-97 TIME: 10:34: 0

PARAMETERS OF THE COMPONENT MOST OUT OF BALANCE:

ITER	NAME	TOTAL MOL	DIFF FXN	LOG ACTVTY	RESIDUAL
0	SO4-2	4.302E-03	4.388E-03	-2.36630	4.388E-03
1	SO4-2	4.302E-03	5.003E-04	-2.54087	4.998E-04
2	SO4-2	4.302E-03	1.053E-02	-2.54499	1.053E-02
3	SO4-2	4.302E-03	-9.435E-04	-3.04269	9.431E-04
4	SO4-2	4.302E-03	-3.354E-04	-2.93237	3.350E-04
5	SO4-2	4.302E-03	-6.109E-05	-2.89735	6.066E-05
6	SO4-2	4.302E-03	-3.894E-06	-2.89125	3.463E-06

PC MINTEQA2 v3.10 DATE OF CALCULATIONS: 23-FEB-97 TIME: 10:34: 1

ITERATIONS= 7: SOLID STRENGITE PRECIPITATES

PART 3 of OUTPUT FILE

PC MINTEQA2 v3.10 DATE OF CALCULATIONS: 23-FEB-97 TIME: 10:34: 1

PARAMETERS OF THE COMPONENT MOST OUT OF BALANCE:

ITER	NAME	TOTAL MOL	DIFF FXN	LOG ACTVTY	RESIDUAL
7	SO4-2	4.302E-03	-2.544E-03	-2.89086	2.544E-03
8	SO4-2	4.302E-03	1.714E-02	-2.22803	1.714E-02
9	SO4-2	4.302E-03	1.449E-03	-2.87091	1.449E-03
10	SO4-2	4.302E-03	-1.306E-04	-2.99604	1.301E-04
11	SO4-2	4.302E-03	-1.178E-03	-2.98385	1.177E-03
12	SO4-2	4.302E-03	2.515E-04	-2.85171	2.510E-04
13	SO4-2	4.302E-03	3.451E-04	-2.87386	3.447E-04
14	SO4-2	4.302E-03	-1.044E-04	-2.90693	1.040E-04
15	SO4-2	4.302E-03	-4.716E-05	-2.89649	4.673E-05
16	SO4-2	4.302E-03	-5.729E-06	-2.89178	5.298E-06

PC MINTEQA2 v3.10 DATE OF CALCULATIONS: 23-FEB-97 TIME: 10:34: 1

ITERATIONS= 17: SOLID HEMATITE PRECIPITATES

PART 3 of OUTPUT FILE

PC MINTEQA2 v3.10 DATE OF CALCULATIONS: 23-FEB-97 TIME: 10:34: 1

PARAMETERS OF THE COMPONENT MOST OUT OF BALANCE:

ITER	NAME	TOTAL MOL	DIFF FXN	LOG ACTVTY	RESIDUAL
17	NO3-1	1.127E-02	-2.801E-03	-2.07233	2.800E-03
18	NO3-1	1.127E-02	5.461E-03	-1.94821	5.460E-03
19	Ca+2	2.369E-03	2.743E-04	-6.20239	2.741E-04

ITERATIONS= 20: SOLID STRENGITE DISSOLVES

PART 3 of OUTPUT FILE

PC MINTEQA2 v3.10 DATE OF CALCULATIONS: 23-FEB-97 TIME: 10:34: 1

PARAMETERS OF THE COMPONENT MOST OUT OF BALANCE:

ITER	NAME	TOTAL MOL	DIFF FXN	LOG ACTVTY	RESIDUAL
20	PO4-3	3.401E-02	4.176E+01	-5.19540	4.176E+01
21	PO4-3	3.401E-02	1.062E+01	-6.19540	1.061E+01
22	PO4-3	3.401E-02	8.976E-01	-7.19540	8.975E-01
23	PO4-3	3.401E-02	-1.455E-02	-8.69758	1.455E-02
24	PO4-3	3.401E-02	5.822E-04	-8.46334	5.788E-04
25	PO4-3	3.401E-02	-5.515E-05	-8.46719	5.175E-05
26	PO4-3	3.401E-02	-4.726E-06	-8.46641	1.325E-06

PC MINTEQA2 v3.10 DATE OF CALCULATIONS: 23-FEB-97 TIME: 10:34: 1

ITERATIONS= 27: SOLID HYDRAPATITE PRECIPITATES

PART 3 of OUTPUT FILE

PC MINTEQA2 v3.10 DATE OF CALCULATIONS: 23-FEB-97 TIME: 10:34: 1

PARAMETERS OF THE COMPONENT MOST OUT OF BALANCE:

ITER	NAME	TOTAL MOL	DIFF FXN	LOG ACTVTY	RESIDUAL
27	NO3-1	1.127E-02	-2.806E-03	-2.07258	2.804E-03
28	NO3-1	1.127E-02	3.968E-03	-1.94821	3.967E-03
29	NO3-1	1.127E-02	2.468E-03	-2.07925	2.467E-03
30	NO3-1	1.127E-02	-5.505E-04	-2.16529	5.494E-04
31	NO3-1	1.127E-02	-8.349E-04	-2.14353	8.337E-04
32	NO3-1	1.127E-02	-5.536E-04	-2.11009	5.524E-04
33	NO3-1	1.127E-02	-2.620E-04	-2.08821	2.609E-04
34	NO3-1	1.127E-02	-8.873E-05	-2.07799	8.760E-05
35	NO3-1	1.127E-02	-1.391E-05	-2.07456	1.279E-05
36	SO4-2	4.302E-03	-7.540E-07	-2.89197	3.238E-07

ID	NAME	ANAL MOL	CALC MOL	LOG ACTVTY	GAMMA	DIFF FXN
140	CO3-2	5.594E-03	7.953E-07	-6.52081	0.379025	-3.543E-09
967	Citrate	3.109E-03	2.314E-03	-3.64721	0.097380	-3.329E-08
732	SO4-2	4.302E-03	3.783E-03	-2.89190	0.339059	-2.706E-08
500	Na+1	7.682E-02	7.582E-02	-1.22863	0.779036	-1.051E-07
460	Mg+2	9.288E-04	3.498E-04	-3.82712	0.425644	-1.545E-09
150	Ca+2	2.369E-03	2.269E-05	-5.03149	0.409806	1.338E-07
180	Cl-1	2.465E-02	2.465E-02	-1.73236	0.751268	-4.735E-08
492	NO3-1	1.127E-02	1.127E-02	-2.07400	0.748529	-2.239E-08
580	PO4-3	3.401E-02	3.121E-08	-8.48011	0.106069	0.000E-01
281	Fe+3	6.029E-04	3.630E-21	-21.20218	0.172948	-4.611E-18
330	H+1	0.000E-01	4.838E-07	-6.40000	0.822856	5.421E-20
2	H2O	0.000E-01	-1.340E-03	-0.00121	1.000000	0.000E-01

PERCENTAGE DISTRIBUTION OF COMPONENTS AMONG
TYPE I and TYPE II (dissolved and adsorbed) species

CO3-2	1.5	PERCENT BOUND IN SPECIES #5001401 NaHCO3 AQ
	58.4	PERCENT BOUND IN SPECIES #3301400 HCO3 -
	40.0	PERCENT BOUND IN SPECIES #3301401 H2CO3 AQ
Citrate	74.4	PERCENT BOUND IN SPECIES # 967 Citrate
	17.4	PERCENT BOUND IN SPECIES #3309671 CITRATEH
	4.7	PERCENT BOUND IN SPECIES #1509671 CACITRATE
	3.3	PERCENT BOUND IN SPECIES #4609671 MGCITRATE
SO4-2	87.9	PERCENT BOUND IN SPECIES # 732 SO4-2
	11.2	PERCENT BOUND IN SPECIES #5007320 NaSO4 -
Na+1	98.7	PERCENT BOUND IN SPECIES # 500 Na+1
Mg+2	37.7	PERCENT BOUND IN SPECIES # 460 Mg+2
	3.6	PERCENT BOUND IN SPECIES #4607320 MgSO4 AQ
	12.5	PERCENT BOUND IN SPECIES #4605801 MgH2PO4 +
	34.2	PERCENT BOUND IN SPECIES #4605802 MgHPO4 AQ
	11.0	PERCENT BOUND IN SPECIES #4609671 MGCITRATE
Ca+2	11.9	PERCENT BOUND IN SPECIES # 150 Ca+2
	1.2	PERCENT BOUND IN SPECIES #1507320 CaSO4 AQ
	7.6	PERCENT BOUND IN SPECIES #1505800 CaHPO4 AQ
	3.0	PERCENT BOUND IN SPECIES #1505802 CaH2PO4 +
	76.1	PERCENT BOUND IN SPECIES #1509671 CACITRATE
Cl-1	100.0	PERCENT BOUND IN SPECIES # 180 Cl-1
NO3-1	100.0	PERCENT BOUND IN SPECIES # 492 NO3-1
PO4-3	1.3	PERCENT BOUND IN SPECIES #5005800 NaHPO4 -
	24.2	PERCENT BOUND IN SPECIES #3305800 HPO4 -2
	73.1	PERCENT BOUND IN SPECIES #3305801 H2PO4 -
Fe+3	9.6	PERCENT BOUND IN SPECIES #2819671 FECITRATE
	90.2	PERCENT BOUND IN SPECIES #2819672 FECITRATEH
H+1	5.0	PERCENT BOUND IN SPECIES #3301400 HCO3 -
	6.9	PERCENT BOUND IN SPECIES #3301401 H2CO3 AQ
	12.2	PERCENT BOUND IN SPECIES #3305800 HPO4 -2
	73.4	PERCENT BOUND IN SPECIES #3305801 H2PO4 -
H2O	97.7	PERCENT BOUND IN SPECIES #3300020 OH-
	2.3	PERCENT BOUND IN SPECIES #4603300 MgOH +

---------- EQUILIBRATED MASS DISTRIBUTION ----------

IDX	NAME	DISSOLVED MOL/KG	DISSOLVED PERCENT	SORBED MOL/KG	SORBED PERCENT	PRECIPITATED MOL/KG	PRECIPITATED PERCENT
140	CO3-2	5.594E-03	100.0	0.000E-01	0.0	0.000E-01	0.0
967	Citrate	3.108E-03	100.0	0.000E-01	0.0	0.000E-01	0.0
732	SO4-2	4.302E-03	100.0	0.000E-01	0.0	0.000E-01	0.0
500	Na+1	7.682E-02	100.0	0.000E-01	0.0	0.000E-01	0.0
460	Mg+2	9.288E-04	100.0	0.000E-01	0.0	0.000E-01	0.0
150	Ca+2	1.915E-04	8.1	0.000E-01	0.0	2.178E-03	91.9
180	Cl-1	2.465E-02	100.0	0.000E-01	0.0	0.000E-01	0.0
492	NO3-1	1.127E-02	100.0	0.000E-01	0.0	0.000E-01	0.0
580	PO4-3	3.270E-02	96.2	0.000E-01	0.0	1.307E-03	3.8
281	Fe+3	5.103E-12	0.0	0.000E-01	0.0	6.029E-04	100.0
330	H+1	6.510E-02	100.0	0.000E-01	0.0	0.000E-01	0.0
2	H2O	3.402E-08	100.0	0.000E-01	0.0	0.000E-01	0.0

Charge Balance: SPECIATED

Sum of CATIONS = 7.670E-02 Sum of ANIONS 9.568E-02

PERCENT DIFFERENCE = 1.101E+01 (ANIONS - CATIONS)/(ANIONS + CATIONS)

EQUILIBRIUM IONIC STRENGTH (m) = 1.058E-01

EQUILIBRIUM pH = 6.400

DATE ID NUMBER: 970223
TIME ID NUMBER: 10340211

Appendix E

Raw Data for Work Discussed in Chapter 6

Table E1: Raw PWP Data for Module I

PWP test Mod 5-6

Date	Stage	Time (min:sec)	Total permeate Weight (kg)	Low pre-mem. press. reading (psi)	High pre-mem. press. reading (psi)	Post-membrane pressure (psi)	Initial weight (kg)	Final weight (kg)	Suction press. to HP pump (psi)	Feed flowrate (LPM)	Recirculation flowrate (LPM)	System temperature (deg. C)	pH meter temperature (deg. C)	pH
7-Jul	Before cleaning	N/A	N/A	194	201	170	0	0.205	21	27.5	27	30	N/A	N/A
		N/A	N/A	196	202	171.5	0	0.23	21	27.5	27	25	N/A	N/A
		N/A	N/A	196	202	172	0	0.219	21	27.5	27	24	N/A	N/A
		N/A	N/A	196	202	172.5	0	0.22	21	27.5	27	24	N/A	N/A
		N/A	N/A	303	311	281.5	0	0.33	26	16	37.5	25	N/A	N/A
		N/A	N/A	300	314	281.5	0.87	1.195	26	16	37.5	24	N/A	N/A
		N/A	N/A	302	316	284	1.7	2.035	25.5	16	37.5	24	N/A	N/A
		N/A	N/A	398	407	377.5	3.344	3.875	25.5	16	37.5	24	N/A	N/A
		N/A	N/A	402	404	380	4.22	4.855	26	16	37.5	24	N/A	N/A
		N/A	N/A	404	406	380	5.25	5.888	26	16	37.5	23	N/A	N/A
		N/A	N/A	487	496	473	7.2	7.777	26	15	38.5	25	N/A	N/A
		N/A	N/A	487	496	473	8.4	8.989	26	15	38.5	25	N/A	N/A
		N/A	N/A	487	496	472	9.5	10.09	26	15	38.5	26	N/A	N/A
		N/A	N/A	605	606	581	11.99	12.7	25.5	15.5	38	25	N/A	N/A
		N/A	N/A	604	605	581	13.4	14.12	25.5	15.5	38	26	N/A	N/A
		N/A	N/A	606	607	583	14.8	15.5	26	15.5	38	26	N/A	N/A
		N/A	N/A	699	702	677.5	17.1	17.89	26	15.5	38	25	N/A	N/A
		N/A	N/A	701	703	678	18.7	19.49	26	15.5	38	25	N/A	N/A
		N/A	N/A	701	704	677.5	20.3	21.09	26	15.5	38	24	N/A	N/A
		N/A	N/A	796	800	776	23.1	23.98	25	16.5	32.25	24	N/A	N/A
		N/A	N/A	797	798	774	24.9	25.77	25	16.5	32.25	24	N/A	N/A
		N/A	N/A	796	797	773.5	26.8	27.67	25	16.5	32.25	25	N/A	N/A
13-Jul	After Triton X-1	N/A	N/A	400	403	377.5	3.85	4.86	25.5	15.5	38.5	24	N/A	N/A
		N/A	N/A	398	401	374.5	5.36	6.17	25.5	15.5	38.5	24	N/A	N/A
		N/A	N/A	399	401	376	6.85	7.67	25.5	16.5	38.5	24.5	N/A	N/A
		N/A	N/A	798	800	777	13	14.61	25	16.5	35.5	24	N/A	N/A
		N/A	N/A	799	801	778	16.1	17.71	25	16.5	35.5	24	N/A	N/A
		N/A	N/A	799	801	777.5	18.9	20.53	25	16.5	35.5	24.5	N/A	N/A
18-Jul	After HCl	10	N/A	397	404	375.5	8.85	9.77	26	14	38	24	24	6.43
		13.35	N/A	397	406	374	11.45	12.39	25.5	14	40	24.5	24.4	6.54
		15	N/A	401	407	380.5	13.6	14.56	25.5	14	40	25	24.7	6.58
		18.4	N/A	400	406	381.5	16.25	17.21	25.5	14	40	25	25	6.63
		22.45	N/A	798	803	778.5	24.1	25.99	25	17	35.5	25	25.6	6.7
		26.33	N/A	796	801	778.5	28.6	30.44	25	17	35.5	25	25.6	7.77
		28.54	N/A	796	802	777.5	33	34.81	24.5	17	35.5	24.5	23.8	7.68
27-Jul	After NaOH+ EDTA	4.1	2.05	196	202	175	3.1	3.67	25	16	40	27	26.4	9.18
		7.04	3.76	197	204	177	4.45	5	25	16	40	25	26.1	9.25
		10	5.38	196	205	176.5	5.25	5.79	25	16	40	25	25.3	9.31
		12.07	6.51	195	202	176	7.25	7.82	25	16	40	26	25.3	9.34
		15.38	8.76	297	306	277.5	10.7	11.59	25	16	38	26	25.9	9.36
		19.07	11.82	297	306	276	12.65	13.53	25	16	38	26	26	9.39
		21.19	13.75	297	309	278.5	14.7	15.57	25	16	38	25	26	9.41
		25.43	17.88	398	406	377	19.3	20.46	25.5	14	40.5	25	25.6	9.45
		28.16	20.8	398	403	377.5	22	23.16	25.5	14	41	25	25.5	9.47
		30.31	23.39	398	404	378.5	24.7	25.86	25.5	14	41	24	25.4	9.47
		35.19	29.26	497	502	476.5	32.2	33.65	25	15	38.5	25	25.3	9.5
		38.35	33.97	496	503	476.5	35.1	36.55	25	15	38.5	25	25.3	9.5
		40.4	36.83	496	503	478	36.3	38.71	25	15	38.5	24	25.1	9.5
		44.4	42.96	596	602	576	45.3	46.99	25	14.5	39	24	25	9.52
		47.17	47.39	596	602	578	48.2	50.94	25	14.5	38.5	24	25	9.52
		49.43	51.49	596	602	577	56	57.75	25	14.5	38.5	25	25.1	9.52
		68.23	17.27	697	706	673	21.3	23.36	25	16	37.5	25	25.3	9.53
		69.37	23.84	691	700	673	25.8	27.87	25	16	37.5	25	25.6	9.55
		71.59	28.66	690	699	674	30.7	32.8	25	16	37.5	25	25.8	9.56
		74.59	35	798	804	781	37.4	39.85	24	17.5	35	26	26.2	9.55
		77.16	40.48	797	803	782.5	45.6	48.08	24	17.5	35	26	26.6	9.56
		80.43	46.86	796	802	780	51	53.52	24	17.5	35	26	27	9.59

Table E2: Raw PWP Data for Module 2

PWP test Mod 3-6

Date	Stage	Time (min.sec)	Total permeate Weight (kg)	Low pre-mem. press. reading (psi)	High pre-mem. press. reading (psi)	Post-membrane pressure (psi)	Initial Permeate weight (kg)	Final Permeate weight (kg)	Station press. to HP pump (psi)	Feed flowrate (LPM)	Recirculation flowrate (LPM)	System temperature (deg. C)	pH meter temperature (deg. C)	pH
14-Aug	Before cleaning	24	8.84	199	293	178.5	8.3	8.89	24	15	38	26	26.2	7.38
		29	10.67	200	294	181.5	11.6	11.88	24.5	15	38	26	26.4	7.42
		34	12.78	201	294	180.5	13.1	13.48	24.5	15	39	26	26.3	7.42
		39	15.2	200	294	281	15.8	16.38	25	14	40	26	26.4	7.53
		44	18.04	200	292	280	18.5	19.05	25	14	40	25	26.1	7.51
		49	20.2	201	295	281.5	20.7	21.34	25	14	40	25	25.7	7.56
		53	23.29	207	403	378.5	23.9	24.6	25	14	40	24	25.2	7.62
		57	26.02	208	403	378.5	26.6	27.29	25	14	40	24	24.9	7.64
		60	28.08	208	402	378.5	28.7	29.39	25	14	40	23.5	24.8	7.66
		64	31.13	405	502	477.5	31.7	32.58	25	14	40	25	24.9	7.68
		67	33.74	407	502	478	34.3	35.17	25	14	40	25	25	7.68
		70	36.34	407	502	479	36.9	37.77	25	14	40	25	25	7.7
		74	40.15	507	603	578.5	43.2	44.26	24.5	14.5	38.75	25	25.4	7.67
		79	45.37	508	604	578	46.3	47.36	24	14.5	38.75	25	25.5	7.72
		82	48.51	508	604	580	49	50.08	24	14.5	38.75	25	25.6	7.72
		86	51.53	606	705	682	52.9	54.11	25	12	41	25	25.6	7.74
		89	55.43	608	705	680	55.6	56.8	25	12	41	25	25.6	7.72
		91	58	606	701	679	58.2	60.4	25	12	41	25	25.6	7.68
		124	6.93	706	799	777.5	5.3	6.69	26	11.5	40.5	25	25.3	7.81
		128	9.77	704	795	776	10.8	12.25	25.5	11.5	40.5	26	25.7	7.81
		130	15.52	708	800	781.5	16.5	17.93	25.5	11.5	40.5	25	26.1	7.76
16-Aug	After Triton X-1	14.3	15.6	306	405	379	16.6	17.68	24	15	38.75	27	26.6	7.28
		19	19.31	307	405	380	19.5	20.58	24	15	38.75	28	28.1	N/A
		20	21.41	308	403	380.5	21.6	22.68	24	15	38.75	26	26.6	7.28
		1	27.88	708	811	778.5	28.4	29.45	25	12	40	26	26.8	7.43
		3	31.76	706	801	777.5	33.3	35.35	25	12	40	26	26.9	7.43
		5	35.8	705	798	778	38	39.01	25	12	40	25	26.8	7.42
17-Aug	After HCl	16.3	18.3	306	403	377	20.2	21.19	25	14	40	25	25.5	6.98
		19.3	22.19	304	404	376.5	22.3	23.27	25	14	40	25	25.4	6.8
		21.15	23.89	305	404	377	24.1	25.08	25	14	40	25	25.4	6.64
		1	29.52	707	802	780.5	30.7	32.67	25	12	40	25	25.6	6.68
		3	33.39	708	812	781.5	34.6	35.75	25	12	40	25	25.8	6.7
		5	37.22	709	808	782.5	38.1	39.89	25	12	40	25	25.8	6.73
18-Aug	After NaOH+ NTA	7	9.68	196	294	178.5	10.3	10.88	23.5	16.75	38	25	24.8	6.28
		10	11.3	195	211	178.5	11.7	12.28	23.5	16.75	38	25	24.8	6.27
		12	12.45	194	211	178.5	13.2	13.77	23.5	16.75	38	25	24.8	6.3
		16	15.07	295	302	276.5	15.8	16.67	24	14	40	25	24.8	6.33
		18	17.78	294	305	278	17.2	18.07	24	14	40	25	25	6.34
		20	18.5	295	308	279	18.3	20.17	24	14	40	25	25	6.35
		24	22.41	397	406	378.5	23.3	24.48	25	13	41	25	25.1	6.37
		26	24.73	398	410	378.5	25.5	26.67	25	13	41	25	25.1	6.38
		28	27.03	397	404	378.5	27.8	28.97	25	13	41	25	25.1	6.39
		32	32.22	497	502	478.5	33.6	35.07	25	12.5	41.75	25	25.2	6.39
		34.3	35.82	497	505	480	36.9	38.34	25	12.5	41.75	24	25.2	6.41
		36.3	38.69	497	502	480	39.5	40.93	25	12.5	41.75	24	25.1	6.34
		44	50.31	600	605	582	51.4	53.1	24	14	38	24	25	6.43
		46	53.69	599	604	582.5	55	56.72	24	14	38	24	24.9	6.37
		48	57.04	599	606	582	58.4	60.11	24	13.5	38	24	24.9	6.43
		61	7.95	694	709 N/A		8.2	11.21	25	13	40	24	24.8	6.67
		63	11.87	700	707	684	14.5	16.53	25	13	40	24	24.9	6.66
		66	17.89	700	705	683	18.5	20.53	25	13	40	24	25	6.6
		69	24.22	706	800	780	25.5	27.79	25	12.5	40	24	25.1	6.66
		71	28.75	706	801	780	29.8	32.2	25	12.5	40	24	25.2	6.66
		73	33.29	705	800	779	34.3	36.6	25	12.5	40	25	25.2	6.67

Table E3: Raw Data for AD/DC Waste Test #1 for Module 1

Mod 5-6
AD/DC waste test #1

Date	Stage	Time (min.sec)	Permeate Weight (kg)	Total permeate Weight (kg)	Low pre-mem. press. reading (psi)	High pre-mem. press. reading (psi)	Post-membrane pressure (psi)	Initial Permeate weight (kg)	Final Permeate weight (kg)	Suction press. to HP pump (psi)	Feed flowrate (LPM)	Recirculation flowrate (LPM)	System temperature (deg. C)	pH meter temperature (deg. C)	pH
1-Aug	After cleaning	0.2	1.55	1.55	397	406	378.5	1.7	2.84	25	15	39	26	26.6	7.58
		5.1	6.97	6.97	396	403	376	7.2	8.31	25	15	38	26	N/A	N/A
		10	12.24	12.24	396	404	376	12.4	13.5	25	15	38	26	26.2	7.68
		15	17.59	17.59	397	407	379	17.7	18.78	25	15	38	25	26	7.66
		20	22.95	22.95	397	410	381.5	24.4	25.47	25	15	38	25	N/A	7.66
		25	28.28	28.28	396	404	377	29.1	30.16	25	15	38	25	N/A	N/A
		30	33.53	33.53	396	406	377	34.6	35.65	25	15	39	25	25.7	7.7
		40	43.87	43.87	396	405	377.5	44.2	45.24	25	15	39	25	N/A	N/A
		60	64.13	64.13	397	406	379	65	66.01	25	15	39	24	25.1	7.75
		80	84.06	84.06	396	404	378	86.3	87.31	25	15	39	24	25.1	7.77
		97.3	100.353	100.353											
		100	0.96	101.313	396	403	375.5	2	2.99	25	14	40	24	24.9	7.8
		140	39.71	140.063	395	402	N/A	40	40.96	25	14	40	24	25	7.83
		180	77.12	177.473	396	410	382	78.9	79.87	25	14	40	24	25	7.87
		204	100.545	200.896											
		205	1.04	201.936	397	406	380	4.2	5.16	25	13.75	40	25	25	7.9
		240	33.93	234.826	396	407	380	34.7	35.64	25	13.75	40	25	24.8	7.94
		280	70.86	271.756	396	407	380.5	71.3	72.22	25	13.75	40	25	24.8	7.96
		284	74.52	275.416	N/A	N/A	N/A	N/A	N/A	N/A	N/A	N/A	N/A	N/A	N/A
		285	75.99	276.886	397	407	380.5	78.3	79.21	25	14	40	25	N/A	N/A
		294	84.02	284.916	394	402	377.5	84.9	85.83	25	14	40	25	25.6	7.85
		312	100.177	301.075	N/A	N/A	N/A	N/A	N/A	N/A	N/A	N/A	N/A	N/A	N/A
		314	3.77	304.845	395	406	377.5	4.8	5.7	24.5	15	38.75	25	24.9	7.96
		354	38.41	339.485	397	405	379	39.4	40.32	25	15	38.75	25	25.8	8.02
		392	75.54	376.615	396	405	378	76.6	77.52	24.5	15	38.75	26	25.7	8.06
		420	100.18	401.255	N/A	N/A	N/A	N/A	N/A	N/A	N/A	N/A	N/A	N/A	N/A
		421	2.17	403.425	397	402	376	3.1	3.95	24	15	38.75	25	25	8.13
		426	6.39	407.645	396	403	377	6.1	6.95	24.5	15	38.75	25	N/A	N/A
		460	34.62	435.875	394	402	376	35.4	36.23	24	15	38.75	25	25	8.17
		500	66.78	468.035	395	406	376.5	67	67.8	24.5	15	38.75	25	25	8.21
		621	98.81	500.065	394	403	377	99.5	100.27	24	15	38.75	25	25.3	8.23
		623	102.106	503.361	N/A	N/A	N/A	N/A	N/A	N/A	N/A	N/A	N/A	N/A	N/A
		626	1.66	505.021	397	406	378.5	1.8	2.56	26	14.5	40	24.5	24.9	8.27
		636	10.82	514.181	397	402	378	11.5	12.28	25	14.5	40	25.5	25.7	8.24
		648	18.52	521.881	397	403	379.5	19.4	20.17	25	14.5	40	25.5	25.7	8.23
		659	26.84	530.201	396	404	380.5	27.6	28.36	25	14.5	40	25	25.7	8.18
		670	35.06	538.421	399	406	382	35.5	36.25	25	14.5	40	25	25.8	8.17
		677	40.2	543.561	402	407	383	40.7	41.43	25	14.5	40	25	25.4	8.16

Table E4: Raw Data for AD/DC Waste Test #2 for Module 1

Mod 5-6
AD/DC waste test #2

Date	Stage	Time (min.sec)	Permeate Weight (kg)	Total permeate Weight (kg)	Low pre-mem. press. reading (psi)	High pre-mem. press. reading (psi)	Post-membrane pressure (psi)	Initial Permeate weight (kg)	Final Permeate weight (kg)	Suction press. to HP pump (psi)	Feed flowrate (LPM)	Recirculation flowrate (LPM)	System temperature (deg. C)	pH meter temperature (deg. C)	pH
3-Aug	After cleaning	0.3	1.99	1.99	396	404	377.5	2.1	3.13	25	13.75	38.75	24.5	24.2	8.22
		5	6.44	6.44	394	400	374.5	6.3	7.26	25	13.75	38.75	23	24.7	8.25
		10	11.34	11.34	395	402	376	11.5	12.53	25	13.75	40	25	25.3	8.27
		18	19.6	19.6	398	410	382.5	19.8	20.87	25	13.75	40	26	25.7	8.29
		20	21.72	21.72	402	411	384	21.9	22.95	25	13.75	40	25	25.4	8.3
		29	30.99	30.99	397	406	381	31.1	32.15	25	13.75	40	25	25.7	8.3
		35	37.22	37.22	398	407	382.5	37.4	38.45	25	13.75	40	25	25.8	8.3
		45	47.54	47.54	398	407	382	47.8	48.83	25	13.75	40	25	25.3	8.31
		60	62.72	62.72	399	407	382	63.3	64.31	25	13.75	40	25	25	8.32
		80	82.32	82.32	400	408	383	82.5	83.48	25	13.75	40	23.5	24.6	8.33
		100	101.84	101.84	400	407	382.5	102.5	103.48	25	13.75	40	24	24.6	8.33
		103	104.37	104.37											
		105	2.64	107.01	399	405	382	3.6	4.62	24	16	37.5	25	25.3	8.32
		150	48.13	152.5	398	407	382	48.4	49.42	24	16	37.5	25	25.7	8.31
		190	89.04	193.41	398	406	380	89.4	90.43	24	16	37.5	26	26.2	8.32
		230	120	224.37											
		232	1.91	226.28	398	404	382	2.8	3.83	24.5	15	39	26	26.3	8.26
		270	39.38	263.75	400	406	383.5	42.5	43.48	24.5	15	39	25	25.8	8.18
		310	77.36	301.73	400	407	384	77.6	78.54	24.5	15	38	25	25.4	8.23
		314	81.135	305.505											
		317	3.23	308.735	398	402	380.5	3.7	4.66	24	15	38	25	25.8	8.24
		360	43.39	348.895	399	404	382	43.6	44.53	24	15	38	26	26.1	8.24
		400	78.09	383.595	402	406	383.5	78.8	79.65	24	15	38	24	24.6	8.27
		428	100.86	406.365	403	407	384.5	101	101.81	24	15	38	24	24.4	N/A
		431	102	407.505											
		435	1.02	408.525	401	404	382	1.2	2.01	25	16	38	24	24.8	8.23
		445	8.95	416.455	396	401	378	9.6	10.39	25	16	37.5	25	25	8.24
		456	17.62	425.125	398	403	379.5	17.8	18.59	24.5	16	37.5	25	25.1	8.23
		465	24.67	432.175	398	402	379.5	24.8	25.58	24.5	16	37.5	25	25.2	8.2
		475	32.43	439.935	400	404	381.5	32.8	33.57	24	16	37.5	25	25.2	8.17
		485	40.15	447.655	402	407	382	40.3	41.07	24	16	37.5	25	25.4	8.14
		495	47.85	455.355	403	411	384	48	48.77	24	16	37.5	25	25.6	8.12
		504	54.61	462.115	398	401	378	55	55.74	24	16	37.5	26	25.7	8.1

Table E5: Raw Data for AD/DC Waste Test #3 for Module 1

Mod 56
AD/DC waste test

Date	Stage	Time (min.sec)	Permeate Weight (kg)	Total permeate Weight (kg)	Low pre-mem. press. reading (psi)	High pre-mem. press. reading (psi)	Post-membrane pressure (psi)	Initial Permeate weight (kg)	Final Permeate weight (kg)	Suction press. to HP pump (psi)	Feed flowrate (LPM)	Recirculation flowrate (LPM)	System temperature (deg. C)	pH meter temperature (deg. C)	pH
8-Aug	5 micron filter removed	2	2.43	2.43	398	406	380.5	2.6	3.59	26	14	40	23	23.6	8.25
		5	5.36	5.36	409	416	389.5	7.7	8.69	26	14	40	22	23.5	8.31
		11	11.26	11.26	399	410	381.5	12	12.96	26	14	40	23	23.9	8.39
		17	17.23	17.23	401	409	383	18	19.02	26	14	40	24	24.3	N/A
		23	23.4	23.4	401	406	384	24.3	25.34	26	14	40	24	N/A	N/A
		32	32.9	32.9	402	410	384	33.8	34.86	26	14	40	25	25.1	8.14
		40	41.37	41.37	398	404	380	42.2	43.26	26	14	40	25	25.4	8.17
		45	46.74	46.74	398	403	379.5	47.6	48.68	26	14	40	25	25.6	8.16
		60	63.03	63.03	398	403	380	65.4	66.49	26	14	40	25	25.3	8.18
		80	84.71	84.71	398	403	380	85.5	86.59	26	14	40	26	25.8	8.2
		100	106.42	106.42	397	402	379.5	107.3	108.39	25.5	14	40	25	25.6	8.18
		103.12	109.804	109.804											
		105	2.53	112.334	404	409	385.5	3.5	4.59	25	15.5	38.5	25	25.6	8.18
		152	54.1	163.904	404	410	384.5	54.9	56	25	15.5	38.5	26	26.1	8.16
		184	88.26	196.064	397	402	379.5	89.2	90.25	25	15.5	38.5	26	25.7	8.18
		197	101.73	211.534	398	403	379	102	103.03	25	15.5	38.5	25	25.3	8.2
		199.47	104.519	214.323						25	15.5	38.5			
		201	1.84	216.163	402	406	383	2.6	3.63	25	15.5	38.5	24	25	8.14
		240	40.97	255.293	403	406	384	43.2	44.19	25	15.5	38.5	24	24.7	8.21
		281	80.79	295.113	402	409	384	81.5	82.47	25	15.5	38.5	24.5	24.7	8.22
		306	104.87	319.193	403	407	384	105	105.97	25	15.5	38.5	24	24.8	8.22
		309	107.621	321.944						25	15.5	38.5			
		311	2.14	324.064	402	404	382	2.8	3.76	25	15.5	38.5	24	24.7	8.24
		346	35.24	357.184	402	405	382.5	36.1	37.05	25	15.5	38.5	25	24.8	8.27
		391	76.75	398.694	403	407	383.5	77.4	78.31	25	15.5	38.5	24	25.1	8.27
		417	100.24	422.184	402	406	383	100.8	101.69	25	15.5	38.5	25	25.2	8.27
		420.13	103.04	424.984						25	15.5	38.5			
		421	0.41	425.394	398	402	379	2.3	3.18	25.5	15.5	38.5	25	25.1	8.28
		430	8.24	433.224	399	402	380	8.8	9.67	25	15.5	38.5	25	25.3	8.27
		440	16.9	441.884	399	403	379.5	17.7	18.57	25	15.5	38.5	25	25.4	8.24
		450	25.49	450.474	400	404	380.5	26.1	26.95	25	15.5	38.5	25	25.6	8.18
		460	34	458.984	400	403	380.5	34.8	35.45	25	15.5	38.5	26	25.7	8.16
		474	45.62	470.604	397	400	376.5	46.1	46.92	25	15.5	38.5	26	25.7	8.12

Table E6: Raw Data for AD/DC Waste Test Performed Before Cleaning for Module 2

Mod 3-6
AD/DC waste test
Before cleaning

Date	Stage	Time (min.sec)	Permeate Weight (kg)	Total permeate Weight (kg)	Low pre-mem. press. reading (psi)	High pre-mem. press. reading (psi)	Post-membrane pressure (psi)	Initial Permeate weight (kg)	Final Permeate weight (kg)	Suction press. to HP pump (psi)	Feed flowrate (LPM)	Recirculation flowrate (LPM)	System temperature (deg. C)	pH meter temperature (deg. C)	pH
9-Aug	5 micron filter installed	1.3	2.37	2.37	395	403	377.5	2.5	3.03	25.5	12.5	41.75	25	25.3	8.18
		6	4.74	4.74	400	406	382.5	4.9	5.44	25.5	12.5	41.75	25	25.5	8.26
		11	7.45	7.45	398	404	379.5	7.7	8.25	25	12.5	41.75	25	25.6	8.27
		16	10.19	10.19	398	402	379	10.3	10.85	25	12.5	41.75	25	25.6	8.28
		20	12.37	12.37	398	402	378	12.8	13.35	25	12.5	41.75	25	25.6	8.28
		25	15.13	15.13	397	400	377.5	15.3	15.86	25	12.5	41.75	25	25.8	8.3
		30	17.87	17.87	399	402	379.5	18.3	18.83	25	12.5	41.75	25	25	8.31
		40	23.18	23.18	399	402	378.5	23.3	23.85	25	12.5	41.75	25	25.3	8.32
		51	29.09	29.09	399	402	378	29.4	29.95	25	12.5	41.75	25	25.2	8.32
		60	33.94	33.94	399	401	378	34.1	34.65	25	12.5	41.75	25	25.2	8.32
		80	44.69	44.69	398	400	378	44.9	45.44	25	12.5	41.75	24	25.2	8.33
		100	55.44	55.44	397	400	377.5	55.5	56.04	25	12.5	41.75	25	25.3	8.33
		122	67.33	67.33	397	400	379	67.5	68.05	25	12.5	41.75	25	25.4	8.33
		155	85.05	85.05	400	402	380	85.2	85.74	25	12.5	41.75	25	25.1	8.33
		186	101.79	101.79	400	402	379.5	101.9	102.44	25	12.5	41.75	25	25.3	
		187.37	102.633	102.633											
		191	1.12	103.753	397	404	378.5	1.6	2.14	24	16	37	24	24.6	8.2
		240	30.93	133.563	404	409	385.5	31.5	32.15	24	16	37.5	27	26.9	8.18
		300	69.81	172.443	398	401	378.5	70.3	70.92	23.5	16	37.5	26	26.1	8.22
		360	103.72	206.353	400	402	380.5	103.8	104.35	23.5	16	37.5	24	24.6	8.26
		362	104.805	207.438											
		365	1.87	209.308	400	406	381.5	2	2.57	24	15.5	38	25	25.1	8.26
		425	37.02	244.458	400	404	381.5	37.1	37.69	24	15.5	38	25	25.5	8.26
		480	69.35	276.788	399	403	380	69.8	70.38	23.5	15.5	38	25	25.7	8.27
		540	103.44	310.878	398	402	380	103.5	104.06	23.5	15.5	37.5	25	25.1	8.22
		542.02	104.504	311.942											
		545	1.76	313.702	400	402	380.5	2.8	3.36	24	14.5	39.5	25	25	8.23
		600	32.36	344.322	397	399	377	32.8	33.35	24	15	38.5	25	25.5	8.23
		660	65.17	377.112	397	399	378	65.6	66.15	24	14.5	38.5	25	25.4	8.25
		713	93.18	405.122	398	400	378.5	93.5	94.01	24	14.5	38.5	24.5	25.1	8.26
		720	95.97	407.912	398	402	379.5	97.1	97.65	23.5	16	38	26	26.3	8.16
		728	100.429	412.371											
		732	2.04	414.411	398	404	381.5	2.7	3.28	25	14.5	38.75	26	26.6	8.2
		745	9.27	421.641	400	404	380.5	9.7	10.23	25	14.5	38.75	25	25.2	8.21
		766	19.69	432.061	402	405	382.5	20.1	20.57	25	14.5	38.75	23	23.5	8.23
		780	26.25	438.621	400	402	380	26.6	27.07	25	14.5	40	23	23.6	8.23
		795	33.37	445.741	400	403	379.5	33.8	34.26	24.5	14.5	40	23	24.2	8.23
		810	40.62	452.991	400	402	380.5	41	41.49	24.5	14.5	40	25	24.7	8.2
		825	47.92	460.291	401	403	381.5	48.3	48.79	24	14.5	40	24	24.8	8.18
		836	54.16	466.531	402	404	381.5	54.5	54.97	24	14.5	40	24	24.8	8.18

Table E7: Raw Data for AD/DC Waste Test #1 for Module 2

Mod 3-6
AD/DC waste test #1
After cleaning with 5 micron filter installed

Date	Stage	Time (min.sec)	Permeate Weight (kg)	Total permeate Weight (kg)	Low pre-mem. press. reading (psi)	High pre-mem. press. reading (psi)	Post-membrane pressure (psi)	Initial Permeate weight (kg)	Final Permeate weight (kg)	Suction press. to HP pump (psi)	Feed flowrate (LPM)	Recirculation flowrate (LPM)	System temperature (deg. C)	pH meter temperature (deg. C)	pH
24-Aug	After cleaning	1.3	1.75	1.75	398	403	384.5	3.2	4.34	25	15	37.5	22	22.4	7.82
		5	5.68	5.68	402	409	386	6.9	8.04	25	15	37.5	22.5	23.1	7.82
		8.3	9.68	9.68	407	411	390	10.4	11.56	25	15	37.5	23	23.5	7.84
		14	15.98	15.98	399	403	382.5	17	18.16	25	15	38.75	23	23.7	7.87
		22.15	25.59	25.59	399	405	383.5	26.5	27.69	25	15	38.75	24	23.8	7.9
		28	32.38	32.38	399	404	382.5	33	34.21	25	15	38.75	24	24.3	7.91
		45	53.03	53.03	398	402	380.5	53.9	55.14	25	15	38.75	25	24.8	7.94
		55.15	65.54	65.54	398	402	381.5	66.4	67.65	25	15	38.75	25	25.2	7.95
		67.3	80.13	80.13	399	402	382.5	80.9	82.11	25	15	38.75	25	25	7.96
		87	103.77	103.77	399	403	381.5	104.6	105.82	25	15	38.75	25	25.2	7.98
		88.53	106.024	106.024											
		90	1.77	107.794	400	404	384.5	2.7	3.91	24.5	16	37.5	25	24.9	8
		110	25.56	131.584	400	402	383.5	26.3	27.49	25	16	37.5	25	24.8	8.02
		128	46.88	152.904	400	402	382.5	49.4	50.59	24.5	16	37.5	25	24.8	8.04
		134	53.82	159.844	398	392	371.5	55	56.04	24.5	16	38.75	23	22.8	8.09
		160	82.7	188.724	396	396	378.5	83.6	84.75	24.5	16	38.75	25	24.4	8.1
		206.07	120	226.024											
		210	3.74	229.764	399	402	382.5	4.7	5.85	25.5	12.5	42	25	24.9	8.14
		235	32.85	258.874	398	402	381.5	33.6	34.74	25	12.5	42	25	25.2	8.16
		248.3	47.41	273.434	422	424	404	48.4	49.46	26	10	43.75	22	22.8	7.99
		273	100.81	326.834	398	402	382.5	101.7	102.77	25	14.5	40.5	25	24	8.01
		298.56	103.139	329.163											
		313	15.04	344.203	399	402	380.5	15.9	16.96	24.5	15	38.75	25	24.4	8.13
		357.15	61.51	390.673	398	401	380.5	62.3	63.34	24	15	38.75	25	25	8.18
		N/A	105.87	435.033	399	402	381.5	106.5	107.47	24.5	15	38.75	25	25	8.21
		403.42	107.974	437.137											
		405	0.99	438.127	398	402	380	1.7	2.65	24.5	16	38.75	25	24.8	8.2
		413	8.49	445.627	398	403	381.5	9.2	10.15	24	16	37.5	25.5	25.5	8.16
		420	14.91	452.047	400	406	382.5	16.3	17.22	24	16	37.5	25	25.1	8.14
		425	19.41	456.547	399	404	382.5	20.1	21	24	16	37.5	25	N/A	N/A

Table E8: Raw Data for AD/DC Waste Test #2 for Module 2

Mod 3-6
AD/DC waste test #2 (repeat of test #1)
After cleaning with 5 micron filter installed

Date	Stage	Time (min.sec)	Permeate Weight (kg)	Total permeate Weight (kg)	Low pre-mem. press. reading (psi)	High pre-mem. press. reading (psi)	Post-membrane pressure (psi)	Initial Permeate weight (kg)	Final Permeate weight (kg)	Suction press. to HP pump (psi)	Feed flowrate (LPM)	Recirculation flowrate (LPM)	System temperature (deg. C)	pH meter temperature (deg. C)	pH
28-Aug	After cleaning	2	2.84	2.84	397	405	384.5	4.4	5.44	25	13.75	40	22	21.8	8.1
		6	6.98	6.98	401	404	384	7.6	8.65	25	13.75	40	22	22.4	8.1
		10	11.19	11.19	400	405	384	12	13.07	25	13.75	40	22	22.8	8.13
		20.15	22.27	22.27	400	406	385.5	23	24.11	25	13.75	40	23	23.3	8.18
		30	33.16	33.16	399	404	383.5	33.9	35.04	25	13.75	40	23	24.1	8.16
		45	50.16	50.16	400	404	383	51	52.14	25	13.75	40	24	24	8.18
		60	67.48	67.48	398	402	380	68.4	69.58	25	13.75	40	25	24.8	8.18
		92	105.59	105.59	398	402	380.5	106 5	107.73	25	13.75	40	25	25.4	8.18
		94.31	108.573	108.573						25					
		96.3	3.26	111.833	400	404	384	4.2	5.4	25	14	39	25	25.3	8.2
		120.3	32.13	140.703	400	404	383	33	34.18	25	14	39	25	25	8.21
		162	79.65	188.223	402	406	385	80.4	81.52	25	14	39	24	24.2	8.23
		186	106.91	217.483	402	406	384.5	109 8	110.93	25	14	39	24	24.4	8.23
		190.12	111.346	219.919						25		39			
		195	5.45	225.369	397	401	378.5	6.5	7.43	25	13.75	40	25	24.8	8.24
		240	56.05	275.969	398	400	378.5	56.8	57.92	25	13.75	40	25	24.9	8.24
		281	101.91	321.829	398	400	379.5	102 6	103.71	25	13.75	40	25	25.1	8.25
		283.13	104.336	324.255						25			25		
		285	2.16	326.415	399	401	380.5	2.9	4	25	13	41	25	25.1	8.25
		325	45.75	370.005	400	401	381.5	46.7	47.77	25	13	40.5	25	24.6	8.31
		360	83.12	407.375	401	402	382.5	83.8	84.86	25	13	40.5	25	25.3	8.29
		384	108.29	432.545	402	404	383	109	110.03	25	13	40.5	25	25.3	8.3
		386.52	111.4	435.655						25			25		
		390.15	4.56	440.215	400	401	381.5	5.2	6.19	25	15	38.75	25	25.1	8.3
		400	14.17	449.825	400	402	380.5	14.8	15.79	25	15	38.75	25	25.2	8.29
		410	23.94	459.595	397	399	379.5	24.6	25.57	25	15	38.75	25	25.4	8.27
		420.15	33.9	469.555	399	402	382	34.5	35.47	25	15	38.75	25	25.5	8.23
		430.15	43.43	479.085	402	403	381.5	43.9	44.84	25	15	38.75	25	25.3	8.21
		440	52.44	488.095	401	402	380.5	54	54.91	24.5	15	38.75	25	25.2	8.18
		445	56.93	492.585	400	401	381.5	57.4	58.29	25	15	38.75	25	25.2	8.18

Table E9: Raw Data for AD/DC Waste Test #3 for Module 2

Mod 3-6
AD/DC waste test #3
After cleaning with 5 micron filter removed

Date	Stage	Time (min.sec)	Permeate Weight (kg)	Total permeate Weight (kg)	Low pre-mem. press. reading (psi)	High pre-mem. press. reading (psi)	Post-membrane pressure (psi)	Initial Permeate weight (kg)	Final Permeate weight (kg)	Suction press. to HP pump (psi)	Feed flowrate (LPM)	Recirculation flowrate (LPM)	System temperature (deg. C)	pH meter temperature (deg. C)	pH
29-Aug	After cleaning	2	3	3	399	403	381.5	3.9	5.02	26	13.75	39	24	24	8.4
		5.3	6.87	6.87	407	409	390.5	7.8	8.71	26	13.75	40	23	24	8.39
		10	11.86	11.86	401	402	382.5	12.5	13.64	26	13.75	40	25	24.8	8.39
		20.15	23.72	23.72	401	402	382	24.7	25.86	26	13	40	25	25.4	8.38
		30	34.86	34.86	400	404	385	35.7	36.86	26	13	40	24.5	24.9	8.39
		45	52.28	52.28	398	400	380.5	53.1	54.27	26	13	40	25	25.4	8.37
		61.15	71.28	71.28	398	400	380.5	72	73.17	26	13	40	25	25.5	8.36
		90	105.05	105.05	398	400	380	105.9	107.07	26	13	40	25	25.7	8.35
		95.26	111.338	111.338						26	13	40			
		97	2.24	113.578	400	402	381.5	3.4	4.55	26	13	40	25	25.2	8.35
		150	61.86	173.198	401	402	381.5	62.5	63.61	26	13	40	24	24.6	8.33
		192	108.16	219.498	400	401	381.5	109	110.1	26	13	40	25	24.8	8.31
		194.31	110.897	222.235							13	40			
		198	4.04	226.275	401	402	384	5.2	6.29	25.5	13.75	40	24	24.5	8.31
		241	50.82	273.055	402	403	382.5	51.5	52.57	25.5	13	40	24	24.6	8.29
		278	104.1	326.335	402	403	384	104.7	105.76	25.5	13	40	25	24.8	8.27
		296.55	110.2	332.435						25.5		40			
		300	2.64	335.075	396	405	380.5	4	5.01	25.5	13	40	23	23.2	8.31
		315	17.8	350.235	397	406	381	18.7	19.75	25.5	13.75	40	25	24.5	8.3
		347	52.63	385.065	396	407	379.5	53.5	54.55	25	13.75	40	25	25	8.3
		375	81.63	414.065	396	405	380.5	82.5	83.51	25	13.75	40	25	24.8	8.31
		405	111.18	443.615	396	406	381.5	112	112.96	25	13.75	40	24	24.4	8.32
		407.27	113.362	445.797							13.75	40			
		410	2.05	447.847	393	400	376.5	3	3.95	26	13.75	40	25	24.9	8.31
		420	11.59	457.387	394	402	378.5	12.5	13.47	26	13.75	39	26	25.5	8.26
		430	21.28	467.077	396	404	379.5	22.1	23.03	26	13.75	39	25	25.3	8.24
		440	30.34	476.137	396	406	380.5	31	31.92	26	13.75	40	25	25.4	8.21

Table E10: Raw Operational Data for Cs and Sr Tests for Module 1

Mod 5-6
Cs and Sr test

Date	Stage	Time (min.sec)	Total permeate Weight (kg)	Low pre-mem. press. reading (psi)	High pre-mem. press. reading (psi)	Post-membrane pressure (psi)	Initial weight (kg)	Final weight (kg)	Suction press. to HP pump (psi)	Feed flowrate (LPM)	Recirculation flowrate (LPM)	System temperature (deg. C)	pH meter temperature (deg. C)	pH
11-Jul	before cleaning	N/A	N/A	198	204	176	1.55	1.782	25	17	37.5	23	N/A	N/A
		N/A	N/A	203	209	178	2.08	2.275	25	17	37.5	24	N/A	N/A
		N/A	N/A	200	208	176.5	2.5	2.716	25	17	37.5	24	N/A	N/A
		N/A	N/A	298	307	280	3.78	4.149	25.5	16	38.5	25	N/A	N/A
		N/A	N/A	300	309	280	4.52	4.894	25.5	16	38.5	26	N/A	N/A
		N/A	N/A	299	311	279.5	5.34	5.718	25.5	16	38.5	26	N/A	N/A
		N/A	N/A	398	402	375.5	8.2	8.67	25.5	16	38.5	25	N/A	N/A
		N/A	N/A	398	402	376	9.13	9.61	25.5	16	38.5	25	N/A	N/A
		N/A	N/A	399	404	378	10.1	10.58	25.5	16	38.5	26	N/A	N/A
		N/A	N/A	498	505	476	12.54	13.15	26	15	39	26	N/A	N/A
		N/A	N/A	498	505	476	14.1	14.71	26	15	39	25	N/A	N/A
		N/A	N/A	499	504	477	14.85	15.56	26	15	39	25	N/A	N/A
		N/A	N/A	598	602	574	18.98	19.72	26	15	38.5	26	N/A	N/A
		N/A	N/A	597	600	573	20.55	21.27	26	15	38.5	25.5	N/A	N/A
		N/A	N/A	598	601	574	22.08	22.79	26	15	38.5	25	N/A	N/A
		N/A	N/A	698	703	675.5	26.5	27.33	25.5	15	38.5	25.5	N/A	N/A
		N/A	N/A	697	701	676	28.2	29.02	26	15	38.5	25	N/A	N/A
		N/A	N/A	696	700	674.5	29.9	30.71	26	15	38.5	25	N/A	N/A
		N/A	N/A	800	803	778.5	34.4	35.32	25	17	38	25	N/A	N/A
		N/A	N/A	798	801	778	36.1	37.01	25	17	38	25	N/A	N/A
		N/A	N/A	798	800	776.5	37.9	38.82	25	17	38	25	N/A	N/A
		N/A	N/A	198	199	173	0.71	0.943	25	17	38	26	N/A	N/A
		N/A	N/A	199	200	173.5	1.86	2.184	25	17	38	26	N/A	N/A
		N/A	N/A	199	199	173.5	2.33	2.559	25	17	38	25	N/A	N/A
		N/A	N/A	300	302	276	6.24	6.61	25.5	16	38	26	N/A	N/A
		N/A	N/A	300	302	275.5	6.94	7.323	25.5	16	38	27	N/A	N/A
		N/A	N/A	299	301	275.5	7.58	7.96	25.5	16	38	26.5	N/A	N/A
		N/A	N/A	398	402	375.5	10.04	10.48	25.5	16	38	25	N/A	N/A
		N/A	N/A	399	401	376	10.9	11.32	25.5	16	38	25	N/A	N/A
		N/A	N/A	398	402	376	11.9	12.35	25.5	16	38	24	N/A	N/A
		N/A	N/A	501	503	478	14.9	15.45	25	16	38	25	N/A	N/A
		N/A	N/A	500	502	477.5	15.9	16.45	25	16	38	25	N/A	N/A
		N/A	N/A	500	503	477.5	16.85	17.43	25	16	38	25	N/A	N/A
		N/A	N/A	601	603	579	19.07	20.12	25.5	16	38	25	N/A	N/A
		N/A	N/A	603	604	580	20.75	21.46	25.5	16	38	25	N/A	N/A
		N/A	N/A	602	604	578.5	22	22.71	25.5	16	38	25	N/A	N/A
		N/A	N/A	701	703	678	24.25	25.06	25.5	16	38	25	N/A	N/A
		N/A	N/A	699	702	678.5	25.7	26.49	25.5	16	38	25	N/A	N/A
		N/A	N/A	700	704	678.5	27.1	27.91	25.5	16	38	25	N/A	N/A
		N/A	N/A	799	803	778.5	30.5	31.43	25	16	38	25	N/A	N/A
		N/A	N/A	798	804	777.5	32.2	33.11	25	16	38	25	N/A	N/A
		N/A	N/A	798	804	776	33.9	34.83	25	16	38	25	N/A	N/A
13-Jul	After Trillon X	N/A	N/A	398	402	376.5	6.4	7.23	25	16	38	24	N/A	N/A
		N/A	N/A	398	402	376.5	8	8.84	25	16	38	24	N/A	N/A
		N/A	N/A	398	402	376.5	9.5	10.36	25	16	38	25	N/A	N/A
19-Jul	After HCl	2	N/A	398	406	377.5	3.5	4.48	25	15	38	25	25	6.77
		5.43	N/A	398	405	377.5	7	7.97	25	15	38	25	25.1	6.79
		8	N/A	396	402	376.5	9.25	10.23	25	15	38	25	25.2	6.81
27-Jul	After NaOH+ EDTA	4.48	4.57	197	203	176.5	5.2	5.82	25	16	40	25	24.7	9.49
		9.24	7.4	193	202	175	8.3	8.92	25	16	39	25	24.5	9.49
		13.43	10.05	190	200	172	10.7	11.31	25	16	39	25	24.6	9.5
		24.27	18.85	396	405	377.5	21.2	22.53	25	16	38	25.5	25.4	9.63
		29.44	26.82	398	407	380.5	28.4	29.73	24.5	16	38	25	25.6	9.48
		34.44	33.4	398	410	380.5	34.9	36.24	24.5	16	38	25.5	25.8	9.46
		45	50.33	593	606	574	53.2	55.13	25	14	39	25	25.9	9.44
		49	57.86	596	610	574	58.8	61.72	25	14	39	25	25.9	9.43
		54	67.26	598	605	574	69.3	71.17	25	14	39	25	25.9	9.4
		5	16.02	798	803	782	19	21.63	24	17.5	35	26	25.9	9.45
		9	26.43	798	802	780.5	27.2	29.79	24	17.5	35	25	26.4	9.45
		12	34.09	798	803	782.5	36	38.6	24	17.5	35	26	26.4	9.45

Table E11: Raw Operational Data for Cs and Sr Tests for Module 2

Mod 3-6
Cs and Sr test

Date	Stage	Time (min:sec)	Total permeate Weight (kg)	Low pre-mem. press. reading (psi)	High pre-mem. press. reading (psi)	Post-membrane pressure (psi)	Initial Permeate weight (kg)	Final Permeate weight (kg)	Suction press. to HP pump (psi)	Feed flowrate (LPM)	Recirculation flowrate (LPM)	System temperature (deg. C)	pH meter temperature (deg. C)	pH
14-Aug	before cleaning	33	10.82	186	188	175.5	10.9	11.24	24	16	38.5	24	24.6	7.77
		36.3	12.02	187	188	176	12.3	[illegible]	24	16	39	24	24.5	7.83
		39	12.87	186	188	175.5	13.1	13.44	24	16	39	24	24.5	7.84
		52	19.06	301	304	281	19.5	20.04	25	13.75	41.75	25	24.8	7.86
		54	20.14	302	305	282.5	20.6	21.14	25	13.75	41.75	25	24.8	7.85
		56	21.23	300	305	281.5	21.6	22.14	25	13.75	41.75	25	24.8	7.86
		9	33.61	398	402	380	31.9	32.63	24	15	39	25	25.3	7.84
		12	32.79	398	402	380	33.1	33.83	24	15	39	25	25.3	7.85
		16	35.71	398	402	380	35.9	36.53	24	15	39	25	25.5	7.84
		7	44.83	504	506	486.5	46	46.82	24	15	39	25.5	25.8	7.85
		9	45.85	505	507	488	47	47.82	24	15	39	25	25.8	7.85
		11	46.46	506	507	486.5	46.7	48.61	24	15	39	25	25.7	7.85
		8	10.21	602	606	584	10.6	11.71	25	14	38.75	25	25.8	7.85
		10	12.41	602	606	584	13.2	14.3	25	14	38.75	25	25.8	7.85
		12	14.59	602	607	584	15.3	16.41	25	14	38.75	25	25.8	7.85
		4	24.32	696	705	675	24.8	26.04	25	12.5	40	25	25.8	7.85
		6	26.78	696	705	676.5	27.5	28.74	25	12.5	40	25	25.8	7.85
		8	29.24	696	705	676	30	31.24	25	12.5	40	25	25.8	7.85
		5	40.76	798	805	777	41.4	42.76	25	11.75	40.5	24	25.5	7.86
		7	43.45	798	805	774	44.3	45.65	25	11.75	40.5	24	25.5	7.86
		9	46.11	796	802	773.5	47.2	48.55	25	11.75	40.5	24	25.4	7.86
16-Aug	After Triton X	15.3	16.83	401	404	381.5	17.5	18.49	24	15	38.75	24	24.9	7.43
		18	18.67	402	403	382	18.8	19.78	24	15	38.75	24	24.9	7.53
		18.3	20.54	402	403	382.5	20.8	21.77	24	15	38.75	24	24.9	7.55
		1.3	28.84	800	803	784	30.1	32.04	25	12	40	24	25	7.58
		3.3	32.75	801	803	784	33.6	35.54	25	12	40	24	25.1	7.58
		7	38.44	801	803	784.5	40.3	42.24	25	12	40	24	25.3	7.59
17-Aug	After HCl	11	11.57	397	405	380.5	12.2	13.18	25	12.5	40	24	24.5	6.5
		13	13.53	400	405	382.5	14.4	15.38	25	13	40.5	24	24.5	6.52
		15.15	15.72	401	404	382.5	16.2	17.18	25	13	40.5	24	24.4	6.54
		2	23.46	801	804	784.5	24.8	26.76	25	12	40	25	24.7	6.6
		4	27.32	800	802	784.5	28.1	30.07	25	12	40	25	24.9	6.63
		6	31.19	800	802	782.5	32.5	34.46	25	12	40	25	25.1	6.65
22-Aug	After NaOH+ NTA	22	14.27	196	206	180	14.6	15.25	24	15	40	25	24.8	8.82
		24	15.56	197	204	180	15.9	16.56	24	15	40	26	25	8.82
		26	16.85	197	205	180.5	17.1	17.77	24	15	40	26	25.2	8.82
		5	27.16	298	307	282.5	28.1	30.13	24.5	13.75	41	26	26.3	8.8
		8.3	30.75	298	307	282.5	31.3	32.33	24.5	13.75	41	26	26.3	8.8
		10.3	32.79	298	310	283.5	33.3	34.33	24.5	13.75	41	26	26.3	8.8
		6	44.37	396	405	378.5	45.8	47.06	24.5	13.75	40	25	25.3	8.81
		8.3	47.46	396	402	378.5	48.2	48.43	24.5	13.75	40	24	25	8.82
		11	50.48	396	402	380	51.4	52.81	24	13.75	40	23	24.8	8.82
		3	58.57	502	507	486.5	60.3	61.84	24	13	40	23	24.5	8.81
		5	62.59	501	507	484.5	63	64.54	24.5	13	40	24	24.6	8.8
		8.3	64.89	500	510	484.5	65.5	67.06	24.5	13	40	24	24.7	8.79
		4	8.33	598	607	583	11.6	13.54	25	12.5	40	25	23.3	8.73
		6.3	14.13	602	610	588	15.3	17.16	25	12.5	40	24	23.7	8.75
		8.3	17.85	604	610	588	19.4	21.34	25	12.5	40	25	24.1	8.76
		4.3	38.14	696	701	680	38.5	41.68	24	11.75	41.75	24	24.7	8.78
		6.3	42.41	695	701	680	43.3	46.53	25	11.75	41.75	25	24.8	8.78
		8.15	46.27	693	700	678	47.5	49.77	26	11.75	41.75	26	25.2	8.77
		3	8.9	794	800	780	11.7	14.26	25	12.5	38.5	25	25.3	8.72
		5	14.06	793	798	778	16.1	18.68	25	12.5	38.5	25	25.6	8.72
		7	20.04	793	798	778	21.1	23.69	25	12.5	38.5	25	25.7	8.72

Table E12: Raw Data for Cs and Sr Rejection Efficiency Tests for Module 1

Mod 5-6

Date	Stage	Pre-membrane Pressure (kPa)	[Cs] Feed mg/L	Permeate mg/L	[Sr] Feed mg/L	Permeate mg/L
11-Jul	before cleaning	1402	45	<10	9032	<10
		2096.1	50	<10	9389	<10
		2761.4	38	24	9717	43
		3459	51	<10	10060	<10
		4132.4	N/A	<10	N/A	<10
		4821.9	40	<10	11680	<10
		5517.1	30	<10	12720	22
		1372.1	39	<10	8750	<10
		2073.1	41	<10	8921	15
		2758	38	<10	9281	38
		3457.8	33	<10	9704	23
		4156.5	28	<10	10010	8
		4835.7	25	<10	10610	11
		5524	26	<10	11580	36
13-Jul	After Trition X	2758	442	22	10300	21
19-Jul	After HCl	2763.7	435	<10	11000	<10
27-Jul	After NaOH+ EDTA	1361.8	155000	3430	117000	20
		2774.1	213000	2050	149000	23
		4146.2	262000	1770	235000	43
		5518.3	227000	910	151000	45

Table E13: Raw Data for Cs and Sr Rejection Efficiency Tests for Module 2

Mod 3-6

Date	Stage	Pre-membrane Pressure (kPa)	[Cs] Feed mg/L	Permeate mg/L	[Sr] Feed mg/L	Permeate mg/L
14-Aug	before cleaning	1359.5	149000	5140	114000	32
		2088	169000	4930	124000	31
		2758	197000	4050	142000	35
		3488.9	234000	4490	169000	44
		4165.7	158000	4030	117000	26
		4829.9	189000	3950	133000	27
		5513.7	229000	4510	164000	38
16-Aug	After Trition X	2775.2	165000	2800	126000	31
		5528.6	221000	3010	158000	44
17-Aug	After HCl	2771.8	169000	4410	127000	42
		5526.3	214000	2420	158000	48
22-Aug	After NaOH+ NTA	1384.7	166000	5500	121000	7
		2089.2	201000	6710	145000	13
		2754.6	222000	4600	176000	23
		3478.5	234000	5550	225000	32
		4172.6	184000	3500	134000	46
		4810.4	203000	3730	180000	58
		5489.6	190000	5260	140000	32

Appendix F

Volume of Pilot-Scale SWRO System Piping

The volume of the piping of the pilot-scale system was determined so that accurate volumetric recoveries could be obtained. The pilot-scale system was completely flushed with deionized water. Then a salt solution of known volume and of a known concentration was recirculated through the pilot-scale system. The change in concentration indicated the volume of the piping in the pilot-scale system.

The volume of salt solution in the wash tank was 30 litres with a conductivity of 17.0 mS/cm. The conductivity of the salt solution after recirculation through the pilot-scale system was 8.71 mS/cm. Based on conservation of mass:

$$V_2 = \frac{N_1 \cdot V_1}{N_2}$$
$$= \frac{17.0 \times 30}{8.71}$$
$$= 58.5 \text{ L}.$$

Therefore, the volume of piping in the pilot-scale system is 58.5-30 = 28.5 L.

TEST TARGET (QA-3)

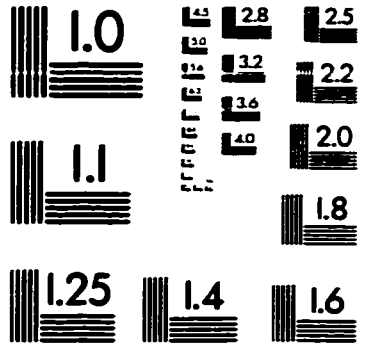

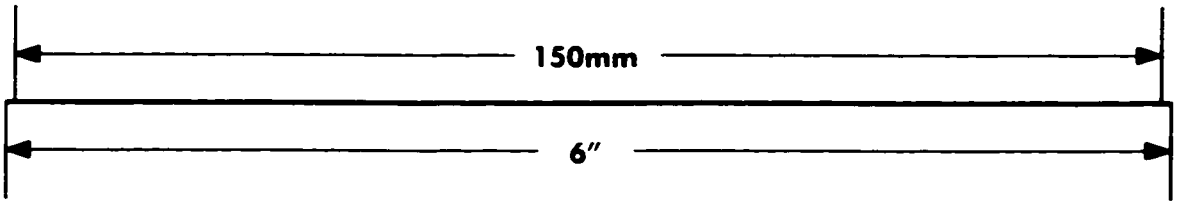

APPLIED IMAGE, Inc
1653 East Main Street
Rochester, NY 14609 USA
Phone: 716/482-0300
Fax: 716/288-5989